THE UNIVERSITY OF OKLAHOMA

GRADUATE COLLEGE

DYNAMIC ANALYSIS OF SUCKER ROD PUMPING

A THESIS

SUBMITTED TO THE GRADUATE FACULTY

in partial fulfillment of the requirements for the

degree of

MASTER OF SCIENCE

By

THOMAS H. NICOL

Norman, Oklahoma

1982

DYNAMIC ANALYSIS OF

SUCKER ROD PUMPING

A THESIS

APPROVED FOR THE DEPARTMENT OF AEROSPACE, MECHANICAL

AND NUCLEAR ENGINEERING

By

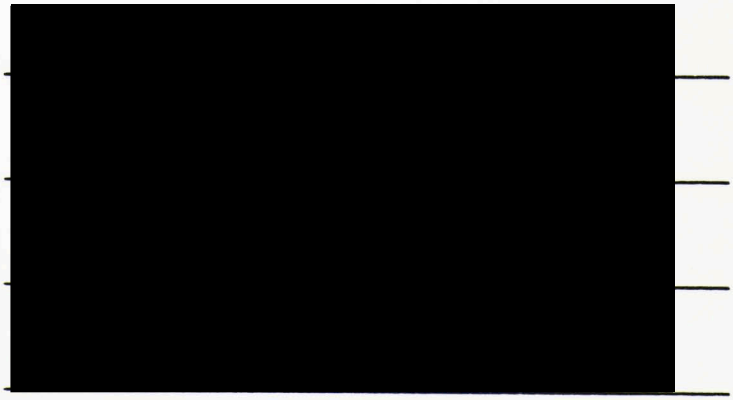

ACKNOWLEDGMENTS

The author would like to thank his thesis committee members, Drs. J. C. Purcupile, W. R. Upthegrove, A. G. Striz, and R. D. Evans for their patience and criticism in evaluation of this report.

Special thanks to Dr. Striz for this author's first comprehensive finite elements introduction and to Dr. Purcupile whose advisement in this and previous works made this project a reality.

Also, to Dr. Luther White, without whose support and encouragement this would not have been possible, thank you.

Finally, the skill and patience of Ms. Tanya Guthrie in her preparation of this manuscript are gratefully acknowledged and much appreciated.

THOMAS H. NICOL
December, 1982

ABSTRACT

The complexity of the interaction between surface and down-hole equipment has made accurate analysis of sucker rod pumping systems difficult at best. Consequently, realistic predictions of performance are seldom, if ever, made in advance of construction.

The petroleum industry has, over the years, compiled a substantial catalog of case histories, in effect, as a data base from which general design guidelines can be developed. However, the analytical work to date has been either sketchy or without sufficient basis in published documentation.

The analysis to be presented here addresses the dynamic behavior of the complete pumping system in, what is hoped to be, a complete and concise manner. The viewpoint is that of the designer or manufacturer of this system. That is, the total dynamic response will be derived based on a given set of input parameters. Factors which are considered consist of, but are not limited to, pumping unit kinematics, rod stress/strain relationships, imposed torques and drive motor slip.

TABLE OF CONTENTS

TABLE OF CONTENTS (cont'd)

LIST OF ILLUSTRATIONS

LIST OF ILLUSTRATIONS (cont'd.)

LIST OF ILLUSTRATIONS (cont'd.)

Chapter 1

INTRODUCTION

1.1 Opening Comments

"The walking beam and sucker rod combination for pumping is a very old method, so old in fact that the first date of its application is not positively known. It is known that the Egyptians used the walking beam principle for drawing water in 476 A.D. This device consisted of a tripod made of poles which supported a wooden beam. A goatskin filled with rocks served as a counterbalance while a servant actuated a rope sucker rod string, as water was drawn in a stone jar."[1]

1.2 Problem Development

One would hope that we have come a long way since those early days, and if we look across the oil fields of the U.S., we see that indeed we have. It is estimated that over 85% of all artificially pumped wells in this country are pumped via the sucker rod method. Large corporations devote entire engineering teams to the design, manufacture, and diagnosis of sucker rod pumping installations.

Still, truly modern technology is only slowly finding its way into the industry. The state of knowledge regarding the dynamic behavior of the complete system exists mainly as a result of an effort by the American Petroleum Institute to catalog as many case histories as possible in an attempt to develop guidelines for proper system design, manufacture, and operation (see ref. 1).

Shell Oil Co. scientists developed finite difference models for the sucker rod string back in the middle 1960's which have been refined and still exist today. Descriptions of their earliest efforts can be found in a report patented under patent number 3,343,409, filed October 1966 and in reference 13, a paper presented at the Society of Petroleum Engineers' Rocky Mountain

---

[1]Bethelehem Steel Company, Sucker Rod Handbook, 1958, page 6.

Regional Meeting in May 1963. However, the details of later work are evidently of a proprietary nature and thus in limited distribution. Unlike many engineering problems, where new solution techniques appear regularly as journal articles, the sucker rod problem has either eluded or been ignored by those who stand the most to gain from its development. Whichever is the case, the problem is as current today as it was twenty years ago.

1.3 Problem Definition

Since the time of the Shell work, new strides have been made in the area of finite elements. This method is well suited toward application in sucker rod dynamics and is, in many ways, more straightforward than the familiar finite difference methods (see chapter 2). For this reason, and in an attempt to broaden the current state of the art, the purpose herein is to apply the finite element method to the solution of the dynamic behavior of the sucker rod string.

In order to familiarize the reader with the well pumping system as a whole, figure 1.1 depicts a typical installation along with some of the more commonly seen nomenclature.

Clearly, the behavior of the rod is but part of the overall problem. A complete system analysis must also include a detailed study of the surface equipment kinematics, torque characteristics, and subsurface pumping equipment. All of these topics are covered in the sections which follow.

The problem at hand has essentially two avenues of approach. First we can look at it from the designer's viewpoint. That is, we can aim the solution toward satisfying the requirements of he who is either designing or manufacturing the system. That person would like to know, given a set of input parameters, what the nature of the behavior will be. What are the maximum rod stresses and where do they occur, what size gearbox is required,

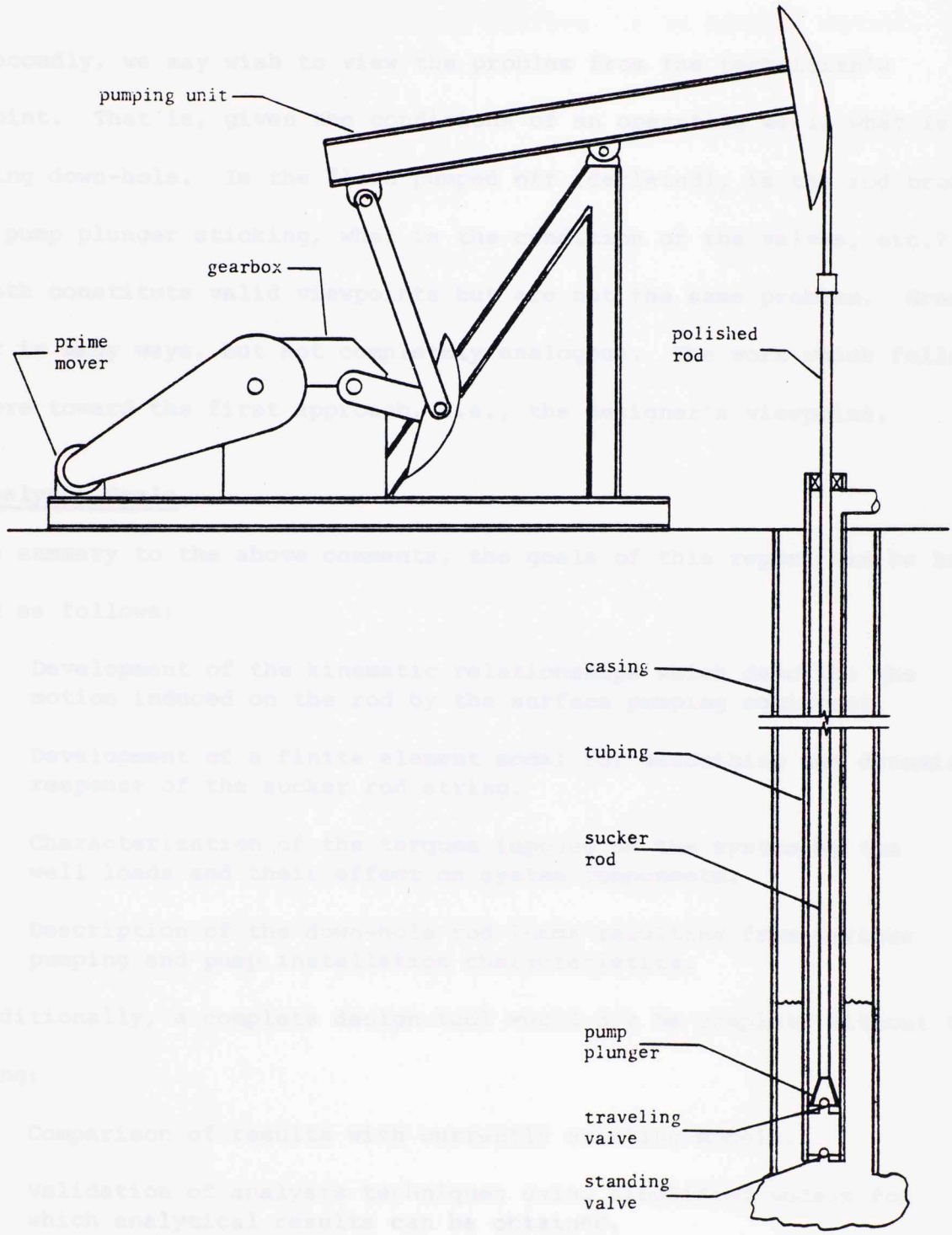

Figure 1.1 - Typical Pumping Installation

what is the average pumping speed, etc? With this information he can intelligently make comparisons among many systems without having to build even one.

Secondly, we may wish to view the problem from the technician's standpoint. That is, given the conditions of an operating well, what is happening down-hole. Is the fluid pumped off (depleted), is the rod broken, is the pump plunger sticking, what is the condition of the valves, etc.?

Both constitute valid viewpoints but are not the same problem. Granted, similar in many ways, but not completely analogous. The work which follows aims more toward the first approach, i.e., the designer's viewpoint.

1.4 Analysis Goals

In summary to the above comments, the goals of this report can be briefly defined as follows:

1. Development of the kinematic relationships which describe the motion induced on the rod by the surface pumping equipment.

2. Development of a finite element model for describing the dynamic response of the sucker rod string.

3. Characterization of the torques imposed on the system by the well loads and their effect on system components.

4. Description of the down-hole rod loads resulting from various pumping and pump installation characteristics.

Additionally, a complete design tool would not be complete without the following:

5. Comparison of results with currently existing models.

6. Validation of analysis techniques using simplified models for which analytical results can be obtained.

Finally, in an attempt to expand even further upon existing techniques the following introductions will be made:

7. Development of a theoretical basis for damping phenomena occuring along the rod surface.

8. Development of effective forms of data reduction aimed at clarification of system behavior.

These end those comments applicable to the introduction of the ensuing report. The sections which follow will address, in an orderly manner, those concepts outlined above.

Chapter 2

THE FINITE ELEMENT METHOD

2.1 Opening Comments

The scope of this work is not meant to include a rigorous appraisal of the finite element method. Volumes of literature exist which accomplish that end. References 7 and 12 are two excellent examples. Nor is it meant to necessarily express superiority of this method over the more familiar finite difference techniques. On the contrary, good agreement between solutions utilizing each of the two would serve to strengthen both.

Owing, however, to the general unfamiliarity with finite elements, a brief synopsis is appropriate here so that subsequent discussions will be more fully understood.

2.2 Finite Difference Methods

Finite difference methods have been in widespread use for many years and still find numerous applications throughout the numerical analysis field. Essentially a function defined over a given region is expanded into the appropriate Taylor-series to the degree of accuracy required. For example, consider the function $y = f(x)$ at $(x_i + \Delta x)$. The Taylor-series expansions about x_i are given by

$$y(x_i + \Delta x) = y_i + y_i'\Delta x + \frac{y_i''\Delta x^2}{2!} + \frac{y_i'''\Delta x^3}{3!} + \cdots \qquad (2.1)$$

and

$$y(x_i - \Delta x) = y_i - y_i'\Delta x + \frac{y_i''\Delta x^2}{2!} - \frac{y_i'''\Delta x^3}{3!} + \cdots \qquad (2.2)$$

Subtracting (2.2) from (2.1) yields

$$y_i' = \frac{y(x_i + \Delta x) - y(x_i - \Delta x)}{2\Delta x} - (\frac{1}{6} y_i'''\Delta x^2 + \ldots). \qquad (2.3)$$

Clearly, we can't deal with an infinite series such as this in the solution of practical problems. Higher order terms are thus truncated past some point deemed to cause little overall error. If we truncate, for example, all terms of order three or higher in (2.3) we arrive at

$$y_i \simeq \frac{y(x_i + \Delta x) - y(x_i - \Delta x)}{2\Delta x} \quad . \qquad (2.4)$$

This is known as the central difference approximation to y_i' at x_i of order Δx^2. Similarly, the comparable approximation is y_i'' is

$$y_i'' \simeq \frac{y(x_i + \Delta x) - 2y(x_i) + y(x_i - \Delta x)}{\Delta x^2} \qquad (2.5)$$

Note that the above expressions require some knowledge of conditions both ahead of and behind the current position, thus the term "central difference". Similar expressions known as forward and backward differences may also be derived if the problem is more suited to those conditions. However, accuracy is generally sacrificed with either of these latter approximations.

2.3 Finite Element Methods

The finite element method, rather than containing Taylor-series expansions of the required functions, relies on the definition of approximating polynomials called shape functions which are defined over the length of each member or element of the discretized space. To illustrate this point, refer to figure 2.1.

The function $y = f(x)$ for which the approximation is desired is given by

$$y = \alpha_1 + \alpha_2 x \qquad (2.6)$$

for the element of length L, bounded by nodes i and j. In this example, y is assumed to vary linearly in x although this is not necessary. Coefficients α_1 and α_2 can be determined by using boundary conditions at the nodes as follows:

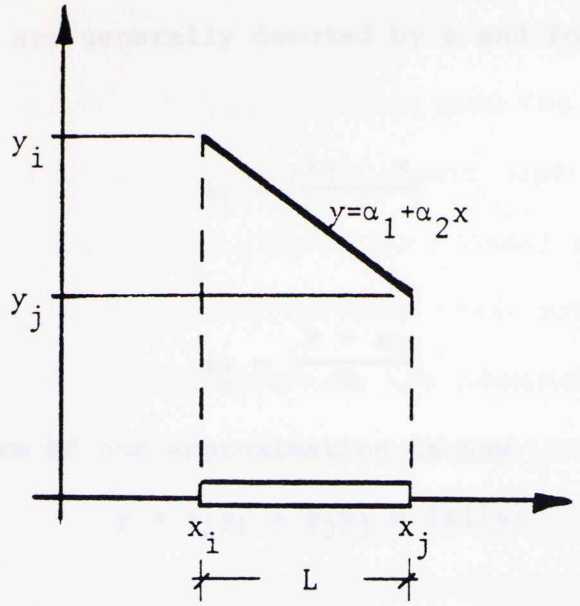

Figure 2.1 - One Element in a Discretized Space

$$y = y_i \text{ at } x = x_i$$

and

$$y = y_j \text{ at } x = x_j \quad .$$

Then,

$$y_i = \alpha_1 + \alpha_2 x_i$$

and

$$y_j = \alpha_1 + \alpha_2 x_j \quad .$$

Solving for α_1 and α_2 yields

$$\alpha_1 = \frac{y_i x_j - y_j x_i}{L}$$

and

$$\alpha_2 = \frac{y_j - y_i}{L}$$

Substituting these results into (2.6) and rearranging terms gives

$$y = \left(\frac{x_j - x}{L}\right) y_i + \left(\frac{x - x_i}{L}\right) y_j \quad . \qquad (2.7)$$

Shape functions are generally denoted by ϕ and for this example are given by

$$\phi_i = \left(\frac{x_j - x}{L}\right)$$

and (2.8)

$$\phi_j = \left(\frac{x - x_i}{L}\right)$$

so that the final form of our approximation is now

$$y = \phi_i y_i + \phi_j y_j = [\phi]\{y\} \quad (2.9)$$

where

$$[\phi] = [\phi_i \phi_j]$$

and

$$\{y\} = \begin{Bmatrix} y_i \\ y_j \end{Bmatrix} .$$

An examination of ϕ_i shows that it has the value of one at node i and zero at node j. Similarly, ϕ_j takes on the values of one at node j and zero at node i. This is characteristic of shape function polynomials, i.e., they are equal to unity at one node and zero at all others.

As hinted at by (2.9), the finite element method is, in essence, a matrix formulation. Individual element matrices, when appropriately assembled, combine to form a system matrix which can be manipulated using conventional matrix procedures. For example, a tensile member consisting of N elements, of the type in the preceding discussion, would be modeled using a set of (N+1) by (N+1) matrices formed by the summation of the individual element matrices previously defined. This point will be clarified in a subsequent section where this assembly is illustrated.

The approximating polynomial defined for the preceding illustrative example was of order one, i.e., linear in x. This need not have been the

case. In fact, any degree polynomial could have been defined. Analogous to the choice of the order of the approximation used for finite difference methods, the degree of this polynomial is chosen such that it adequately describes the physical situation. Generally, higher order equations decrease the sparsity of the system matrices (produce fewer zeros in the off-diagonal terms), but do not significantly increase the complexity of the formulation.

It can be shown that, if the shape function polynomial truly reflects the actual physical situation, the resulting solution will be exact if the boundary conditions are defined correctly. For example, the deflection of a prismatic bar in tension is a linear function of the applied load. Thus, its finite element equivalent which employs a linear shape function will yield exact results for deflection versus load. Similarly, a beam element in bending can be precisely modeled using a third order shape function (cubic spline) (see ref. 12, page 37).

One of the advantages of the finite element method, at least from this author's viewpoint, is the manner in which boundary condition terms are incorporated into the model. In the finite difference method, boundary condition expressions are reduced to their series expansions in a manner analogous to the discussion in section 2.2. Satisfaction of these conditions must be insured with each solution iteration. This is similarly true in the finite element method, however, in this case, boundary condition coefficients are simply added to the correct matrix positions. For this reason, the entire problem can be formulated without regard to boundary conditions. Then after matrix assembly, the appropriate corrections at the boundaries are incorporated. This concept greatly simplifies the overall solution and facilitates the use of a general formulation in the solution of many individual problems. This too will be illustrated more completely in an upcoming discussion.

It can be additionally shown that the finite elements treat non-homogeneous and anisotropic material properties with little difficulty whereas finite difference techniques can not (at least not so easily). Also, elements can be of varying shapes and forced to conform to irregular boundaries. Although these two properties do not necessarily apply to the problem at hand, they are nonetheless important considerations.

Finally, and again in this author's opinion, the finite element method lends itself well to efficient, orderly implementation for computer generated solutions, which, in this day and age, constitutes a distinct advantage.

With these thoughts in mind, we can turn our attention to the proposed problem and hopefully, have some insight into the nature of the resulting formulation.

Chapter 3

SUCKER ROD MODEL FORMULATION

3.1 Opening Comments

As indicated in chapter one, the dynamic analysis of a sucker rod pumping system actually consists of separate solutions to several problems, each of which can essentially stand alone. There is the problem of pumping unit kinematics, i.e., the derivation of the equations of motion for the surface equipment. Then too, there is the torque analysis of the drive system including both the gearbox and the prime mover and coupled with this, the treatment of variations in pumping speed as a result of these applied torques. Finally, and the subject of this section, there is the modeling of the sucker rod string from the finite element standpoint.

In order to proceed with this development, we must first define a coordinate system, some of the nomenclature, and the sign conventions to be used in this and the following sections. Figure 3.1 depicts an arbitrary element of the string and some required notation.

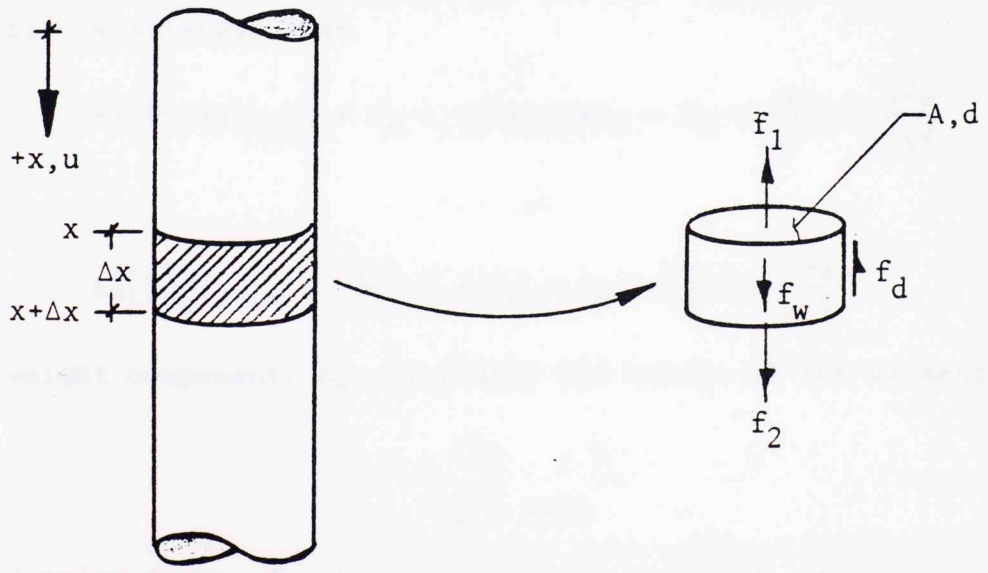

Figure 3.1 Model Development

where:

u = displacement
$\partial u/\partial t$ = velocity
$\partial^2 u/\partial t^2$ = acceleration
} all "+" in "+" x-dir

A = rod cross-sectional area
d = rod diameter
w = rod material weight density
f_1, f_2 = static/dynamic forces
f_w = weight component
f_d = damping force

3.2 Derivation of the Governing Equation

With figure 3.1 in mind we may proceed. The free body diagram shown at the top right of the above depicts all of the terms required for a summation of forces on the element of length Δx. From Newton's second law we have $\Sigma F = ma$ which, for this case yields

$$\Sigma F_x = f_2 + f_w - f_1 - f_d = m \frac{\partial^2 u}{\partial t^2}$$

or

$$f_2 + f_w - f_1 - f_d = \left(\frac{w}{g}\right) A\Delta x \frac{\partial^2 u}{\partial t^2} \quad . \tag{3.1}$$

Recognizing that $\sigma_x = f_1/A$ (stress at x) and $\sigma_{x+\Delta x} = f_2/A$ and assuming an elastic, Hookian material where, for the one dimensional case, $E\varepsilon = E(\partial u/\partial x)$, we may write immediately that

$$EA(\partial u/\partial x)_{x+\Delta x} + f_w - EA(\partial u/\partial x)_x - f_d = \left(\frac{w}{g}\right)A\Delta x \frac{\partial^2 u}{\partial t^2}$$

or

$$EA\left[\left(\frac{\partial u}{\partial x}\right)_{x+\Delta x} - \left(\frac{\partial u}{\partial x}\right)_x\right] + f_w - f_d = \left(\frac{w}{g}\right)A\Delta x \frac{\partial^2 u}{\partial t^2} \tag{3.2}$$

The weight component, f_w, is simply the weight of the element Δx and is given by

$$f_w = wA\Delta x \tag{3.3}$$

The damping force, f_d, is somewhat more involved. If we imagine that the damping force arises from the skin friction between the rod and the fluid

column, we can view f_d as being a function of the rod surface area, some damping factor, c, and the rod velocity. We will see later that this damping factor is actually related to the resulting shear stress acting at the rod boundary. Using the above arguments gives

$$f_d = c\pi d\Delta x \frac{\partial u}{\partial t} .$$

Since $d = 2\sqrt{A/\pi}$ we can rewrite this as

$$f_d = 2c\sqrt{A\pi}\ \Delta x \frac{\partial u}{\partial t} \tag{3.4}$$

Now, substitution of (3.3) and (3.4) into (3.2) yields

$$EA\left[\left(\frac{\partial u}{\partial x}\right)_{x+\Delta x} - \left(\frac{\partial u}{\partial x}\right)_x\right] + wA\Delta x - 2c\sqrt{A\pi}\ \Delta x \frac{\partial u}{\partial t} = \left(\frac{w}{g}\right) A\Delta x \frac{\partial^2 u}{\partial t^2} . \tag{3.5}$$

Finally, dividing by Δx and taking the limit as $\Delta x \to 0$ gives

$$\lim_{\Delta x \to 0} \frac{EA}{\Delta x}\left[\left(\frac{\partial u}{\partial x}\right)_{x+\Delta x} - \left(\frac{\partial u}{\partial x}\right)_x\right] + wA - 2c\sqrt{A\pi}\ \frac{\partial u}{\partial t} = \frac{w}{g} A \frac{\partial^2 u}{\partial t^2}$$

or

$$EA \frac{\partial^2 u}{\partial x^2} + wA - 2c\sqrt{A\pi}\ \frac{\partial u}{\partial t} = \frac{w}{g} A \frac{\partial^2 u}{\partial t^2} . \tag{3.6}$$

If we now define temporary replacements for the constant terms in (3.6) as

$$\begin{aligned} \alpha &= EA \\ \beta &= 2c\sqrt{A\pi} \\ \gamma &= -wA \end{aligned} \tag{3.7}$$

and

$$\rho = \left(\frac{w}{g}\right)A$$

we can rewrite (3.6) (after rearranging) as

$$\alpha \frac{\partial^2 u}{\partial x^2} - \rho \frac{\partial^2 u}{\partial t^2} - \beta \frac{\partial u}{\partial t} - \gamma = 0 \tag{3.8}$$

which we recognize as the one-dimensional wave equation with damping and one constant coefficient. This then defines the governing equation for the dynamic behavior of the sucker rod string.

3.3 Initial and Boundary Conditions

For solution of (3.8) we need a set of both initial and boundary conditions applicable to the physical system. These are introduced here for completeness but will be treated in detail in chapter seven.

At the start of the solution procedure the following initial conditions apply:

$$\begin{aligned} u(x,0) &= u_o(x): \quad \text{displacement at } t = 0 \\ \frac{\partial u}{\partial t}(x,0) &= \dot{u}_o(x): \quad \text{velocity at } t = 0 \\ \frac{\partial^2 u}{\partial t^2}(x,0) &= \ddot{u}_o(x): \quad \text{acceleration at } t = 0. \end{aligned} \tag{3.9}$$

That is, at $t = 0$, the displacement of all nodes will be specified, as will their respective velocities and accelerations. In this case, nodal displacement will be determined from a static analysis, velocities and accelerations will be set equal to zero (start from rest).

The boundary conditions which must be satisfied at each solution interval are given by

$$u(0,t) = f(t): \quad \text{displacement at } x = 0 \text{ is given as some function of time} \tag{3.10}$$

and

$$a' \frac{\partial u}{\partial x}(L,t) + b' \frac{\partial^2 u}{\partial t^2}(L,t) + c' \frac{\partial u}{\partial t} + d'u(L,t) - p(t) = 0$$

where

a', b', c', d' = non-negative coefficients

$p(t)$ = prescribed pump loading condition

The coefficients for the bottom boundary condition must be non-negative in order to assure non-singularity of the system matrices. A complete discussion of these coefficients and the loading function, $p(t)$, will be given in chapter seven.

3.4 Finite Element Adaptation

Using concepts outlined in chapter two, we now begin the development of our finite element representation of (3.8).

The unknown functions to be determined are the displacements at points along the rod as functions of time, i.e., u(x,t). The shape functions, ϕ, are functions of the space variable only. Thus, the unknown u(x,t) is approximated as a linear combination of these and the function u(t), displacement as a function time only. That is

$$u(x,t) \simeq \sum_{i=1}^{N} u_i(t)\,\phi_i(x) \tag{3.11}$$

where the space is discretized into N elements.

Substitution of (3.11) into (3.8) while dropping the (x) on ϕ_i for convenience gives

$$\alpha \sum_{i=1}^{N} u_i(t)\frac{d^2\phi_i}{dx^2} - \rho \sum_{i=1}^{N} \frac{d^2u_i(t)}{dt}\,\phi_i - \beta \sum_{i=1}^{N} \frac{du_i(t)}{dt}\,\phi_i - \gamma = 0$$

Multiplying through by $(-\phi_j)$ to facilitate the steps which follow yields

$$-\alpha \sum_{i=1}^{N} u_i(t)\frac{d^2\phi_i}{dx^2}\,\phi_j + \rho \sum_{i=1}^{N} \frac{d^2u_i(t)}{dt^2}\,\phi_i\phi_j + \beta \sum_{i=1}^{N} \frac{du_i(t)}{dt}\,\phi_i\phi_j + \gamma\phi_j = 0\ .$$

Now, in order to account for the contribution of all points along each element we need to integrate with respect to x along each element of length L. This yields

$$\int_0^L \Big[-\alpha \sum_{i=1}^{N} u_i(t)\frac{d^2\phi_i}{d_{x2}}\,\phi_j\Big]dx + \int_0^L \Big[\rho \sum_{i=1}^{N} \frac{d^2u_i(t)}{dt^2}\,\phi_i\phi_j\Big]dx +$$

$$\int_0^L \Big[\beta \sum_{i=1}^{N} \frac{du_i(t)}{dt}\,\phi_i\phi_j\Big]dx + \int_0^L \big[\gamma\phi_j\big]dx = 0. \tag{3.12}$$

Integration of all terms is straightforward except for

$$\int_0^L \left[-\alpha \sum_{i=1}^{N} u_i(t) \frac{d^2\phi_i}{dx^2} \phi_j\right]dx$$

which must be integrated by parts. Rewriting this as

$$\int_0^L \left[-\alpha \sum_{i=1}^{N} u_i(t)\phi_j \frac{d}{dx}\left(\frac{d\phi_i}{dx}\right)\right]dx$$

and recognizing that $\phi_j = u$ and $\frac{d\phi_i}{dx} = v$ we have the standard form for integration by parts

$$\int udv = uv - \int vdu$$

which, for this case, gives

$$\int_0^L \left[-\alpha \sum_{i=1}^{N} u_i(t)\phi_j \frac{d}{dx}\left(\frac{d\phi_i}{dx}\right)\right]dx = -\alpha \sum_{i=1}^{N} u_i(t)\left[\frac{d\phi_i}{dx}\phi_j\Big|_0^L - \int_0^L \frac{d\phi_i}{dx}\frac{d\phi_j}{dx}dx\right] .$$

The final result from (3.12) then is

$$\left[-\alpha \sum_{i=1}^{N} u_i(t)\left[\frac{d\phi_i}{dx}\phi_j\Big|_0^L - \int_0^L \frac{d\phi_i}{dx}\frac{d\phi_j}{dx}dx\right] + \rho \sum_{i=1}^{N} \frac{d^2u_i(t)}{dt^2} \int_0^L \phi_i\phi_j dx + \right.$$

$$\beta \sum_{i=1}^{N} \frac{du_i(t)}{dt} \int_0^L \phi_i\phi_j dx + \gamma \int_0^L \phi_j dx = 0$$

or in slightly different form

$$\alpha \sum_{i=1}^{N} u_i(t)\left[\int_0^L \frac{d\phi_i}{dx}\frac{d\phi_j}{dx}dx - \frac{d\phi_i}{dx}(L) + \frac{d\phi_i}{dx}(0)\phi_j(0)\right] +$$

$$\rho \sum_{i=1}^{N} \frac{d^2u_i(t)}{dt^2} \int_0^L \phi_i\phi_j dx + \beta \sum_{i=1}^{N} \frac{du_i(t)}{dt} \int_0^L \phi_i\phi_j dx + \gamma \int_0^L \phi_j dx = 0 \qquad (3.13)$$

We now recognize (3.13) as being of the form

$$[M]\{\ddot{u}\} + [C]\{\dot{u}\} + [K]\{u\} + \{f\} = 0 \qquad (3.14)$$

where

$$[M] = \rho \sum_{i=1}^{N} \int_0^L \phi_i \phi_j dx$$

$$[C] = \beta \sum_{i=1}^{N} \int_0^L \phi_i \phi_j dx$$

$$[K] = \alpha \sum_{i=1}^{N} \left[\int_0^L \frac{d\phi_i}{dx} \frac{d\phi_j}{dx} dx - \frac{d\phi_i}{dx}(L)\phi_j(L) + \frac{d\phi_i}{dx}(0)\phi_j(0) \right] \qquad (3.15)$$

$$\{f\} = \gamma \int_0^L \phi_j dx \quad .$$

So using the approximation given in (3.11) we have transformed the second order hyperbolic partial differential equation in (3.8) into a second order system of ordinary differential equations. This sytem is that which now governs our dynamic analysis.

3.5 Shape Function Determination

Before we can evaluate the integrals in (3.15) we must first define the shape functions, $\phi(x)$. It is worth noting here that the entire formulation thus far has not relied on any knowledge of these functions, save for their existence.

Refer to figure 3.2 below for the notation required in defining $\phi(x)$.

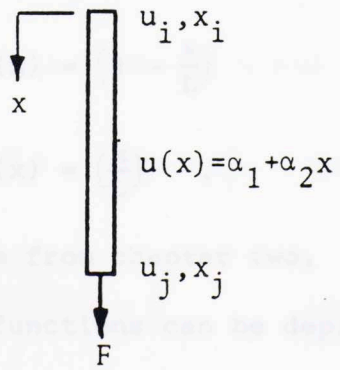

Figure 3.2 - Shape Function Notation

For this analysis we shall assume a linear form for the nodal displacements, u(x). This function is then given by

$$u(x) = \alpha_1 + \alpha_2 x \tag{3.16}$$

which we recognize from chapter two. At the boundaries

$$u(0) = \alpha_1 + \alpha_2 \cdot 0 = u_i$$

or

$$\alpha_1 = u_i \tag{3.17}$$

and

$$u(L) = \alpha_1 + \alpha_2 L = u_j \tag{3.18}$$

Substituting (3.17) into (3.18) yields

$$u_i + \alpha_2 L = u_j$$

or

$$\alpha_2 = \frac{u_j - u_i}{L} \tag{3.19}$$

Substituting (3.17) and (3.19) into (3.16) gives

$$u(x) = \left(1 - \frac{x}{L}\right)u_i + \left(\frac{x}{L}\right)u_j \tag{3.20}$$

which can be rewritten as

$$u(x) = \phi_i(x)u_i + \phi_j(x)u_j \tag{3.21}$$

where

$$\phi_i(x) = \left(1 - \frac{x}{L}\right)$$

$$\phi_j(x) = \left(\frac{x}{L}\right) \quad .$$

Again we may recall this form from chapter two.

Graphically, the shape functions can be depicted as in figure 3.3 below.

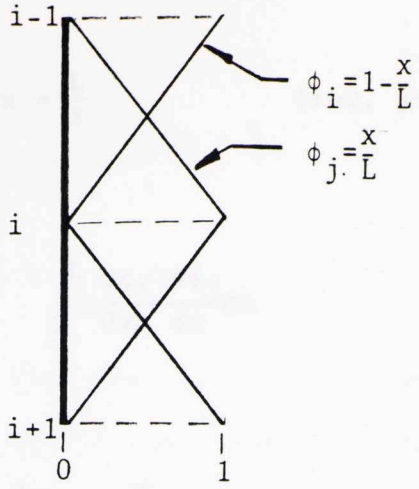

Figure 3.3 - Graphical Illustration of Shape Functions

The first derivatives of $\phi(x)$ also appear in (3.15). These are given as simply

$$\frac{d\phi_i}{dx} = -\frac{1}{L}$$

and

$$\frac{d\phi_j}{dx} = \frac{1}{L} \quad .$$

3.6 Element Matrix Derivation

In order to determine the element matrices given by (3.15), we must evaluate the integrals given there. Matrices [M] and [C] contain the term

$$\int_0^L \phi_i \phi_j dx \quad .$$

Evaluation of this for all combinations of i and j yields

$$\int_0^L \left(1 - \frac{x}{L}\right)\left(1 - \frac{x}{L}\right)dx = \frac{L}{3} \qquad (i=1,\ j=1)$$

$$\int_0^L \left(1 - \frac{x}{L}\right)\left(\frac{x}{L}\right)dx = \frac{L}{6} \qquad (i=1,\ j=2)$$

$$\int_0^L \left(\frac{x}{L}\right)\left(1 - \frac{x}{L}\right)dx = \frac{L}{6} \qquad (i=2,\ j=1)$$

$$\int_0^L \left(\frac{x}{L}\right)\left(\frac{x}{L}\right)dx = \frac{L}{3} \qquad (i=2,\ j=2) \quad .$$

Matrix [K] contains

$$\int_0^L \frac{d\phi_i}{dx}\frac{d\phi_j}{dx}dx$$

which gives

$$\int_0^L \left(-\frac{1}{L}\right)\left(-\frac{1}{L}\right)dx = \frac{1}{L} \qquad (i=1,\ j=1)$$

$$\int_0^L \left(-\frac{1}{L}\right)\left(\frac{1}{L}\right)dx = -\frac{1}{L} \qquad (i=1,\ j=2)$$

$$\int_0^L \left(\frac{1}{L}\right)\left(-\frac{1}{L}\right)dx = -\frac{1}{L} \qquad (i=2,\ j=1)$$

$$\int_0^L \left(\frac{1}{L}\right)\left(\frac{1}{L}\right)dx = \frac{1}{L} \qquad (i=2,\ j=2) \quad .$$

Finally, {f} contains

$$\int_0^L \phi_j dx$$

which results in

$$\int_0^L \left(1 - \frac{x}{L}\right)dx = \frac{L}{2} \qquad (j=1)$$

$$\int_0^L \left(\frac{x}{L}\right)dx = \frac{L}{2} \qquad (j=2) \quad .$$

In matrix form these may be represented as

$$[M]^{(e)} = \rho\int_0^L \phi_i\phi_j dx = \frac{\rho L}{6}\begin{bmatrix} 2 & 1 \\ 1 & 2 \end{bmatrix}$$

$$[C]^{(e)} = \beta\int_0^L \phi_i\phi_j dx = \frac{\beta L}{6}\begin{bmatrix} 2 & 1 \\ 1 & 2 \end{bmatrix}$$

$$[K]^{(e)} = \alpha \int_0^L \frac{d\phi_i}{dx} \frac{d\phi_j}{dx} dx = \frac{\alpha}{L} \begin{bmatrix} 1 & -1 \\ -1 & 1 \end{bmatrix}$$

$$\{f\}^{(e)} = \gamma \int_0^L \phi_j \, dx = \frac{\gamma L}{2} \begin{Bmatrix} 1 \\ 1 \end{Bmatrix} \qquad (3.22)$$

where superscript (e) reminds us that these are element matrices. Note too that in the above expression for $[K]^{(e)}$, the right hand terms in (3.15) do not appear. These terms apply only at the boundary, thus not entering the general element matrix.

These then completely define the element mass matrix, damping matrix, stiffness matrix, and force vector, respectively.

3.7 System Matrix Assembly

The summation or assembly of the element matrices given in (3.22) is a simple process which is best explained through illustration.

Suppose we have a rod discretized into three elements as below.

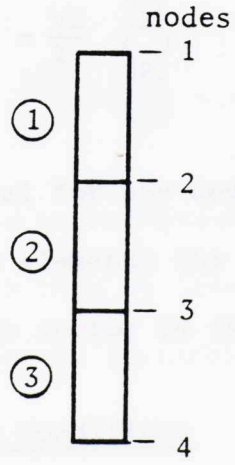

Figure 3.4 - Sample Rod Discretization

where ①, ②, and ③ denote element numbers. Recognize that elements ① and ② share node 2 while ② and ③ share node 3. The element matrices must then overlap at these points. For example, the mass matrix for the rod is assembled as below.

$$[M] = \frac{\rho L}{6}$$

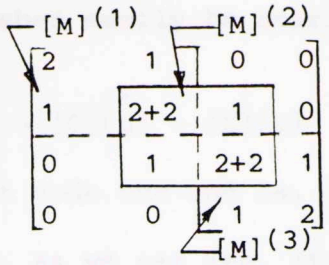

The remaining three matrices are similarly given by

$$[C] = \frac{\beta L}{6} \begin{bmatrix} 2 & 1 & 0 & 0 \\ 1 & 4 & 1 & 0 \\ 0 & 1 & 4 & 1 \\ 0 & 0 & 1 & 2 \end{bmatrix}$$

$$[K] = \frac{\alpha}{L} \begin{bmatrix} 1 & -1 & 0 & 0 \\ -1 & 2 & -1 & 0 \\ 0 & -1 & 2 & -1 \\ 0 & 0 & -1 & 1 \end{bmatrix}$$

and

$$\{f\} = \frac{\gamma L}{2} \begin{Bmatrix} 1 \\ 2 \\ 2 \\ 1 \end{Bmatrix} .$$

This procedure is identical for any degree of discretization desired. We see that for a division into N elements the square matrices are of dimension (N+1) by (N+1) while the column vector is (N+1) by (1).

3.8 Incorporation of Boundary Conditions

Only now does it become necessary to look in detail at the handling of boundary condition terms. As we saw in (3.10), two equations exist, one for each end of the rod. The first dictates that the displacement at the top of the rod (x = 0) must be specified at each time step. As we will see in chapter four, the displacement, velocity, and acceleration will all be known. This being the case, we need only to solve for the uppermost component of the

force vector, {f}. This is accomplished easily be rewriting (3.14) as

$$\{f\} = -[M]\{\ddot{u}\} - [C]\{\dot{u}\} - [K]\{u\} \quad . \tag{3.23}$$

This is done only for the solution at node one and is, in fact, one of the peculiarities in this analysis. But, as we can see, it poses no real problems.

At the bottom of the rod, the latter of (3.10) applies. Looking at the first term we have

$$a' \frac{\partial u}{\partial x} (L,t)$$

which we rewrite as

$$a' \frac{\partial u}{\partial x} (L,t) \simeq u(t)_N \frac{d\phi_1}{dx} + u(t)_{N+1} \frac{d\phi_2}{dx}$$

using the shape functions defined previously. This may be written as

$$a' \frac{\partial u}{\partial x} (L,t) \simeq - \frac{1}{L} u(t)_N + \frac{1}{L} u(t)_{N+1}$$

where N is the number of elements. Using this we rewrite the latter of (3.10) as

$$- \frac{a'}{L} u(t)_N + \frac{a'}{L} u(t)_{N+1} + b' \frac{\partial^2 u}{\partial t^2} (L,t) + c' \frac{\partial u}{\partial t} (L,t) + d'u(L,t) - p(t) = 0 \tag{3.24}$$

In effect this equation is superimposed on the existing equation at the bottom boundary. We accomplish this by inserting coefficients a' through d' into the proper position within the existing system matrices. For example, recall that

$$[M] = \frac{\rho L}{6} \begin{bmatrix} 2 & 1 & 0 & 0 \\ 1 & 4 & 1 & 0 \\ 0 & 1 & 4 & 1 \\ 0 & 0 & 1 & 2 \end{bmatrix} \quad .$$

In (3.24) the coefficient on the $\{\ddot{u}\}$ term is b' so, b' is simply added to the lower right corner of [M] (the position associated with the bottom node).

This gives the corrected [M] as

$$[M] = \frac{\rho L}{6}\begin{bmatrix} 2 & 1 & 0 & 0 \\ 1 & 4 & 1 & 0 \\ 0 & 1 & 4 & 1 \\ 0 & 0 & 1 & 2 + \frac{6b'}{\rho L} \end{bmatrix}$$

where $(6/\rho L)$ accounts for the $(\rho L/6)$ out front. Similarly, the remaining three matrices are

$$[C] = \frac{\beta L}{6}\begin{bmatrix} 2 & 1 & 0 & 0 \\ 1 & 4 & 1 & 0 \\ 0 & 1 & 4 & 1 \\ 0 & 0 & 1 & 2 + \frac{6c'}{\beta L} \end{bmatrix}$$

$$[K] = \frac{\alpha}{6}\begin{bmatrix} 1 & -1 & 0 & 0 \\ -1 & 2 & -1 & 0 \\ 0 & -1 & 2 & -1 \\ 0 & 0 & -1 - \frac{a'L}{L\alpha} & 1 + \frac{a'L}{L\alpha} \end{bmatrix}$$

and

$$\{f\} = \frac{\gamma L}{2}\begin{Bmatrix} 1 \\ 2 \\ 2 \\ 1 - \frac{2p(t)}{\gamma L} \end{Bmatrix} .$$

Clearly, such a treatment readily facilitates the use of any type of boundary condition desired. The identification of coefficients a' through d' will be left to a subsequent discussion.

3.9 Rod Buoyancy

Buoyant forces exerted on the rod have not been mentioned thus far, but any complete analysis must take them into account.

Archimedes first proposed the law of buoyancy in the third century B.C. It states simply that the buoyant force acting on a submerged body is the difference between the vertical component of pressure acting below the surface

and that acting above. No horizontal pressure component can exert a buoyant force. Figure 3.5 depicts a typical lower rod section.

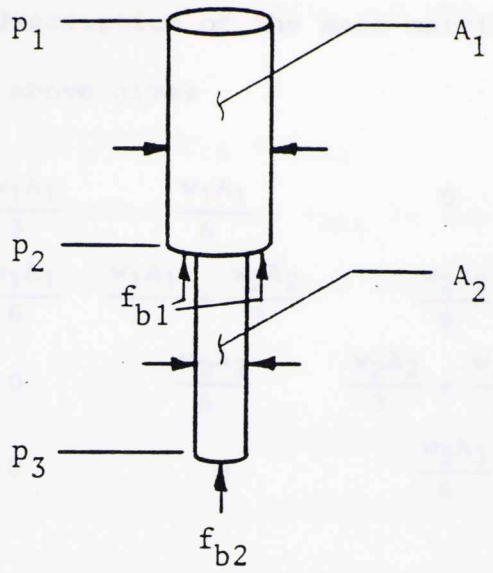

Figure 3.5 - Buoyancy Analysis Notation

From this figure we see that buoyant forces can exist only at the bottom of the rod and at the junction between A_1 and A_2. These forces are simply the product of the acting pressure and the exposed horizontal area. That is, at the rod junction

$$f_{b1} = p_2(A_1 - A_2)$$

while at the bottom

$$f_{b2} = p_3 A_2 \quad .$$

As was the case in handling conventional boundary condition terms, the buoyant forces are added to the appropriate existing matrix terms, this time, to {f}. Note, however, that these forces exist only at nodes where a change in cross section occurs.

3.10 Treatment of Tapered Rod Strings

As one might guess, particularly in light of the preceding discussion, it is desirable to consider rods composed of several different section diameters.

Recalling from (3.7) that

$$\rho = \left(\frac{w}{g}\right)A$$

let's look at the complete description of the mass matrix [M]. Taking $(\rho/6)$ inside and substituting the above gives

$$[M] = \frac{L}{g}\begin{bmatrix} \frac{w_1A_1}{3} & \frac{w_1A_1}{6} & 0 & 0 \\ \frac{w_1A_1}{6} & \frac{w_1A_1}{3}+\frac{w_2A_2}{3} & \frac{w_2A_2}{6} & 0 \\ 0 & \frac{w_2A_2}{6} & \frac{w_2A_2}{3}+\frac{w_3A_3}{3} & \frac{w_3A_3}{6} \\ 0 & 0 & \frac{w_3A_3}{6} & \frac{w_3A_3}{3}+\frac{b'g}{L} \end{bmatrix}.$$

Note that this is still the system matrix from the example of figure 3.4. Now, however, w_1A_1, w_2A_2, and w_3A_3 are products of the weight density and cross sections of elements 1 , 2 and 3 , respectively.

From the above it is clear that the incorporation of varying rod sizes into our finite element model is only a matter of choosing the appropriate coefficients for each of the individual element matrices. In fact, we could just as easily handle rods assembled from different materials. Our only restriction is that any change in geometry must occur at a nodal point. Completely similar conditions exist for each of [C], [K], and {f}.

3.11 Differential Equation Solution

The sections thus far presented in chapter three have defined completely that system of equations given in (3.14). Due to the nature of the boundary conditions we take two approaches to its solution. From section 3.8 we saw that for node one we rewrote (3.14) as

$$\{f\} = -[M]\{\ddot{u}\} - [C]\{\dot{u}\} - [K]\{u\} \quad . \tag{3.23}$$

Because we will know $\ddot{u}$, $\dot{u}$, and u at node one from the pumping unit kinematic analysis (chapter four), the above can be solved immediately for {f(1)}. This component consists of two terms, the body force and the force at the well head known as polished rod load. That is

$$\{f(1)\} = f_{1b} + f_{PRL} \tag{3.25}$$

where f_{1b} is the body force contribution and f_{PRL} is the polished rod load. Body forces being constant, we are able to solve for the polished rod load at each solution iteration.

For the remaining nodes we know the components of {f} but not of $\{\ddot{u}\}$,{u} or {u}. Multiplying (3.14) by the inverse of the mass matrix, $[M]^{-1}$, we have

$$[M]^{-1}[M]\{\ddot{u}\} + [M]^{-1}[C]\{\dot{u}\} + [M]^{-1}[K]\{u\} + [M]^{-1}\{f\} = 0$$

or, after rearranging,

$$\{\ddot{u}\} = - [M]^{-1}[C]\{\dot{u}\} - [M]^{-1}[K]\{u\} - [M]^{-1}\{f\} \quad . \tag{3.26}$$

For simplicity we define

$$[M]^{-1}[C] = [C]^*$$

$$[M]^{-1}[K] = [K]^*$$

and

$$[M]^{-1}\{f\} = \{f\}^*$$

with which (3.26) may be written

$$\{\ddot{u}\} = -[C]^*\{\dot{u}\} - [K]^*\{u\} - \{f\}^* \quad . \tag{3.27}$$

Integrating (3.27) twice with respect to time yields both the velocity and displacement at all remaining nodes. That is

$$\dot{u}_{i+1} = \dot{u}_i + \int \ddot{u}_i dt$$

and

$$u_{i+1} = u_i + \int \dot{u}_i dt$$

where subscript i refers to values at the current time and i+1 to values at $t+\Delta t$.

A fourth order Runge-Kutta integration of $\ddot{u}$ yields the required results (error of order four) without the need for predictions and corrections as in schemes such as Euler's method.

Given $\ddot{u}_i$, $\dot{u}_i$, and u_i, the Runge-Kutta algorithm yields the following (see ref. 5).

$$\dot{x}_{i+1} = \dot{x}_i + \frac{1}{6}(k_1 + 2k_2 + 2k_3 + k_4)$$

and

$$x_{i+1} = x_i + \dot{x}_i \Delta t + \frac{\Delta t}{6}(k_1 + k_2 + k_3)$$

where

$$k_1 = \ddot{u}(u_i, \dot{u}_i)\Delta t$$

$$k_2 = \ddot{u}(u_i + \frac{\Delta t}{2}\dot{u}_i,\ \dot{u}_i + \frac{k_1}{2})\ \Delta t$$

$$k_3 = \ddot{u}(u_i + \frac{\Delta t}{2}\dot{u}_i + \frac{\Delta t}{4}k_1,\ \dot{u} + \frac{k_2}{2})\ \Delta t$$

and

$$k_4 = \ddot{u}(u_i + \dot{u}_i \Delta t + \frac{\Delta t}{2}k_2,\ \dot{u}_i + k_3)\Delta t \quad .$$

Thus we have a complete solution procedure for the dynamic equation, (3.14).

3.12 Closing Remarks

This completes the formulation needed to analyze the dynamic behavior of the sucker rod string. Summarizing briefly, we began with the second order partial differential equation, (3.8), developed from a free body diagram on an arbitrary rod section (figure 3.1). Using the finite element approximation to u(x,t) we reduced this to the set of ordinary differential equations given by (3.14). To this system were added the appropriate boundary condition terms as defined in (3.10) and the effects of rod buoyancy. Finally, rearrangement of (3.14) and integration of $\{\ddot{u}\}$ yielded a method of solution for all previously

unknown physical and dynamical properties.

In order to utilize this model we must now address both the nature of the motion applied via the surface equipment and the forces imposed at the pump. The former constitutes the subject of chapter four.

Chapter 4

PUMPING UNIT KINEMATICS

4.1 Opening Comments

If we are to effectively use the formulation developed in chapter three, we need some mechanism by which to drive the sucker rod/pump combination. This is the function of the surface pumping equipment. There exist essentially two types of mechanisms in common use throughout the petroleum industry. They are classified as the "conventional" and "Mark-II" types as shown in figures 4.1 and 4.2, respectively.

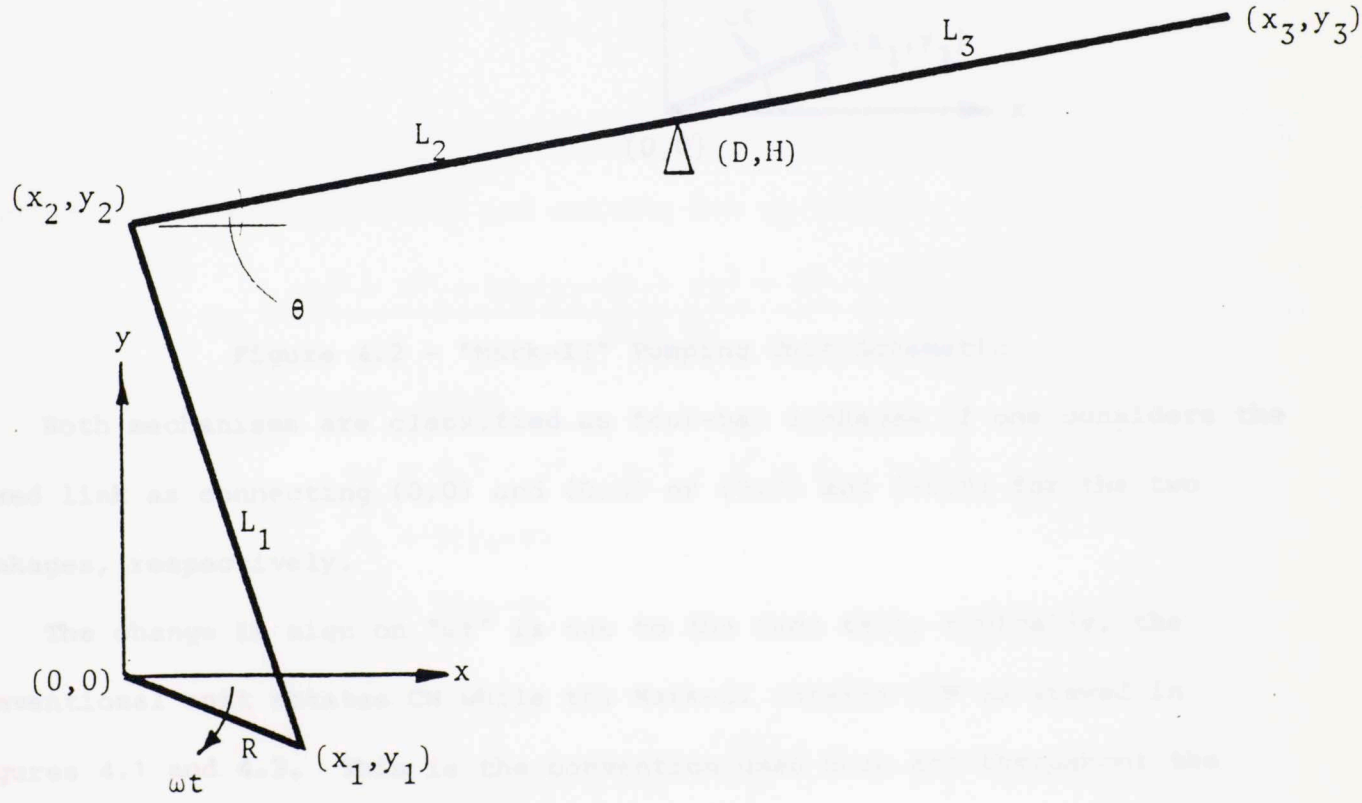

Figure 4.1 - "Conventional" Pumping Unit Schematic

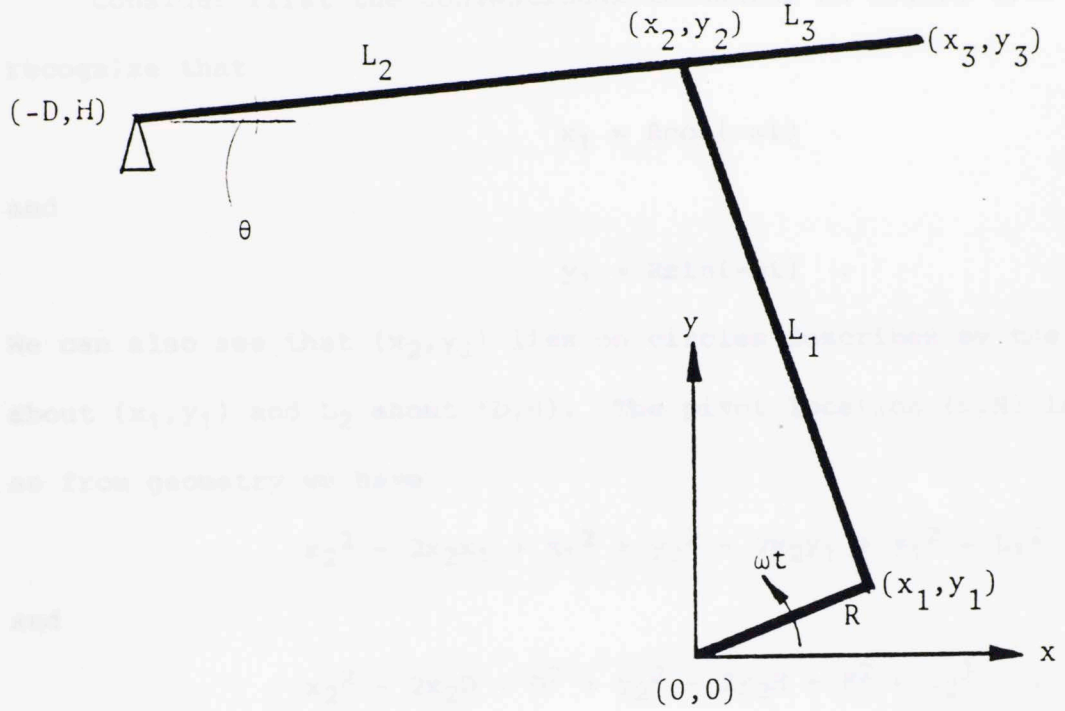

Figure 4.2 - "Mark-II" Pumping Unit Schematic

Both mechanisms are classified as four-bar linkages if one considers the fixed link as connecting (0,0) and (D,H) or (0,0) and (-D,H) for the two linkages, respectively.

The change in sign on "ωt" is due to the fact that, typically, the conventional unit rotates CW while the Mark-II rotates CCW as viewed in figures 4.1 and 4.2. This is the convention used here and throughout the remaining analyses.

4.2 Derivation of the Equations of Motion

Our primary interest is in the motion at (x_3,y_3), however, in the torque analysis in chapter five we will need the positions of (x_1,y_1) and (x_2,y_2) so the following derivation will detail these as well.

Consider first the conventional mechanism in figure 4.1. Immediately we recognize that

$$x_1 = R\cos(-\omega t)$$

and

$$y_1 = R\sin(-\omega t) \quad .$$

We can also see that (x_2,y_2) lies on circles described by the rotation of L_1 about (x_1,y_1) and L_2 about (D,H). The pivot location (D,H) is a known entity, so from geometry we have

$$x_2^2 - 2x_2x_1 + x_1^2 + y_2^2 - 2y_2y_1 + y_1^2 = L_1^2 \qquad (4.1)$$

and

$$x_2^2 - 2x_2D + D^2 + y_2^2 - 2y_2H + H^2 = L_2^2 \quad . \qquad (4.2)$$

Subtracting (4.2) from (4.1) and solving for x_2 yields

$$x_2 = \frac{x_1^2 - D^2 - 2y_2(y_1-H) + y_1^2 - H^2 - L_1^2 + L_2^2}{2(x_1-D)} \quad . \qquad (4.3)$$

If we define replacement terms

$$c_1 = x_1^2 - D^2 + y_1^2 - H^2 - L_1^2 + L_2^2$$

$$c_2 = 2(y_1-H)$$

$$c_3 = 2(x_1-D)$$

we can rewrite (4.3) as

$$x_2 = \frac{c_1}{c_3} - \frac{c_2y_2}{c_3} \quad .$$

Substituting this back into (4.1) and performing a great deal of manipulation yields, upon solving for y_2

y2 =

$$\frac{\frac{2c_1c_2}{c_3^2} + 2y_1 - \frac{2c_2x_1}{c_3} + \sqrt{\left(\frac{-2c_1c_2}{c_3^2} - 2y_1 + \frac{2c_1}{c_3}x_1\right)^2 - 4\left(\frac{c_2}{c_3}+1\right)\left[\left(\frac{c_1}{c_3}\right)^2 + x_1^2 + y_1^2 - \frac{2c_1x_1}{c_3} - L_1^2\right]}}{\left[\left(\frac{c_2}{c_3}\right)^2 + 1\right]^2}$$

Defining additional replacement terms

$$c_4 = \frac{c_1}{c_3}$$

$$c_5 = \frac{c_2}{c_3}$$

and again performing some manipulation, y_2 can be expressed as

$$y_2 = \frac{c_4c_5 + y_1 - c_5x_1 + \sqrt{c_5^2L_1^2 + L_1^2 - (c_5y_1 + x_1 - c_4)^2}}{(c_5^2 + 1)} \quad .$$

Referring again to figure 4.1 we can also write

$$y_3 = H + L_3\sin\theta = H + L_3\left(\frac{H-y_2}{L_2}\right)$$

and

$$x_3 = D + L_3\cos\theta = D + L_3\left(\frac{D-x_2}{L_2}\right) \quad .$$

Summarizing all of the displacement relations for the conventional mechanism we have

$$x_1 = R\cos(-\omega t)$$

$$y_1 = R\sin(-\omega t)$$

$$x_2 = c_4 - c_5\, y_2$$

$$y_2 = \frac{c_4c_5 + y_1 - c_5x_1 + \sqrt{c_5^2L_1^2 + L_1^2 - (c_5y_1 + x_1 - c_4)^2}}{(c_5^2 + 1)} \quad . \qquad (4.4)$$

$$x_3 = D + L_3\left(\frac{D-x_2}{L_2}\right)$$

$$y_3 = H_3 + L_3\left(\frac{H-y_2}{L_2}\right) \quad .$$

Turning our attention to the Mark-II mechanism and referring to figure 4.2 we recognize that

$$x_1 = R\cos(\omega t)$$

and

$$y_1 = R\sin(\omega t) \quad .$$

An analysis completely similar to that for the conventional linkage results in expressions for x_2 and y_2 that are identical to those in (4.4). However, terms c_4 and c_5 are slightly modified and are given by

$$c_4 = \frac{x_1^2 - D^2 + y_1^2 - H^2 - L_1^2 + L_2^2}{2(x_1 + D)}$$

and

$$c_5 = \frac{y_1 - H}{x_1 + D} \quad .$$

From figure 4.2 we see that

$$x_3 = x_2 + L_3\cos\theta = x_2 + L_3\left(\frac{x_2 + D}{L_2}\right)$$

and finally,

$$y_3 = y_2 + L_3\sin\theta = y_2 + L_3\left(\frac{y_2 - H}{L_2}\right) \quad .$$

Because we are interested in all aspects of the behavior at the end of L_3 we need not only its position, but also its corresponding velocity and acceleration. Owing to the fact that $y_3(t)$ is known to be well behaved this writer elected to use finite difference approximations to both $\dot{y}_3$ and $\ddot{y}_3$. As illustrated in chapter two, these expressions are derived from the Taylor-series expansions of y_3 about (t_i). For the sake of accuracy, fourth order central difference expressions are used. These can be found in a number of sources. Reference 5 contains the following:

$$\dot{y}_i = \frac{-y_{i+2} + 8y_{i+1} - 8y_{i-1}\ y_{i-2}}{12(\Delta t)}$$

and

$$\ddot{y}_i = \frac{-y_{i+2} + 16y_{i+1} - 30y_i + 16y_{i-1} - y_{i-2}}{12(\Delta t)^2} \quad .$$

Comparison of results using these approximations with analytical results on equations similar in nature to those describing $y_3(t)$ indicate accuracy to better than two decimal places, or a fraction of one percent.

4.3 Closing Remarks

Completion of the above analysis now allows us, given the physical dimensions of the linkage, to describe completely not only the motion at all joints, but the velocity and acceleration at the top of the rod as well. Upon comparing the notation here with that in chapter three, we have complete equivalence between

$$y_3(t) \text{ and } u(0,t)$$

$$\dot{y}_3(t) \text{ and } \frac{\partial u}{\partial t}(0,t)$$

and between

$$\ddot{y}_3(t) \text{ and } \frac{\partial^2 u}{\partial t^2}(0,t).$$

We now proceed to considerations of the torque imposed on the gearbox and prime mover via the load in the rod string.

Chapter 5

APPLIED TORQUE CHARACTERISTICS

5.1 Opening Comments

The torque imposed on the system drive components arises from two primary sources. First the well load acts through the equivalent pumping unit lever arm and applies a torque directly to the gearbox output shaft. Second, attached to the output shaft are counterweights which also produce an applied torque. The resultant of these two components yields the net torque on the gearbox which is that torque required from the drive motor (when modified by the overall reduction ratio). It may help to refer back to figure 1.1 in considering these effects.

5.2 Torque Factor Derivation

The equivalent pumping unit lever arm mentioned above is known as the "torque factor" throughout the industry. Being a lever arm it has units of length and varies continuously throughout a pumping cycle. Any investigation into the torque characteristics of a given pumping system must begin with a look at this parameter.

As in the discussion on kinematics, we must treat the conventional and Mark-II units separately. Figures 5.1 and 5.2 illustrate the notation required in the derivations which follow. The coordinate systems and coordinate point designations are identical to those in figures 4.1 and 4.2.

Consider, first, the conventional unit. Dimension t_1, t_2, and t_3 are all perpendicular distances from end or pivot points to their respective links. By inspection we see that

$$t_1 = R\sin(180-\gamma) = R\sin\gamma \qquad (5.1)$$

$$t_2 = L_2\sin\phi \qquad (5.2)$$

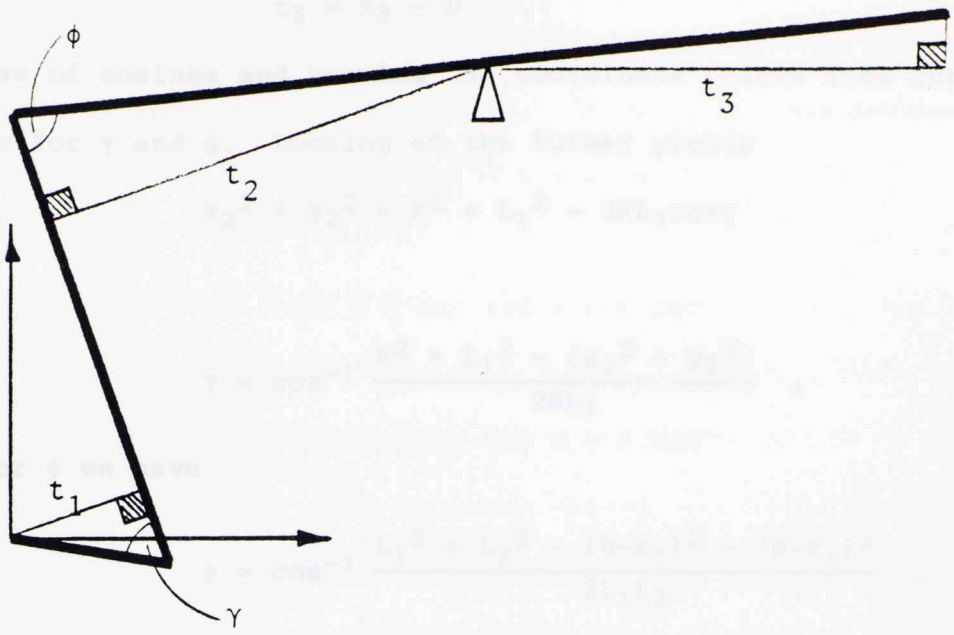

Figure 5.1 - Conventional Unit Torque Factor Notation

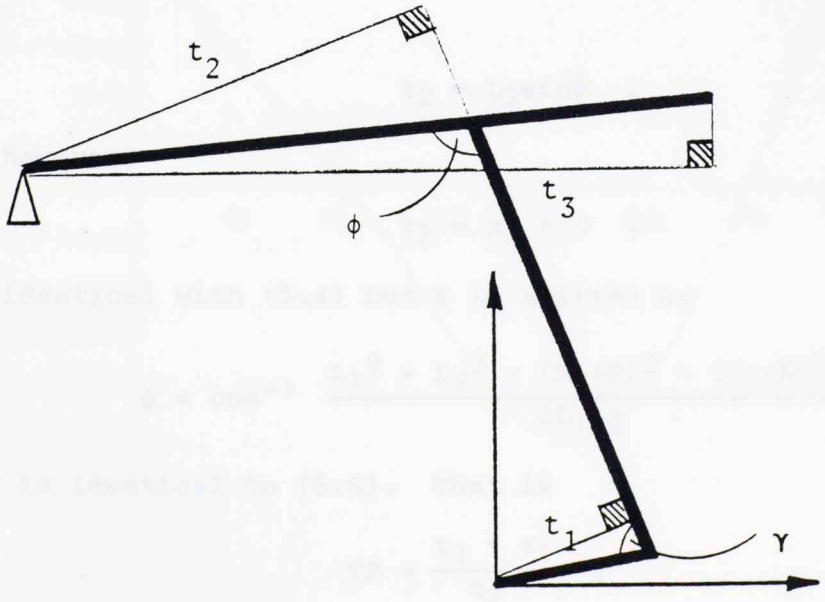

Figure 5.2 - Mark-II Torque Factor Notation

and

$$t_3 = x_3 - D \tag{5.3}$$

Using the law of cosines and knowing the coordinate points from chapter four, we can solve for γ and ϕ. Looking at the former yields

$$x_2^2 + y_2^2 = R^2 + L_1^2 - 2RL_1\cos\gamma$$

or

$$\gamma = \cos^{-1} \frac{R^2 + L_1^2 - (x_2^2 + y_2^2)}{2RL_1} \quad . \tag{5.4}$$

Similarly for ϕ we have

$$\phi = \cos^{-1} \frac{L_1^2 + L_2^2 - (D-x_1)^2 - (H-y_1)^2}{2L_1L_2} \quad . \tag{5.5}$$

The torque factor, TF, is given simply by

$$TF = \frac{t_3 \cdot t_1}{t_2} \quad . \tag{5.6}$$

Looking now at figure 5.2 we see that for the Mark-II we again have

$$t_1 = R\sin\gamma$$

and

$$t_2 = L_2\sin\theta \quad .$$

This time, however,

$$t_3 = x_3 + D \quad . \tag{5.7}$$

Angle γ is identical with (5.4) but ϕ is written as

$$\phi = \cos^{-1} \frac{L_1^2 + L_2^2 - (x_1+D)^2 - (y_1-H)^2}{2L_1L_2} \quad . \tag{5.8}$$

Finally, TF is identical to (5.6). That is

$$TF = \frac{t_3 \cdot t_1}{t_2} \quad .$$

It may not be obvious from the above expressions, but the torque factor for any given unit is a periodic function taking both positive and negative values. Since torque is defined by the "right hand rule", any well load which produces a torque out of the page (ref. figures 5.1 and 5.2) is positive.

Using this convention, the unit in figure 5.1 is shown in a positive torque factor position. Figure 5.2 shows a negative position. The sign of the torque factor is governed by the angle γ. In fact, for the conventional unit

$$TF \geq 0 \text{ for } 0 \leq \gamma \leq 180°$$

and

$$TF \leq 0 \text{ for } 180 \leq \gamma \leq 360°$$

whereas for the Mark-II

$$TF \geq 0 \text{ for } 180 \leq \gamma \leq 360°$$

and

$$TF \leq 0 \text{ for } 0 \leq \gamma \leq 180°.$$

Figure 5.3 shows a typical plot of the torque factor as a function of crank position.

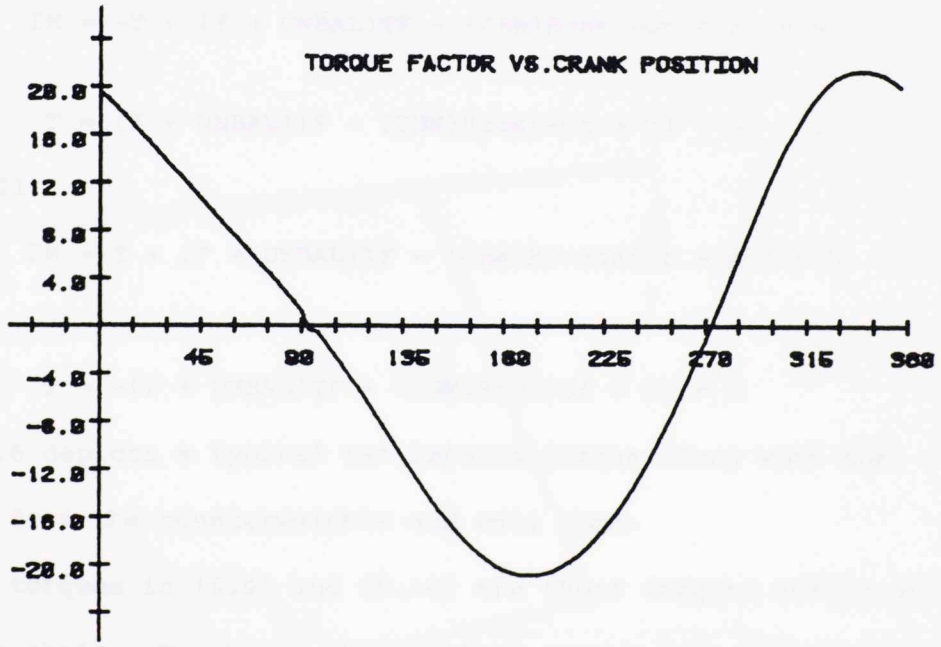

Figure 5.3 - Typical Torque Factor Curve

5.3 Torque Analysis

Figures 5.4 and 5.5 show the additional notation necessary in discussing the torques applied to the system from all sources. Again, notation common to earlier discussions is identical with these.

Briefly, the load applied at the end of L_3 is the combination of the well load, F, and the unbalance load, UNBAL. The latter is the structural unbalance of the unit and is taken as positive for "horsehead heavy" mechanisms. The counterbalance weight, CBW, are assumed to act at a distance, R, from the crank centerline. The angle, β, allows the counterweights to be "phased" with respect to the crank arm, and is defined as positive CCW from the crank arm centerline.

With these thoughts in mind, we can now sum moments about the output shaft center. For the conventional unit

$$\Sigma M = -T + (F + UNBAL)TF - (CBW)R\cos(-\omega t + \beta) = 0$$

or

$$T = (F + UNBAL)TF - (CBW)R\cos(-\omega t + \beta) = 0 \quad . \tag{5.9}$$

For the Mark-II

$$\Sigma M = T + (F + UNBAL)TF - (CBW)R(-\cos(\omega t + \beta)) = 0$$

or

$$T = -(F + UNBAL)TF + (CBW)R\cos(\omega t + \beta) = 0 \tag{5.10}$$

Figure 5.6 depicts a typical net imposed torque along with the contributions from the counterweights and well load.

Note the torques in (5.9) and (5.10) are those torques acting on the gearbox output shaft. To obtain the required torque from the drive motor, we simply divide this by the overall speed reduction ratio. That is

$$T_m = \frac{T}{RATIO} \tag{5.11}$$

where T_m is the motor torque delivered. The above neglects losses through the belt drive and gearbox.

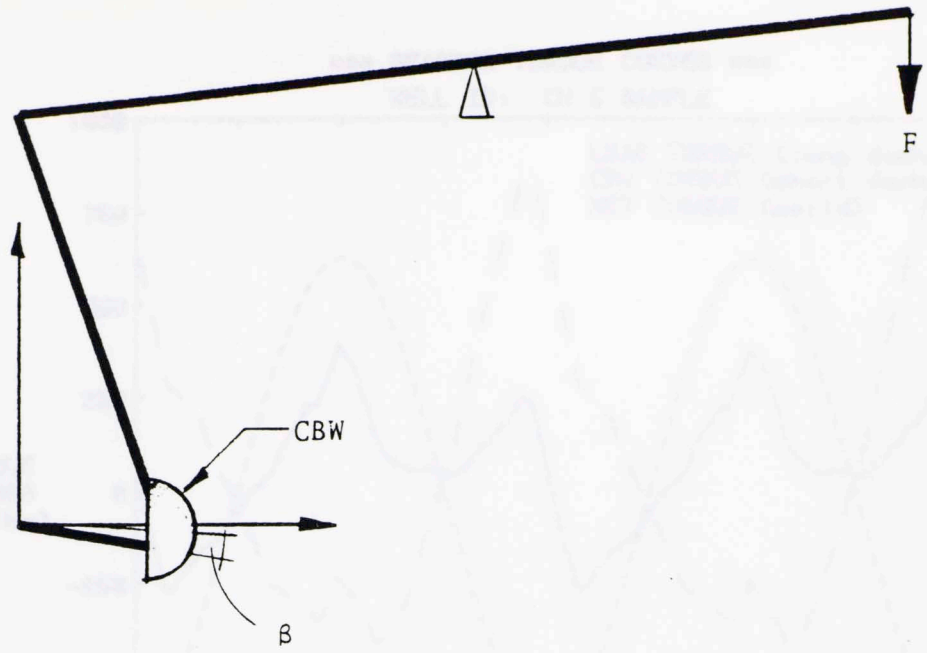

Figure 5.4 - Conventional Unit Torque Notation

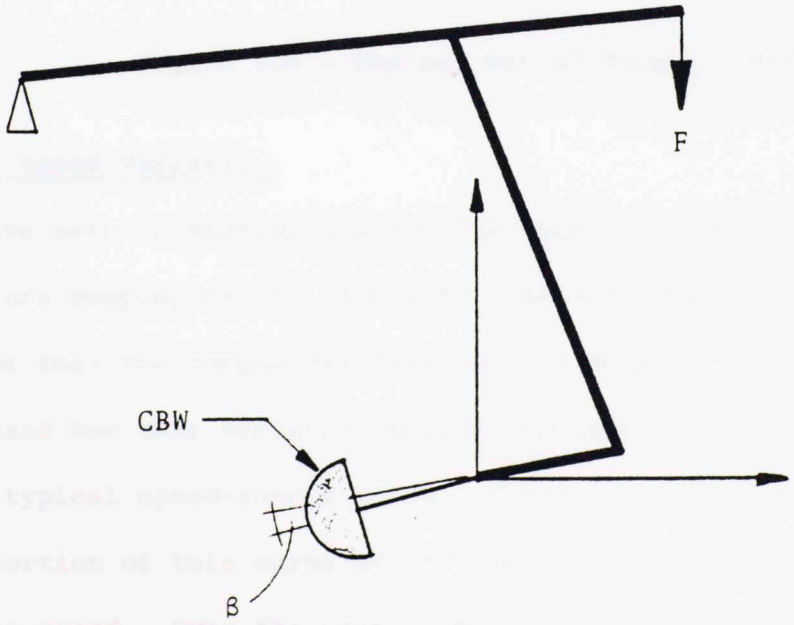

Figure 5.5 - Mark-II Torque Notation

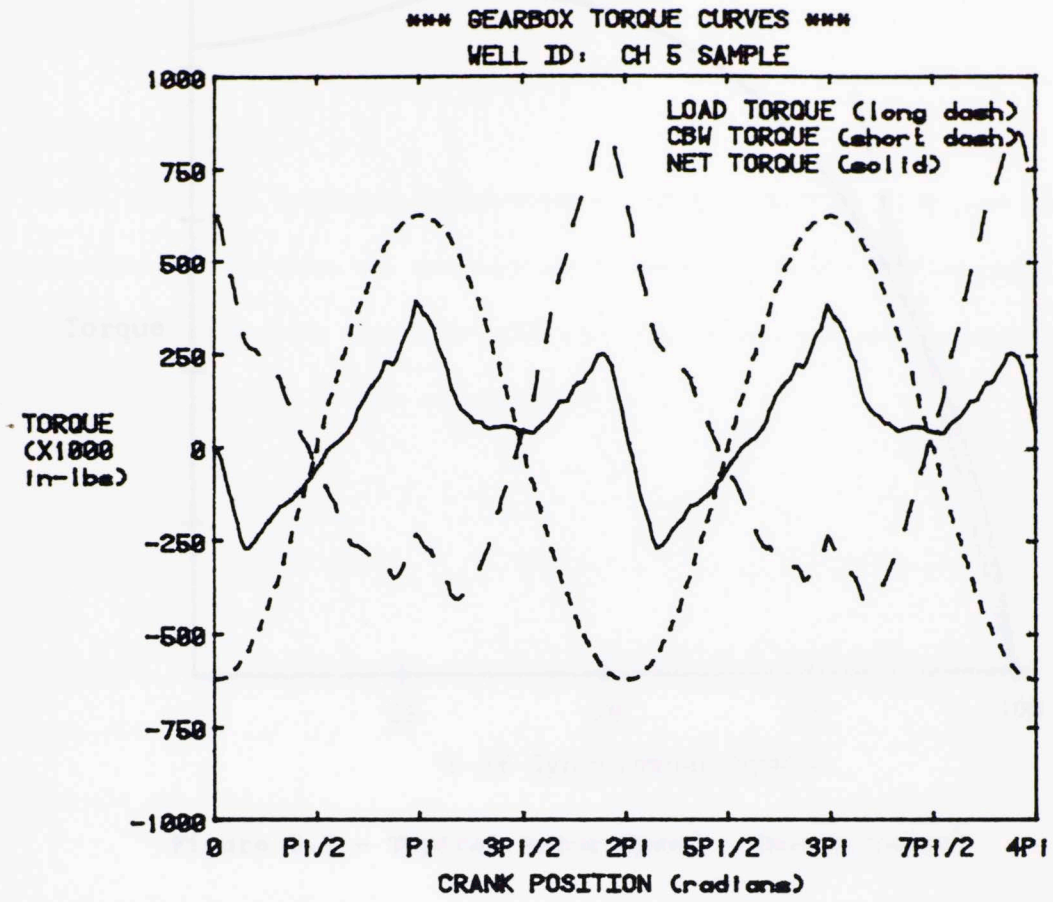

Figure 5.6 - Typical Set of Torque Curves

5.4 Motor Speed Variation

We have seen in section 5.3 how the torque on the system varies over the course of one pumping cycle. Assuming that the reduction ratio is constant, we conclude that the torque delivered by the motor must also vary. In order to understand how this variation affects the motor speed, it is instructive to look at a typical speed-torque curve. Figure 5.7 shows such a curve.

The portion of this curve of interest is roughly that from 100% to 80% of synchronous speed. Over the course of this range the torque can be approximated as a linear function of speed as shown by the dashed line. This is common practice and allows us to readily compute the motor speed, given the

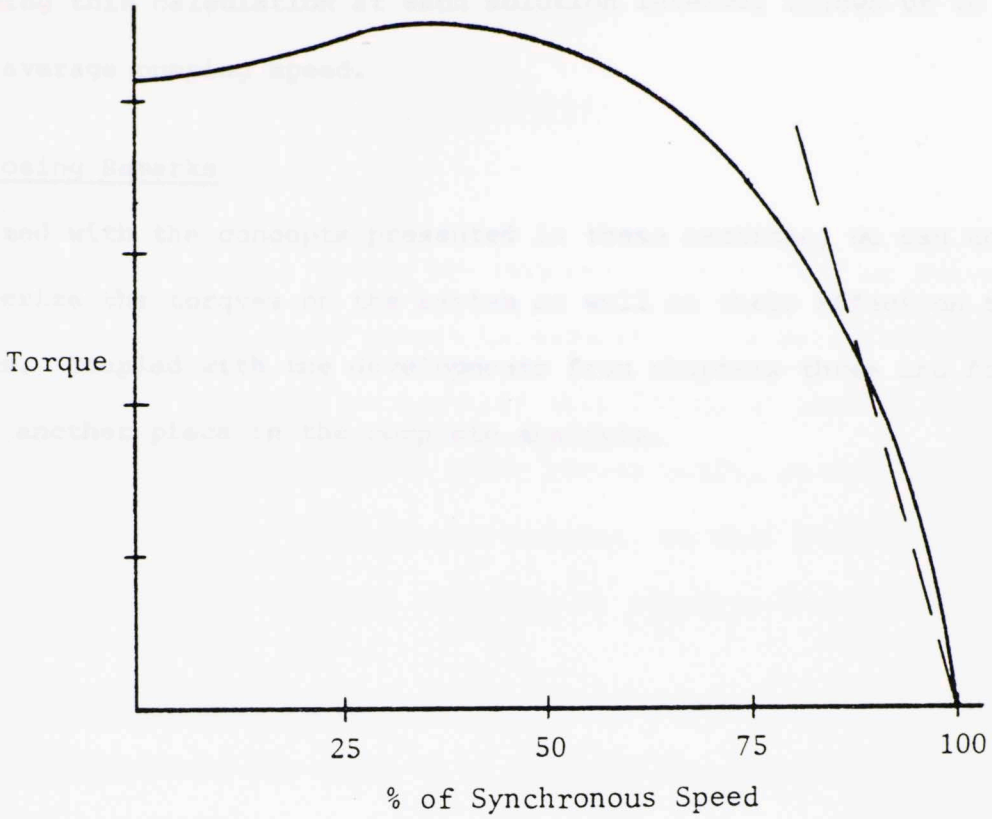

Figure 5.7 - Typical Motor Speed - Torque Curve[1]

output torque. For example, suppose the instantaneous required torque is 18000 in-lb, the synchronous speed is 1200 RPM, and the torque at 1000 RPM is 20000 in-lb. We want to know the instantaneous speed. A linear interpolation gives the following:

Speed (RPM)	Torque (in-lb)
1200	0
RPM?	18000
1000	20000

$$\text{RPM?} = \left(\frac{18000-0}{20000-0}\right)(1000-1200) + 1200$$

or

$$\text{RPM?} = 1020 \text{ RPM} \quad .$$

---

[1]Courtesy of Westinghouse Electric Corp., Buffalo, NY

Performing this calculation at each solution interval allows us to keep track of the average pumping speed.

5.5 Closing Remarks

Armed with the concepts presented in these sections, we can now characterize the torques on the system as well as their effect on the dynamics. Coupled with the developments from chapters three and four they provide another piece in the complete analysis.

Chapter 6

FLUID DAMPING

6.1 Opening Comments

As outlined in chapter three, the damping force exerted on the rod by its relative motion with the fluid column is developed by a skin friction effect at the rod surface. In order to quantify this force, we look at the nature of annular pipe flow, specifically the shear stress acting at the inner boundary. Rather than flow through a conventional annulus, we will look at the case where the center section has some velocity, v, relative to the outer wall.

6.2 Derivation of Shear Stress

Figure 6.1 depicts the model to be used and the required notation. We look in detail at the fluid shell of thickness Δr.

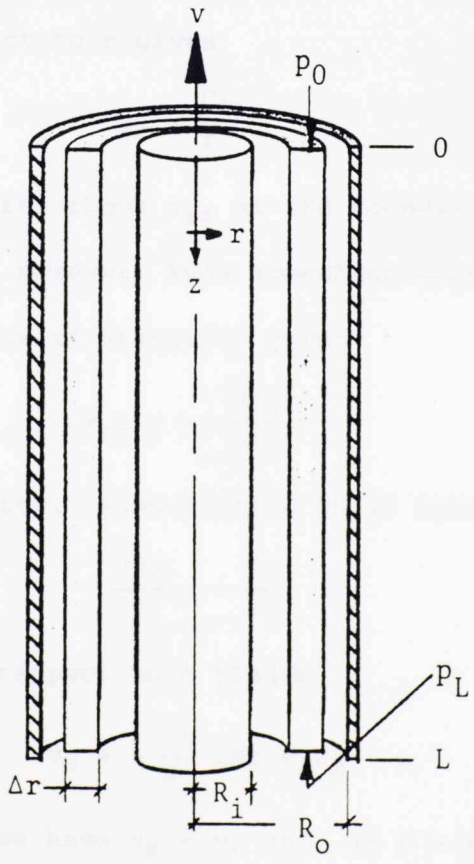

Figure 6.1 - Annular Flow Model

A momentum balance on the fluid shell yields

$$(2\pi rL\tau_{rz})\big|_r - (2\pi rL\tau_{rz})\big|_{r+\Delta r} + (2\pi r\Delta r\gamma v_z^2)\big|_{z=0} - (2\pi r\Delta r\gamma v_z^2)\big|_{z=L} + 2\pi r\Delta rL\gamma g + 2\pi r\Delta r(p_o - p_L) = 0 \tag{6.1}$$

If we assume an incompressible fluid then v_z at z = o and z = L are equal so terms three and four drop out. Dividing by $2\pi L\Delta r$ and taking the limit as $\Delta r \to 0$ gives

$$\lim_{\Delta r\to 0} \frac{(r\tau_{rz})\big|_{r+\Delta r} - (r\tau_{rz})\big|_r}{\Delta r} = \left(\frac{p_o - p_L}{L} + \gamma g\right)r$$

or

$$\frac{d(r\tau_{rz})}{dr} = \left(\frac{p_o - p_L}{L} + \gamma g\right)r \quad . \tag{6.2}$$

Taking $p_o = 0$ (pressure at the surface) and recognizing that $p_L = \gamma gL$, we may eliminate the right hand side of (6.2). We are left with

$$\frac{d(r\tau_{rz})}{dr} = 0 \quad .$$

Integrating once with respect to r gives

$$\tau_{rz} = \frac{C_1}{r} \quad . \tag{6.3}$$

Unfortunately, we know nothing about τ_{rz} at the boundaries which would allow us to determine C_1. We do, however, know something about the velocities at both R_i and R_o. Newton's law of viscosity gives

$$\tau_{rz} = -\mu \frac{dv_z}{dr} \tag{6.4}$$

where μ is the fluid viscosity. Substituting (6.4) into (6.3) gives us

$$\frac{dv_z}{dr} = -\frac{C_1}{\mu r} \quad .$$

Integrating once more with respect to r yields

$$v_z = -\frac{C_1}{\mu} \ln r + C_2 \quad .$$

Recognizing that at $r = R_i$ we have $v_z = v$, and at $r = R_o$, $v_z = 0$, we can solve for C_1 and C_2 as follows.

at $R = R_i$ $$v = -\frac{C_1}{\mu} \ln R_i + C_2 \qquad (6.5)$$

at $r = R_o$ $$0 = -\frac{C_1}{\mu} \ln R_o + C_2 \qquad (6.6)$$

Subtracting (6.6) from (6.5) gives

$$v = -\frac{C_1}{\mu} \ln\left(\frac{R_i}{R_o}\right)$$

or

$$C_1 = -\frac{v\mu}{\ln\left(\frac{R_i}{R_o}\right)} \quad . \qquad (6.7)$$

Substituting (6.7) into (6.6) and solving for c_2 we have

$$C_2 = -\frac{v \ln R_o}{\ln\left(\frac{R_i}{R_o}\right)}$$

or finally

$$v_z = \frac{\ln\left(\frac{r}{R_o}\right)}{\ln\left(\frac{R_i}{R_o}\right)} v \quad . \qquad (6.8)$$

Recalling that v is the rod velocity, (6.8) gives us the fluid velocity at any position, r.

Again referring to (6.4) we can derive an expression for τ_{rz} based on (6.8). This yields

$$\tau_{rz} = -\mu \frac{d}{dr}\left[\frac{\ln\left(\frac{r}{R_o}\right)}{\ln\left(\frac{R_i}{R_o}\right)}\right] v$$

or

$$\tau_{rz} = -\frac{\mu v}{r \ln\left(\frac{R_i}{R_o}\right)} \quad .$$

At the rod surface where $r = R_i$ this gives

$$\tau_{rz} = -\frac{\mu v}{R_i \ln\left(\frac{R_i}{R_o}\right)} \quad . \qquad (6.9)$$

In chapter three we derived the damping force in terms of a damping factor, c, as

$$f_d = 2c\sqrt{A\pi}\ \Delta x \frac{\partial u}{\partial t} \quad . \tag{3.4}$$

Using τ_{rz} and referring to figure 3.1, the equivalent force will be given by

$$f_d = 2\tau_{rz}\sqrt{A\pi}\ \Delta x \tag{6.10}$$

Equivalence requires that

$$c = \frac{\tau_{rz}}{v} \tag{6.11}$$

where we recall that $\frac{\partial u}{\partial t}$ is simply v from the above discussion. Substituting (6.9) into (6.11) gives the final form for c as

$$c = -\frac{\mu}{R_i \ln\left(\frac{R_i}{R_o}\right)} \quad . \tag{6.12}$$

The required units on μ in (6.12) are $lb_f\text{-sec/in}^2$.

6.3 Closing Remarks

It should be noted that the momentum balance given by (6.1) is valid only for laminar flow. A quick check of the Reynolds number for a typical configuration yields the following.

Let

$$R_i = 0.5 \text{ in}$$

$$R_o = 1.0 \text{ in}$$

$$v_z = 30 \text{ in/sec}$$

$$\gamma = 8.2 \times 10^{-5}\ lb_m\text{-sec}^2/\text{in}^4$$

$$\mu = 1.5 \times 10^{-6}\ lb_f\text{-sec/in}^2 \quad (10cp).$$

The Reynolds number is given by (see ref. 4, page 54)

$$R_e = \frac{2R_o\left(1 - \frac{R_i}{R_o}\right) v_z \gamma}{\mu}$$

which yields

$$R_e = 1640 \quad .$$

This is well below the transition Reynolds number of 2100 so our assumption of laminar flow is valid.

Chapter 7

DOWN-HOLE CONSIDERATIONS

7.1 Opening Comments

Sections 3.3 and 3.8 served as introductions to the subject of the boundary conditions which apply at the ends of the rod string. The surface condition was treated adequately there when coupled with the developments in chapter four. Several unaddressed questions remain regarding the bottom-hole conditions. Specifically, we need to look in detail at the loading function, p(t), and coefficients a' through d' in (3.10). This section expands upon earlier discussions on this bottom boundary condition. Reiterating, the latter of (3.10) is repeated here.

$$a'\frac{\partial u}{\partial x}(L,t) + b'\frac{\partial^2 u}{\partial t^2}(L,t) + c'\frac{\partial u}{\partial t}(L,t) + d'u(L,t) - p(t) = 0 \quad (3.10)$$

where

a',b',c',d' = non-negative coefficients
p(t) = prescribed pump loading condition

7.2 Pump Action Analysis

In order to understand the loading function, p(t), it is helpful to look at figure 7.1 which illustrates the four stages involved in rod loading. Recall from figure 1.1 the existence of the standing and traveling values.

Figure 7.1a depicts the period at bottom dead center when the load is being transferred from the tubing to the rod. The traveling valve is closing causing the full weight of the fluid to bear on the tubing string. The standing value is ready to open. In (b) the rod is moving up, bearing the full weight of the fluid column. The traveling valve is closed, the standing valve is open. It should be noted that while the standing valve is open, any

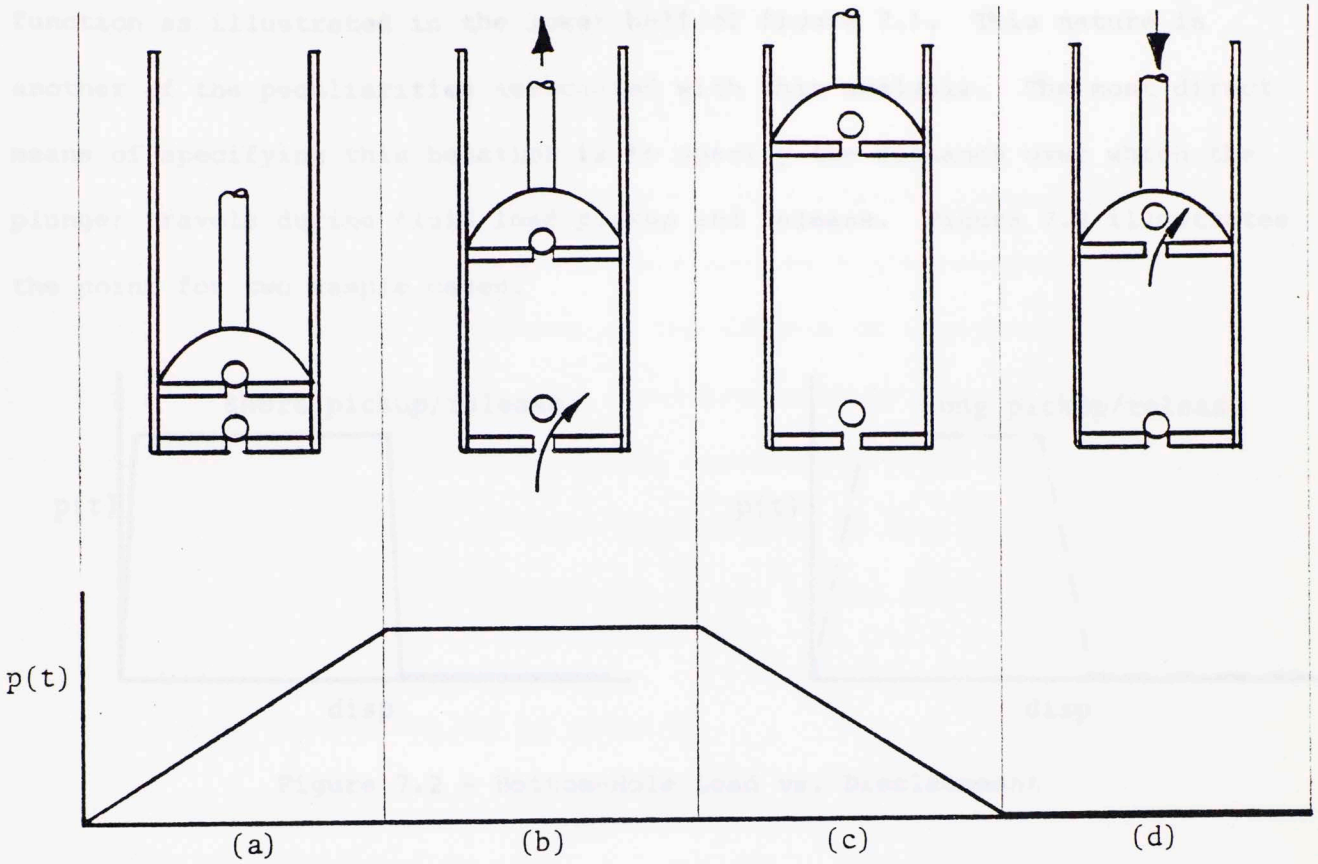

Figure 7.1 - Four Stages of Pump Action

pressure due to a fluid level in the casing acts directly on the underside of the plunger. The net rod load, p(t), in (b) is given by

$$p(t) = \text{TOPFOR} - \text{BOTFOR}$$

where

TOPFOR = fluid pressure above plunger times plunger area
BOTFOR = bottom-hole pressure times plunger area

Figure 7.1c illustrates the top dead center position at which load begins transferral back to the tubing. The traveling value begins to open, the standing valve begins to close. Finally, (d) shows the rod on its way down, moving freely through the fluid. The traveling valve is open, the standing valve is closed. In (d), p(t) = 0. Following (d) the cycle repeats.

From this description of the cycle we see that p(t) is a periodic function as illustrated in the lower half of figure 7.1. This nature is another of the peculiarities associated with this analysis. The most direct means of specifying this behavior is to specify the distance over which the plunger travels during fluid load pickup and release. Figure 7.2 illustrates the point for two sample cases.

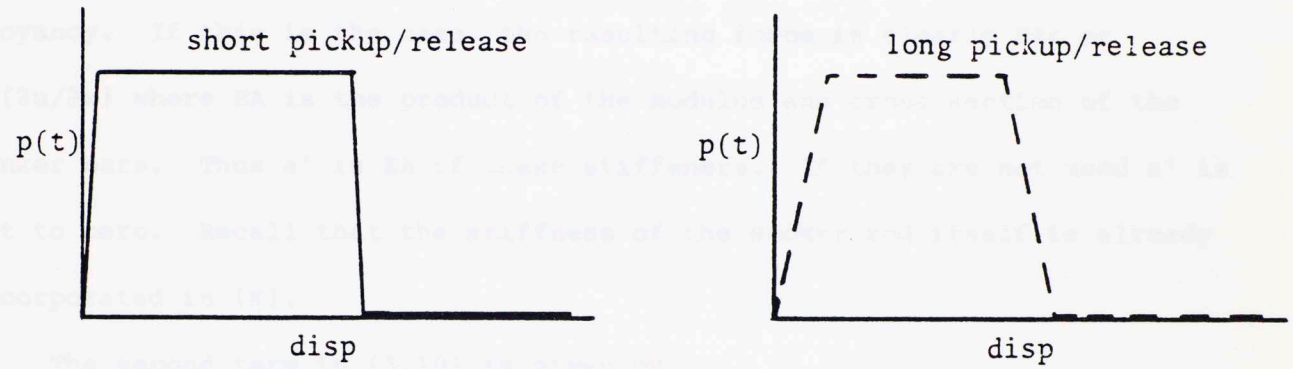

Figure 7.2 - Bottom-Hole Load vs. Displacement

The value of p(t) at any point during pickup (or release) is obtained by taking the ratio of Δu for the current interval to the total pickup (or release) distance, times the quantity (TOPFOR-BOTFOR). That whole quantity is then added to the previous p(t) as an incremental change in pump load. During the remainder of the up/downstrokes, the loads are as defined earlier.

The determination of these pickup and release distances is based upon whether or tubing anchors are installed and, if not, on the tubing size, fluid weight, etc.. For the anchored case, illustrated by the dashed curve, the distances, which can be as great as 2 ft., are determined from the static tube deflection due to fluid weight.

7.3 Boundary Condition Coefficients

As one of the last loose ends to tie up, we address coefficients a' through d' in (3.10). Referring to the latter of (3.10), this explanation is

best served by looking in detail at each term individually.

The first of these is

$$a' \frac{\partial u}{\partial x} (L,t) \quad .$$

This is simply a stress generated force on any stiffness element added at the pump. For example, stiffeners known as sinker bars are sometimes added to the bottom of the sucker rod to counteract the effects of compressive loads due to buoyancy. If this is the case, the resulting force is clearly $EA\varepsilon$ or $EA(\partial u/\partial x)$ where EA is the product of the modulus and cross section of the sinker bars. Thus a' is EA of these stiffeners. If they are not used a' is set to zero. Recall that the stiffness of the sucker rod itself is already incorporated in [K].

The second term in (3.10) is given by

$$b' \frac{\partial^2 u}{\partial t^2} (L,t) \quad .$$

In this term b' is nothing more than the mass of the fluid column. The only special consideration needed is the determination of when this term applies. On upward acceleration it clearly exists. On deceleration the mass is uncoupled and b' goes to zero. Likewise, on the downstroke the fluid weight, and hence mass, is borne by the tubing. During this part of the cycle b' is again set to zero.

The damping term

$$c' \frac{\partial u}{\partial t} (L,t)$$

is probably the one for which we have the most intuitive feel. Fluid friction exists at all points in the cycle. On the upstroke there is drag between the plunger and pump body as well as a damping effect from fluid flow through the standing valve. On the downstroke, plunger drag again exists as does damping through the traveling valve. The combined factor c' takes these effects into account.

Finally, the last term

$$d'u(L,t)$$

allows one to apply a force as strictly a function of plunger displacement. Frankly, it is not clear that d' has immediate physical significance. In this analysis it is set to zero but included to maintain generality. The intent of this work was not to identify precisely all of these coefficients. It is hoped that at some future time, experimental data will be available to either corroborate or redefine their significance.

A similar argument holds for c'. Although its meaning seems straightforward, its magnitude is not known exactly. For this work it is assumed to be related to fluid viscosity much like the rod damping discussed previously.

7.4 Closing Remarks

With these thoughts, we close the bulk of the analysis required in the solution to the problem posed in chapter one. The discussion which follows addresses the implementation of solution techniques and results from selected design situations.

CHAPTER 8

DATA REDUCTION

8.1 Opening Comments

In any analysis with the scope of that presented in the previous chapters, one is faced with the task of selecting how one wishes to view the results. The data selected should be both indicative of the behavior of the system being analyzed and informative. Clearly, we don't want results which are obscured by ambiguous display. The following discussions deal with those forms of data reduction chosen for the analysis in chapters three through seven.

8.2 Forms of Data Presentation

As in most engineering problems, we would ultimately like some graphical output from our solution. Numerical values, although sometimes more precise, don't represent a visual picture of system behavior. Nor do they make comparisons between various cases as meaningful as they might be. In the output from the sucker rod dynamic analysis, we will display numerically only some chosen extreme values for certain system characteristics, e.g., maximum stresses, max/min torques and pumping speeds, etc. The bulk of the output will be graphical.

The standard form of system response throughout the petroleum industry is known as a dynagraph. Its origin dates back to the early days of modern sucker rod pumping. A dynagraph is generated by attaching a load cell in line with the polished rod. The output from the load cell, coupled with a means of recording the position of the rod, produces a load vs. displacement plot analogous to a lissajous pattern common in electrical circuit analysis. Figure 8.1 shows a typical dynagraph from an actual well study.

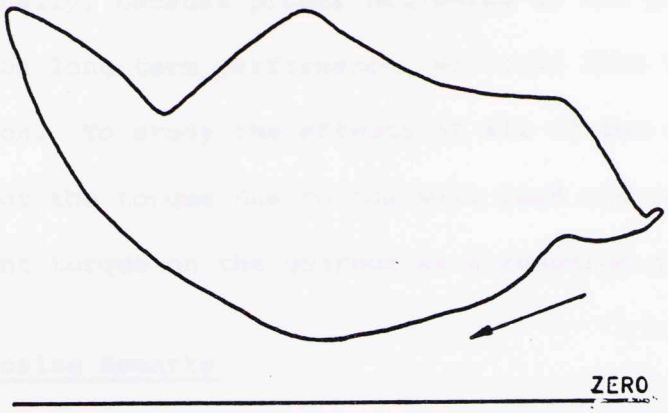

MAX LOAD	16,200 LB
MIN LOAD	2,700 LB
RANGE	13,500 LB
SPEED	23 SPM
STROKE	64 IN.
POL ROD HP	27.5
ENGINE RPM	940
TIME	4:00 PM

Figure 8.1 - Dynagraph Card

It is not clear that the dynagraph form of data presentation is the most useful way of displaying load results, but it is widely used and well understood. Therefore, a dynagraph will be simulated in this analysis as a means of bridging the technology gap in sucker rod dynamics.

One would also like to know the effects of pumping unit behavior on induced rod stresses. Because two pumping mechanisms which generate the same stroke length can do so in different ways, e.g., they may have different durations for the up/down strokes. It is natural to assume that the resulting rod stresses will also be different. As a result, we will plot the acceleration at the top of the rod and the rod stress vs. position. Such information could be used in optimization of minimum rod stress for a given desired stroke.

Some interest has been proposed in developing the load transfer characteristics of the sucker rod. Although this is not the intent of this analysis, it is a simple matter to provide this information as a starting

point for future investigations. Essentially this amounts to little more than displaying the dynagraph data in a more conventional format.

Finally, because proper balancing of the pumping unit has a dramatic effect on long term performance, we would like to know precisely its balance condition. To study the effects of all of the various torque components, we will plot the torque due to the well load and counterweights as well as their resultant torque on the gearbox as a function of crank position.

8.4 Closing Remarks

The four forms of data presentation described should provide not only some continuity with existing analysis but adequate information on which to judge any proposed design as well. The various plots described will be included in sample analyses in the following sections and in the appropriate appendices.

CHAPTER 9

SOLUTION DEVELOPMENT AND UTILIZATION

9.1 Opening Comments

It should be clear by now that the computations and analyses presented in the preceding sections do not lend themselves to hand manipulation. For this reason, a computer program called "DYNA1" has been written which performs the required operations. DYNA1 is written in FORTRAN 77 and is presently being run interactively on a VAX 11/780 computer. The source code occupies approximately 100 blocks (50K) including the graphics subroutines. PLOT10 subroutines from Tektronix produce binary output which drives any of their 4000 series graphics terminals.

9.2 Program Synopsis

DYNA1 consists of a main routine and twenty-one subroutines each of which handles one aspect of the previous analyses. The main routine acts as the coordinator for these subroutines as well as variable initializer and output controller. In addition, it keeps tabs on max/min values of pertinent parameters. Below is a list of all subroutines and a brief description of their function.

ASSEMB: assembles system matrices [M], [C], and [K] from individual element matrices . . . entry ASSEMF assembles the force vector {f}

DATGEN: interactively creates input data file "DATSET"

DYNAGR: plots surface and pump load data in dynagraph format

ECHO: echoes input data to file "SUMMARY"

INCOND: generates the initial conditions on $\ddot{u}$, $\dot{u}$, u

INVERT: inverts [M] (or any square matrix)

LINK: calculates the displacement, velocity, and acceleration at the top of the rod based on pumping unit geometry

LOADGR: plots surface and pump loads vs. crank position

MESH: generates the mesh connectivity data and the x-coordinates of all nodal points

MSPEED: calculates the motor speed based on torque requirements

MULT: multiplies two matrices . . . entry VMULT multiplies a matrix times a vector

PLOAD: determines pump plunger position and the corresponding load p(t)

RKUTT: integrates $\ddot{u}$ to find $\dot{u}$ and u (4th order Runge-Kutta)

SHAPE: defines and initializes shape function matrices $[\phi]$ and $[d\phi/dx]$

SIGRAF: plots rod stress and top acceeleration vs. crank position

SOLVE: solves the system of ODE's for {f(1)} and $\{\ddot{u}\}$

STRESS: solves for element stresses at each iteration based on end point displacements

TORQF: calculates the torque factor of the pumping unit based on its present position

TORQGR: plots the torques due to well load and counterweights and their resultant vs. crank position

TORQUE: calculates gearbox and motor torques given polished rod load, torque factor, and reduction ratio

UPDATE: adds boundary condition terms to system matrices and updates $[M]^{-1}$, [C]*, and [K]* when necessary

It should be clear from the above that each point of the preceding analyses has been suitably addressed. The liberal use of subroutines not only tends to make a program more readable but also allows revisions to be made more readily.

As mentioned in section 9.1, DYNA1 is an interactive program. If a data file exists ("DATSET") the user responds with an "f" (file) when prompted.

The program will then read the input data file and begin computations. If a data file does not exist or if a new set of input is desired, the user responds with an "i" (interactive) when prompted. DYNA1 will then prompt for all required input. At the same time, a new file, "DATSET", will be written automatically, superseding any that might have already existed.

In addition to the plotted output, there are potentially three output data files generated. The first, called "DIAGNOS", is written only if requested. It provides some diagnostic output should results be suspect for some reason. The second output file, called "SUMMARY" is always written and supersedes any that previously existed. It contains a list of the input data as well as a summary of final results. A third file, "PLTDAT", is generated when plotted output is desired. It is read by the various plot routines but is otherwise transparent to the user.

When plotted output is desired, four binary files are written, "DYNAPLOT", "LOADPLOT", "SIGPLOT", and "TORQPLOT". They contain the dynagraph, load, stress, and torque plot, respectively. They must be output to a Tektronix 4000 series graphics terminal. Otherwise, useless garbage will be displayed on the screen (at best).

9.3 Input Data Requirements

As mentioned in section 9.2, DYNA1 will prompt for required input data. Briefly, that data is listed below.

Well Identification:	20 characters, self explanatory
Diagnostics/Plot Flags:	1 = yes, 0 = no . . . one response for each
Rod Length:	enter length in feet
Plunger Diameter:	enter diameter in inches
No. of Different Rod Diameters:	enter 1 through 5 as required

Diameter, Begin/End Element:	enter the diameter of each rod size plus the beginning and ending element number (see discussion later in this section)
Tubing Anchor Flag:	1 = anchored, 0 = unanchored
Tubing OD:	enter tube OD in inches if tubing is unanchored
Fluid Height and Specific Gravity:	enter the casing fluid height above the plunger in feet and the specific gravity of the fluid
Linkage Parameters:	enter linkage type, 1 = conventional, 2 = Mark II, and the dimensions D, H, L_1, L_2, L_3 and R in inches (see figures 4.1 and 4.2)
Desired Strokes per Minute:	typically 5 through 20
Motor Speed Variation Flag:	1 = variable speed, 0 = constant speed
Counterweights, Phase Angle, Unbalance:	enter the weight of the counterbalance in pounds, angle β in degrees (see figures 5.4 and 5.5, and the structural unbalance in pounds ("+" for horsehead heavy units)
Synchronous Speed and Slip Speed/ Torque:	if motor speed is variable, enter the synchronous speed in RPM and a speed from the motor curve with its associated torque in inch-pounds
Motor Speed:	if motor speed is constant, enter the motor speed in RPM
Fluid Viscosity:	enter the value in centipoises
Sinker Bars:	if sinker bars are used, enter their diameter in inches

The above completes the input data required by DYNA1. The prompts are hopefully self explanatory in all cases. One area may, however, need some elaboration here in order to be fully understood.

As we have seen from chapter three, the finite element method relies on a discretization of the model being analyzed. Naturally, the finer the

discretization, the better the simulation, but the longer the computation time. Conversely, with few elements, we gain computation time but lose resolution. In this analysis, a five element model was chosen as a compromise between computation time and resolution. The resulting mesh is shown in figure 9.1.

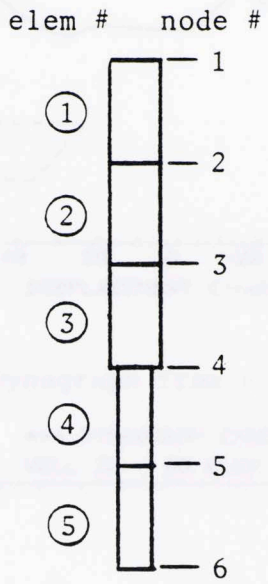

Figure 9.1 - Finite Element Mesh

Recall that changes in geometry can occur only at nodes, thus, referring to the diameter input segment discussed earlier, a single taper 1" rod would have a diameter of 1", the beginning element number is 1 and the ending element number is 5. A two taper string with 2000' of 7/8" and 3000' of 3/4" rod would have a diameter of 0.875 from elements 1 through 2 and a diameter of 0.750" from element 3 through 5.

Figures 9.2 and 9.3 are included to confirm the accuracy of a five element model. Both are results from the same input data.

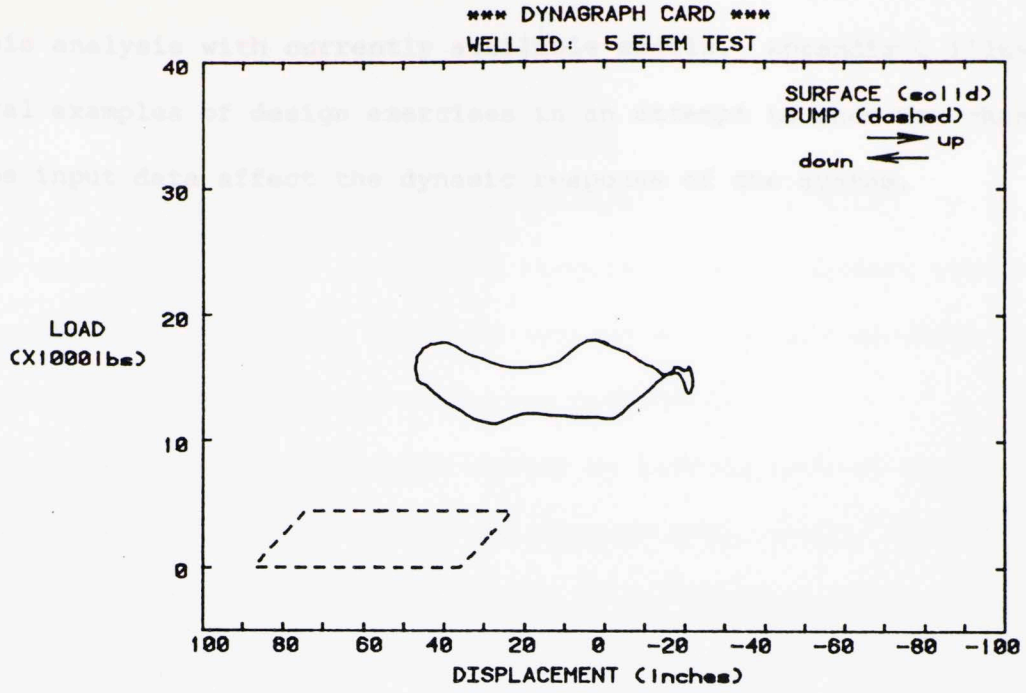

Figure 9.2 - Dynagraph from a 5-Element Mesh

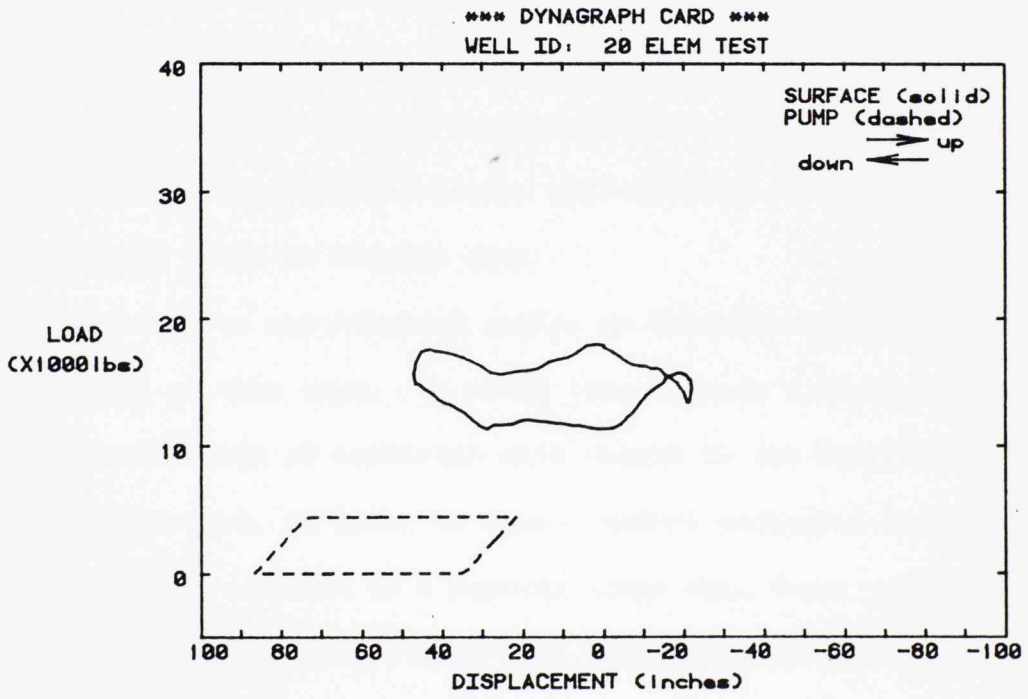

Figure 9.3 - Dynagraph from a 20-Element Mesh

9.4 Closing Remarks

Examples of these plotted outputs and the form of the summary of results will be illustrated in appendices B and C. Appendix B contains comparisons of

of this analysis with currently available models. Appendix C illustrates several examples of design exercises in an attempt to show how changes to some of the input data affect the dynamic response of the system.

CHAPTER 10

SUMMARY

It is difficult to summarize an analysis such as this. It is not as though we have attempted to solve a singularly posed problem with a unique solution. Rather, we have tried to develop a procedure by which we can effectively analyze a family of design situations.

Conclusion is probably best served by looking back at the analysis goals set forth in section 1.4. Items one through four, seven, and eight in that section, outline the theoretical goals of our solution, i.e., development of the pumping unit kinematics, the finite element model, torque characterization, pump load simulation, fluid damping, and forms of data reduction. All of these items have been fully described in chapters three through eight. Verification of the procedure discussed in items five and six of section 1.4 will be treated in appendices A through C. Hopefully, all of these dicussions constitute a clear, well defined, and well documented outline to the problem posed in chapter one.

In addition to our original goals, we have the unspoken goals which apply to any report of this type. We would like to know that somehow we have added to the existing body of knowledge with regard to the problem at hand. We can feel confident that, in fact, we have. Modern mathematical techniques have been successfully applied to a problem older than those techniques themselves. Industry accepted "rules of thumb" and "dimensionless parameters" have not been relied upon anywhere. Finally, the nature of the solution has been left general enough to facilitate upgrading as experimental data becomes available for more precise characterization of such things as boundary condition coefficients.

In short, we have addressed the problem from a new light and done so in purely analytical fashion. The result being a solution which escapes some of the pitfalls of previous analyses, most notably, instabilities in handling shallow wells and difficulty in defining damping factors for heavy crudes. Our approach thus takes us many steps forward in understanding and addressing the dynamic behavior of sucker rod pumping systems.

REFERENCES

Books

1. American Petroleum Institute, Sucker Rod Pumping System Design Book, Dallas, 1970.

2. Bethlehem Steel Corporation, Sucker Rod Handbook, New York, 1958.

3. Bird, R. B., Stewart, W. E., and Lightfoot, E. N., Transport Phenomena, New York: John Wiley and Sons, Inc., 1960.

4. Craft, B. C., Holden, W. R., and Graves, E. D., Well Design: Drilling and Production, New Jersey: Prentice-Hall, Inc., 1962.

5. James, M. L., Smith, G. M., and Wolford, J. C., Applied Numerical Methods for Digital Computation, New York: Harper and Row, 1977.

6. Schlichting, Hermann, Boundary Layer Theory, New York: McGraw-Hill, 1968.

7. Segerlind, L. J., Applied Finite Element Analysis, New York: John Wiley and Sons, Inc., 1976.

8. Seto, William W., Mechanical Vibrations, New York: McGraw-Hill, 1964.

9. Slonneger, J. C., Dynagraph Analysis of Sucker Rod Pumping, Houston: Gulf Publishing Co., 1961.

10. Timoshenko, S. P. and Goodier, J. N., Theory of Elasticity, New York: McGraw-Hill, 1970.

11. White, Frank M., Fluid Mechanics, New York: McGraw-Hill, 1979.

12. Zienkiewicz, O. C., The Finite Element Method, London: McGraw-Hill, 1977.

Papers

13. Gibbs, S. G., "Predicting the Behavior of Sucker-Rod Pumping Systems," Journal of Petroleum Technology, July, 1963.

APPENDIX A

TESTING OF THE FINITE ELEMENT MODEL

To give us peace of mind, we would like to test some of the more complex notions described in this report. Particularly, the solution to the system of differential equations and the integration routine. We accomplish this by comparing the results given by the developed model with those determined analytically for a case which possesses an analytical solution.

Such a solution exists for the vibration of a prismatic bar of length L, free at one end.

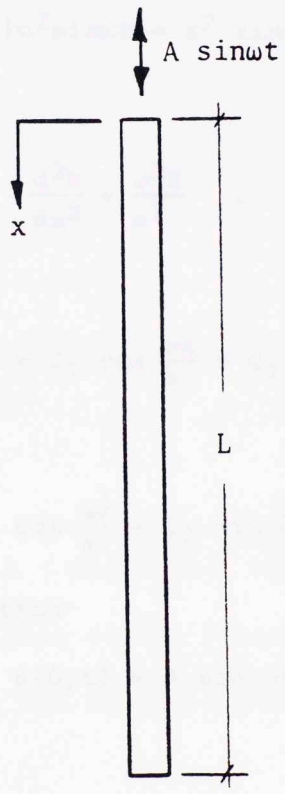

Figure A.1 - Test Case Model

The general differential equation for longitudinal vibrations in this bar is given by

$$\frac{\partial^2 u}{\partial t^2} = a^2 \frac{\partial^2 u}{\partial x^2} \tag{A.1}$$

where $a^2 = E/\rho$

u = displacement at any cross section.

The boundary conditions are

$$u(0,t) = A \sin\omega t$$

$$\frac{\partial u}{\partial x}(L,t) = 0.$$

For steady state vibration, $u(x,t) = U(x) \sin\omega t$ is the general form of solution. Substituting this into (A.1) yields

$$-U(x)\omega^2 \sin\omega t = a^2 \sin\omega t \frac{d^2U}{dx^2}$$

or

$$\frac{d^2U}{dx^2} + \frac{\omega^2 X}{a^2} \quad . \tag{A.2}$$

The solution to (A.2) is then

$$U(x) = C_1 \cos\frac{\omega x}{a} + C_2 \sin\frac{\omega x}{a}$$

from which

$$u(x,t) = \left(C_1 \cos\frac{\omega x}{a} + C_2 \sin\frac{\omega x}{a}\right) \sin\omega t \quad . \tag{A.3}$$

From the first boundary condition

$$u(0,t) = A \sin\omega t$$

so

$$C_1 = A$$

From the second boundary condition

$$\frac{\partial u}{\partial x}(L,t) = \frac{\omega}{a}\left[-A\sin\frac{\omega L}{a} + C_2 \cos\frac{\omega L}{a}\right] \sin\omega t = 0$$

from which

$$C_2 = A \tan \frac{\omega L}{a} \quad .$$

The steady state vibration is thus given by

$$u(x,t) = A \left[\cos \frac{\omega x}{a} + \tan \frac{\omega L}{a} \sin \frac{\omega x}{a}\right] \sin \omega t \quad . \qquad (A.4)$$

A plot of u(x,t) for an arbitrary set of conditions yields the following figure.

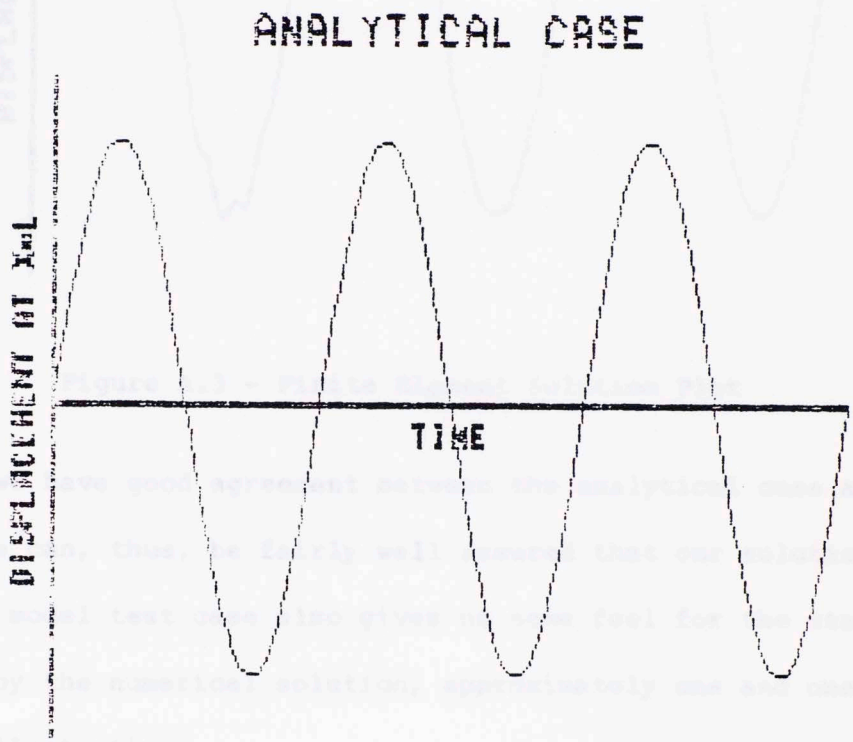

Figure A.2 - Analytical Solution Plot

Applying the same conditions to the finite element model yields the figure below. The horizontal and vertical axis scales are identical in these two figures.

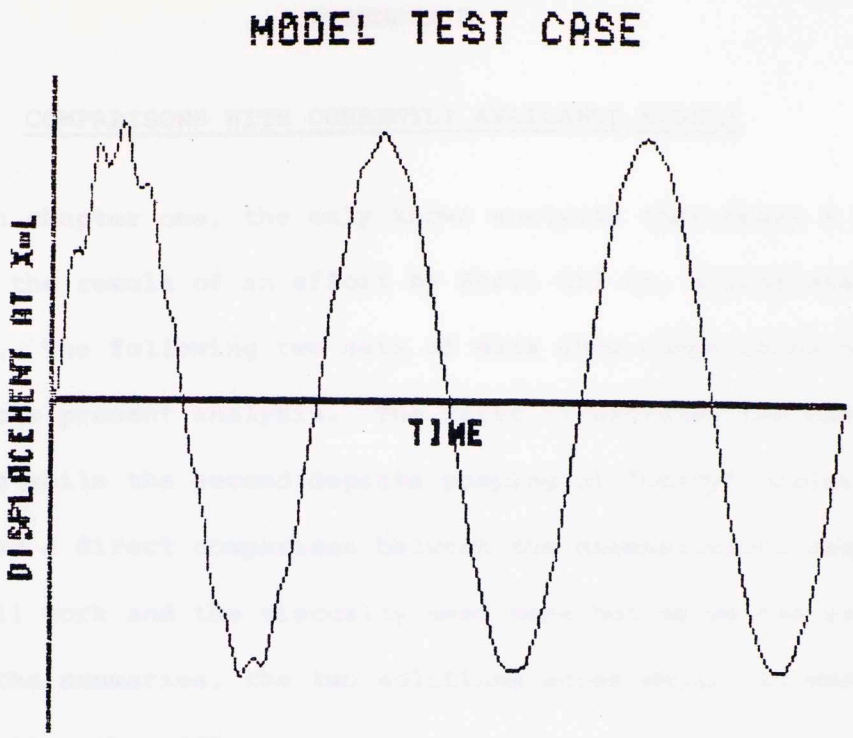

Figure A.3 - Finite Element Solution Plot

Clearly, we have good agreement between the analytical case and our simulation. We can, thus, be fairly well assured that our solution technique is valid. The model test case also gives us some feel for the stabilization time required by the numerical solution, approximately one and one-half cycles in the above illustration.

APPENDIX B

COMPARISONS WITH CURRENTLY AVAILABLE MODELS

As noted in chapter one, the only known analysis that bears a resemblance to this work is the result of an effort by Shell Oil Co. scientists in the 1960's and 70's. The following two sets of data show comparisons between the Shell work and the present analysis. The first illustrates the case of "normal" damping while the second depicts pumping of "heavy" crudes. It is difficult to draw a direct comparison between the dimensionless damping factor used in the Shell work and the viscosity used here but as we can see from the dynagraphs and the summaries, the two solutions agree well. In most instances, to better than 10%.

```
WELL IDENTIFICATION.....?TN1
DIRECTION OF ROTATION(CW/CCW).....(DOR)?CW
STRUCTURAL UNBALANCE.....(SUB)?-500
DIMENSION OF PUMPING UNIT ACCORDING TO API RP-11E
(A,C,P,H,I,G,R) .....(DPU)
 ?150,172.5,150,200,150,50,50
PUMP PLUNGER DIAMETER.....(PPD)?2.
PUMP DEPTH.....(DEP)?5000
FLUID DEPTH.....(FD)?5000
SPECIFIC GRAVITY OF FLUID.....(SPG)?.9
PUMPING SPEED.....(SPM)?10
SUCKER RODS OR CORODS(SR/CR).....(SC)?SR
API NUMBER OF ROD STRING.....(API)??6
LENGTH OF LARGEST ROD.....(RL)?3000
ENTER LENGTH OF NEXT SMALLER ROD.....(NL)?2000
SINKER BARS(YES/NO).....(SB)?NO
TUBING ANCHORED(YES/NO).....(TA)?NO
TUBING SIZE.....(TS)?2
PERCENT OF PUMP FILLAGE.....(PPF)?100
THE DAMPING FACTOR TO BE ENTERED FOR NORMAL FRICTION
IS 10 PERCENT.  ENTER DAMPING FACTOR.....(DCO)?10
```

Figure B.1-Shell Program Input - Case 1

SURFACE DYNAGRAPH PREDICTION FOR CONVENTIONAL GEOMETRY.

WELL IDENTIFICATION...TN1

* * * TUBING UNANCHORED * * *

PUMP FILLING.....	100.	PERCENT
POLISHED ROD STROKE LENGTH.....	90.	INCHES
PUMP PLUNGER STROKE LENGTH.....	74.	INCHES
FLUID LOAD ON PUMP PLUNGER.....	6120.	POUNDS
STANDING VALVE LOAD.....	8797.	POUNDS
TRAVELING VALVE LOAD.....	14917.	POUNDS
CBE AT 90 DEGREES.....	12569.	POUNDS
MAXIMUM POLISHED ROD LOAD.....	17642.	POUNDS
MINIMUM POLISHED ROD LOAD.....	6166.	POUNDS
MAXIMUM GEARBOX TORQUE.....	344101.	INCH-POUNDS
MINIMUM GEARBOX TORQUE.....	-181388.	INCH-POUNDS
POLISHED ROD POWER.....	11.1	HORSEPOWER

Figure B.2-Shell Program Output - Case 1

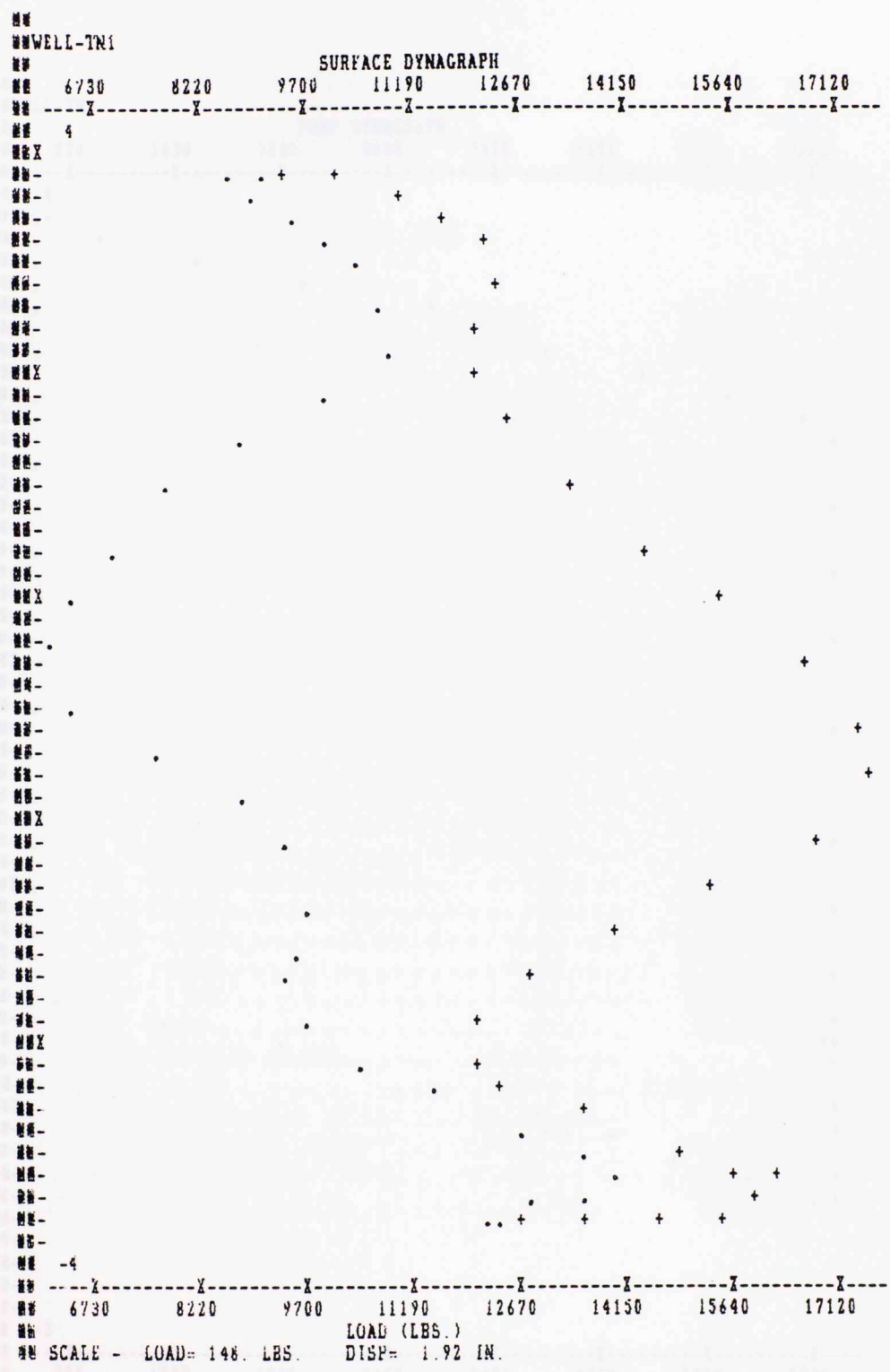

Figure B.3-Shell Program Surface Dynagraph - Case 1

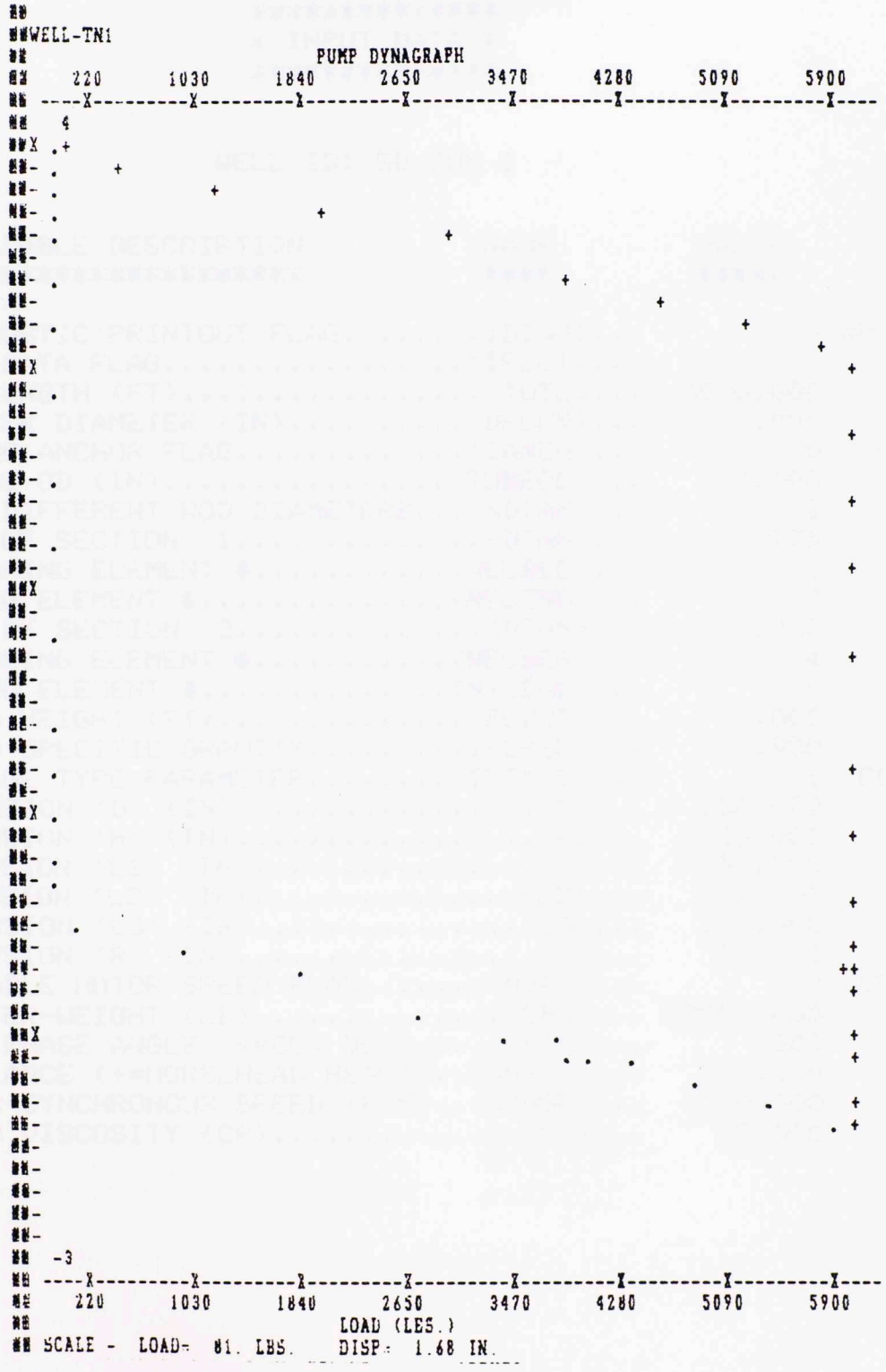

Figure B.4-Shell Program Pump Dynagraph - Case 1

```
              **************
              * INPUT DATA *
              **************

                  WELL ID: SD CHK 1

  VARIABLE DESCRIPTION              NAME          VALUE        REMARKS
  ********************              ****          *****        *******

DIAGNOSTIC PRINTOUT FLAG.......(IDIAG)...           0 NO DIAGNOSTICS
PLOT DATA FLAG.................(IPLOT)...           1      PLOT DATA
ROD LENGTH (FT)................(TOTL)....  5000.000
PLUNGER DIAMETER (IN)..........(DPLUN)...     2.000
TUBING ANCHOR FLAG.............(IANCH)...           0   UNANCHORED
TUBING OD (IN).................(TUBOD)...     2.000
# OF DIFFERENT ROD DIAMETERS...(NDIAM)...         2
DIAM OF SECTION  1.............(DIAM)....      .875
BEGINNING ELEMENT #............(NELBEG)...         1
ENDING ELEMENT #...............(NELEND)...         3
DIAM OF SECTION  2.............(DIAM)....      .750
BEGINNING ELEMENT #............(NELBEG)...         4
ENDING ELEMENT #...............(NELEND)...         5
FLUID HEIGHT (FT)..............(FLDHT)....      .000
FLUID SPECIFIC GRAVITY.........(SPGR)....      .900
LINKAGE TYPE PARAMETER.........(IPTYPE)...         1  CONVENTIONAL
DIMENSION 'D' (IN).............(D).......   150.000
DIMENSION 'H' (IN).............(H).......   150.000
DIMENSION 'L1' (IN)............(L1)......   150.000
DIMENSION 'L2' (IN)............(L2)......   172.500
DIMENSION 'L3' (IN)............(L3)......   150.000
DIMENSION 'R' (IN).............(R).......    50.000
VARIABLE MOTOR SPEED FLAG......(MVAR)....           0  CONSTANT SPD
COUNTER-WEIGHT (LB)............(CBW).... 12500.000
C-WT PHASE ANGLE (+=CCW DEG)...(BETA)....      .000
UNBALANCE (+=HORSEHEAD HEAVY)..(UNBAL)...   500.000
MOTOR SYNCHRONOUS SPEED (RPM)..(SYNSP)...  1200.000
FLUID VISCOSITY (CP)...........(MU)......    15.000
```

Figure B.5-Finite Element Input - Case 1

```
                    **********************
                    * SUMMARY OF RESULTS *
                    **********************

MAXIMUM ROD STRESSES (PSI)
**************************

ELEMENT #  1:  25512.
ELEMENT #  2:  22062.
ELEMENT #  3:  18390.
ELEMENT #  4:  20855.
ELEMENT #  5:  16965.


POLISHED ROD LOADS (LB)
***********************
MAXIMUM PRL= 16345.
MINIMUM PRL=  6075.


GEARBOX/MOTOR TORQUES (IN-LB)
*****************************
MAXIMUM GEARBOX TORQUE=  333611.
MINIMUM GEARBOX TORQUE= -232484.
MAXIMUN MOTOR TORQUE=      2780.
MINIMUM MOTOR TORQUE      -1937.


PUMPING RATES (STROKES/MIN)
***************************
MAXIMUM= 10.00
MINIMUM= 10.00


MISCELLANEOUS
*************
SURFACE STROKE (IN)=                87.40
PUMP STROKE (IN)=                   71.61
POLISHED ROD HORSEPOWER=            10.21
WEIGHT OF ROD IN AIR (LB)=        9126.87
WEIGHT OF ROD IN FLUID (LB)=      8078.73
MAX FLUID LD ON PLUNGER (LB)=     6126.11
```

Figure B.6-Finite Element Output - Case 1

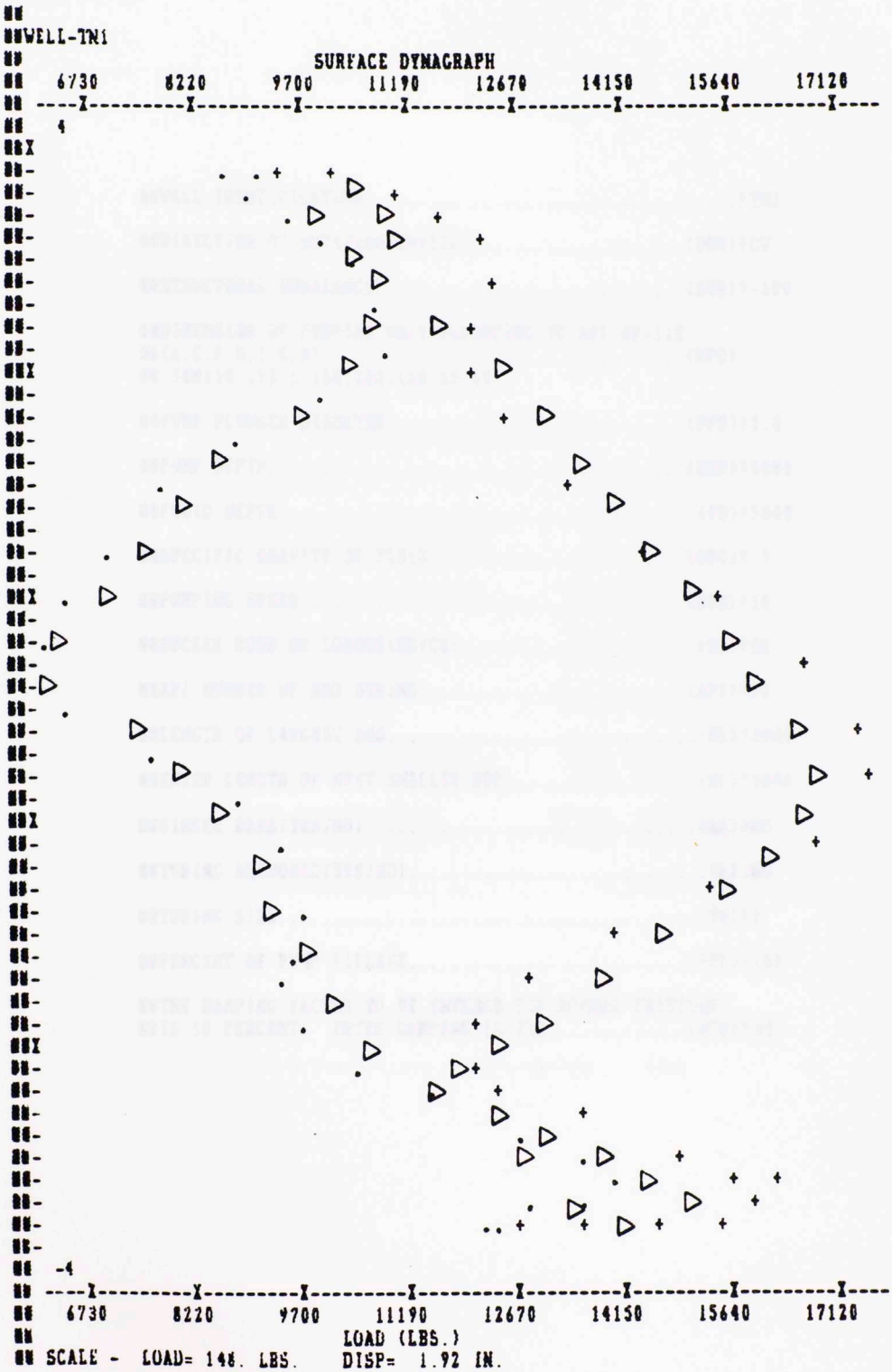

Figure B.7-Shell Program/Finite Element (Δ) Comparison - Case 1

```
WELL IDENTIFICATION.....?TN1

DIRECTION OF ROTATION(CW/CCW).....(DOR)?CW

STRUCTURAL UNBALANCE.....(SUB)?-500

DIMENSION OF PUMPING UNIT ACCORDING TO API RP-11E
(A,C,P,H,I,G,R) .....(DPU)
 ?150,172.5,150,200,150,50,50

PUMP PLUNGER DIAMETER.....(PPD)?2.0

PUMP DEPTH.....(DEP)?5000

FLUID DEPTH.....(FD)?5000

SPECIFIC GRAVITY OF FLUID.....(SPG)?.9

PUMPING SPEED.....(SPM)?10

SUCKER RODS OR CORODS(SR/CR).....(SC)?SR

API NUMBER OF ROD STRING.....(API)?76

LENGTH OF LARGEST ROD.....(RL)?3000

ENTER LENGTH OF NEXT SMALLER ROD.....(RL)?2000

SINKER BARS(YES/NO).....(SB)?NO

TUBING ANCHORED(YES/NO).....(TA)?NO

TUBING SIZE.....(TS)?2

PERCENT OF PUMP FILLAGE.....(PPF)?100

THE DAMPING FACTOR TO BE ENTERED FOR NORMAL FRICTION
IS 10 PERCENT.  ENTER DAMPING FACTOR.....(DCO)?30.
```

Figure B.8-Shell Program Input - Case 2

```
SURFACE DYNAGRAPH PREDICTION FOR CONVENTIONAL GEOMETRY.


  WELL IDENTIFICATION...TN1

          * * * TUBING UNANCHORED * * *

    PUMP FILLING.....                100. PERCENT

    POLISHED ROD STROKE LENGTH.....   90. INCHES
    PUMP PLUNGER STROKE LENGTH.....   72. INCHES

    FLUID LOAD ON PUMP PLUNGER.....  6120. POUNDS

    STANDING VALVE LOAD.....         8797. POUNDS
    TRAVELING VALVE LOAD.....       14917. POUNDS

    CBE AT 90 DEGREES.....          12569. POUNDS

    MAXIMUM POLISHED ROD LOAD.....  18329. POUNDS
    MINIMUM POLISHED ROD LOAD.....   5286. POUNDS

    MAXIMUM GEARBOX TORQUE..... 359193. INCH-POUNDS
    MINIMUM GEARBOX TORQUE.....-152105. INCH-POUNDS

    POLISHED ROD POWER.....          14.4 HORSEPOWER
```

Figure B.9-Shell Program Output - Case 2

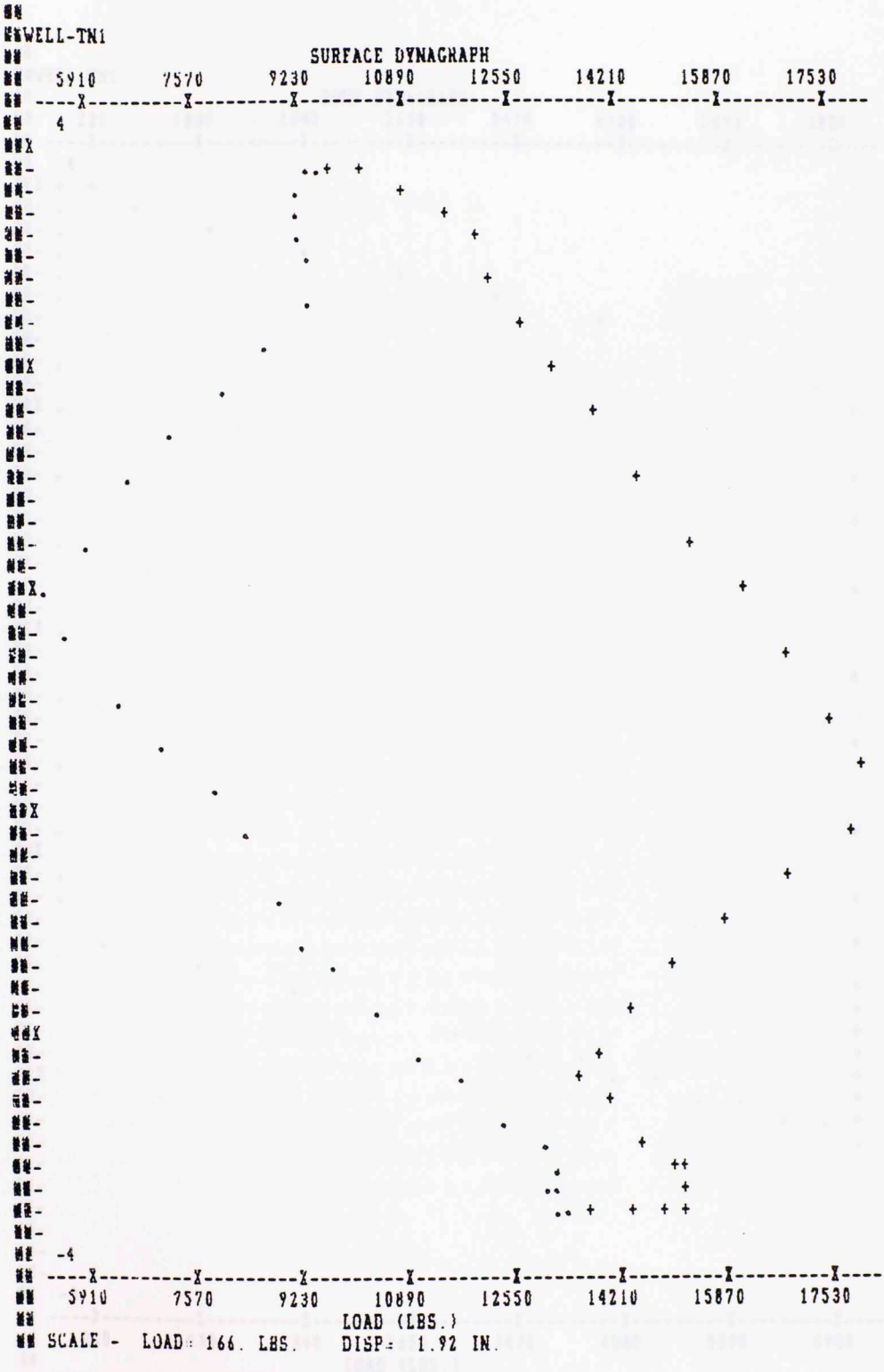

Figure B.10-Shell Program Surface Dynagraph - Case 2

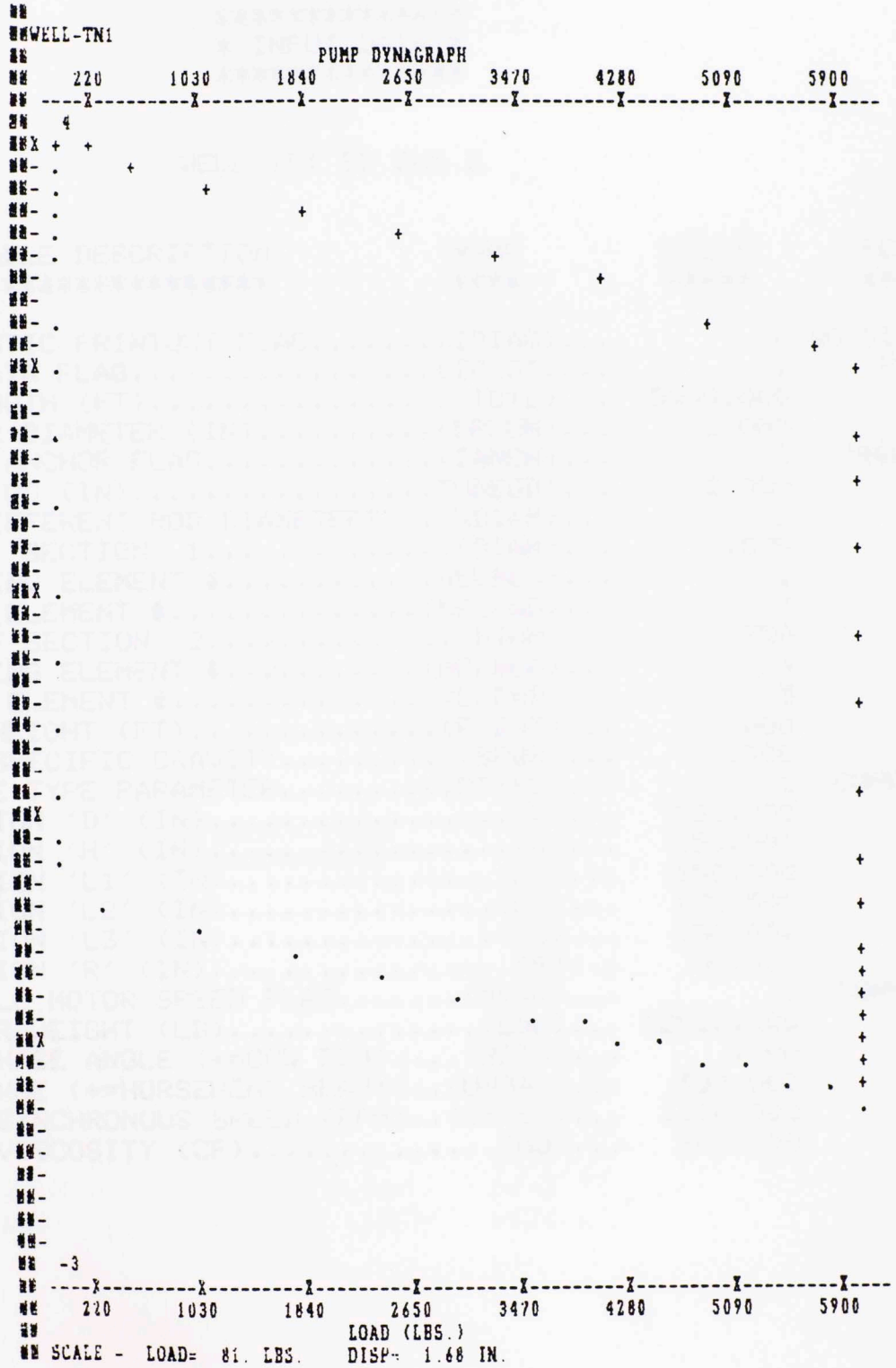

Figure B.11-Shell Program Pump Dynagraph - Case 2

```
**************
* INPUT DATA *
**************

WELL ID: SD CHK 2

  VARIABLE DESCRIPTION                NAME          VALUE       REMARKS
  ********************                ****          *****       *******

DIAGNOSTIC PRINTOUT FLAG.......(IDIAG)...              0 NO DIAGNOSTICS
PLOT DATA FLAG.................(IPLOT)...              1    PLOT DATA
ROD LENGTH (FT)................(TOTL)...     5000.000
PLUNGER DIAMETER (IN)..........(DPLUN)...        2.000
TUBING ANCHOR FLAG.............(IANCH)...              0   UNANCHORED
TUBING OD (IN).................(TUBEOD)...        2.000
# OF DIFFERENT ROD DIAMETERS...(NDIAM)...              2
DIAM OF SECTION  1.............(DIAM)...         .875
BEGINNING ELEMENT #............(NELBEG)...              1
ENDING ELEMENT #...............(NELEND)...              3
DIAM OF SECTION  2.............(DIAM)...         .750
BEGINNING ELEMENT #............(NELBEG)...              4
ENDING ELEMENT #...............(NELEND)...              5
FLUID HEIGHT (FT)..............(FLDHT)...         .000
FLUID SPECIFIC GRAVITY.........(SPGR)...         .900
LINKAGE TYPE PARAMETER.........(IPTYPE)...              1  CONVENTIONAL
DIMENSION 'D' (IN).............(D)...       150.000
DIMENSION 'H' (IN).............(H)...       150.000
DIMENSION 'L1' (IN)............(L1)...       150.000
DIMENSION 'L2' (IN)............(L2)...       172.500
DIMENSION 'L3' (IN)............(L3)...       150.000
DIMENSION 'R' (IN).............(R)...        50.000
VARIABLE MOTOR SPEED FLAG......(MVAR)...              0  CONSTANT SPD
COUNTER-WEIGHT (LB)............(CBW)...    12500.000
C-WT PHASE ANGLE (+=CCW DEG)...(BETA)...         .000
UNBALANCE (+=HORSEHEAD HEAVY)..(UNBAL)...     500.000
MOTOR SYNCHRONOUS SPEED (RPM)..(SYNSP)...    1200.000
FLUID VISCOSITY (CP)...........(MU)...        300.000
```

Figure B.12-Finite Element Input - Case 2

```
                    **********************
                    * SUMMARY OF RESULTS *
                    **********************

MAXIMUM ROD STRESSES (PSI)
**************************

ELEMENT #  1:  26973.
ELEMENT #  2:  23153.
ELEMENT #  3:  19125.
ELEMENT #  4:  21565.
ELEMENT #  5:  17305.


POLISHED ROD LOADS (LB)
***********************
MAXIMUM PRL= 17305.
MINIMUM PRL=  5338.


GEARBOX/MOTOR TORQUES (IN-LB)
*****************************
MAXIMUM GEARBOX TORQUE=  362470.
MINIMUM GEARBOX TORQUE= -216924.
MAXIMUN MOTOR TORQUE=      3021.
MINIMUM MOTOR TORQUE      -1808.


PUMPING RATES (STROKES/MIN)
***************************
MAXIMUM= 10.00
MINIMUM= 10.00


MISCELLANEOUS
*************
SURFACE STROKE (IN)=                  87.40
PUMP STROKE (IN)=                     70.87
POLISHED ROD HORSEPOWER=              12.96
WEIGHT OF ROD IN AIR (LB)=          9126.87
WEIGHT OF ROD IN FLUID (LB)=        8078.73
MAX FLUID LD ON PLUNGER (LB)=       6126.11
```

Figure B.13-Finite Element Output - Case 2

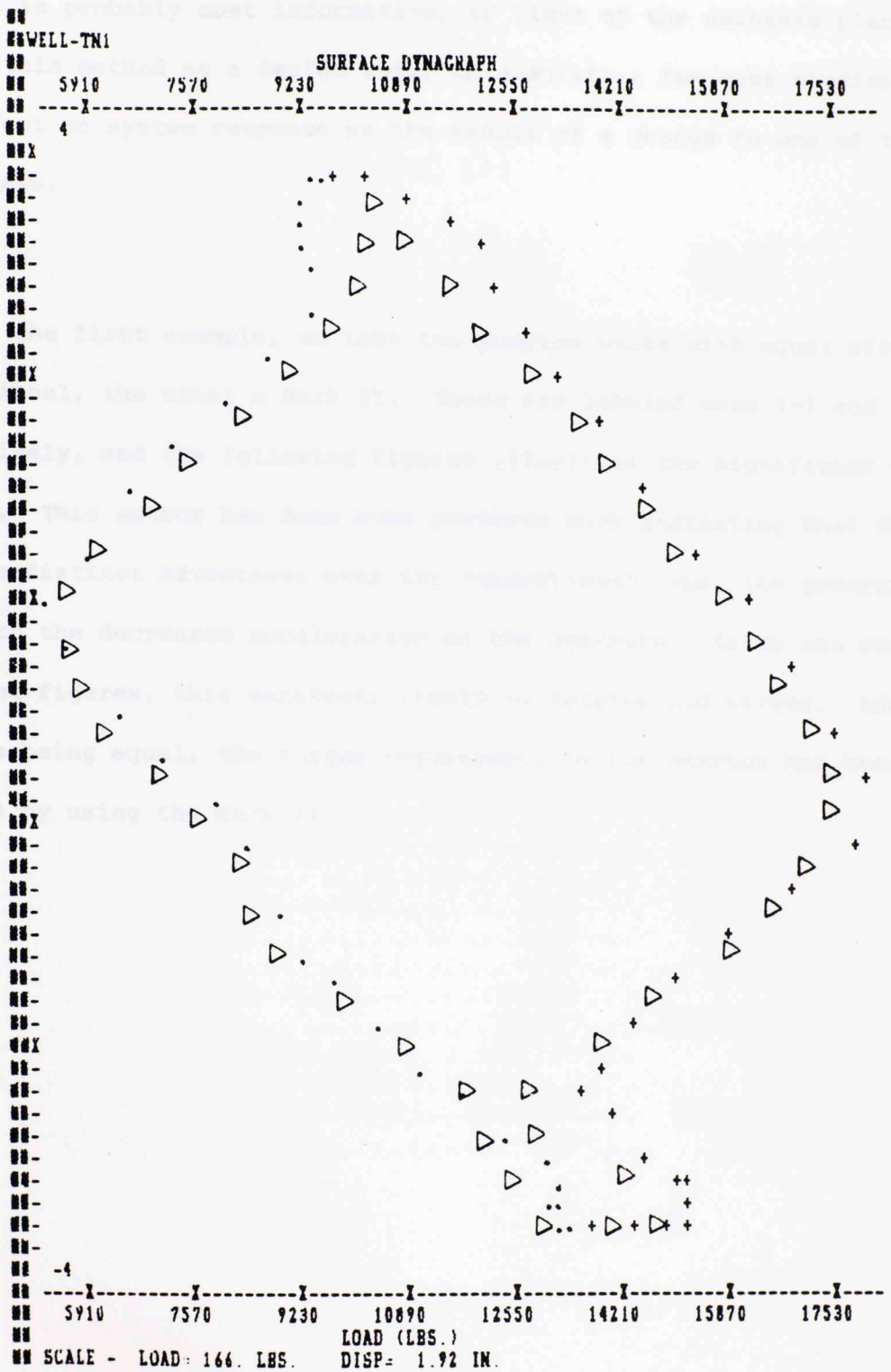

Figure B.14-Shell Program/Finite Element (Δ) Comparison - Case 2

APPENDIX C

SAMPLE CASE STUDIES

It is probably most informative, in light of the emphasis placed on the use of this method as a design tool, to simulate a few case studies to view the effect on system response as the result of a change to one of the input parameters.

Case 1

In the first example, we take two pumping units with equal strokes, one conventional, the other a Mark II. These are labeled case 1-1 and 1-2, respectively, and the following figures illustrate the significant output results. This author has done some previous work indicating that the Mark II has some distinct advantages over the conventional type, (in general) due mainly to the decreased acceleration on the upstroke. As we can see from the following figures, this manifests itself in reduced rod stress. Additionally, all else being equal, the torque requirement on the gearbox has been reduced a full 28% by using the Mark II.

```
**************
* INPUT DATA *
**************

WELL ID: CASE 1-1

  VARIABLE DESCRIPTION              NAME          VALUE        REMARKS
  ********************              ****          *****        *******

DIAGNOSTIC PRINTOUT FLAG.......(IDIAG)...              0 NO DIAGNOSTICS
PLOT DATA FLAG.................(IPLOT)...              1     PLOT DATA
ROD LENGTH (FT)................(TOTL)...       5000.000
PLUNGER DIAMETER (IN)..........(DPLUN)...          1.750
TUBING ANCHOR FLAG.............(IANCH)...              0   UNANCHORED
TUBING OD (IN).................(TUBEOD)...          2.000
# OF DIFFERENT ROD DIAMETERS...(NDIAM)...              2
DIAM OF SECTION  1.............(DIAM)...           .875
BEGINNING ELEMENT #............(NELBEG)...              1
ENDING ELEMENT #...............(NELEND)...              3
DIAM OF SECTION  2.............(DIAM)...           .750
BEGINNING ELEMENT #............(NELBEG)...              4
ENDING ELEMENT #...............(NELEND)...              5
FLUID HEIGHT (FT)..............(FLDHT)...        500.000
FLUID SPECIFIC GRAVITY.........(SPGR)...           .900
LINKAGE TYPE PARAMETER.........(IPTYPE)...              1  CONVENTIONAL
DIMENSION 'D' (IN).............(D)...           150.000
DIMENSION 'H' (IN).............(H)...           150.000
DIMENSION 'L1' (IN)............(L1)...           150.000
DIMENSION 'L2' (IN)............(L2)...           172.500
DIMENSION 'L3' (IN)............(L3)...           150.000
DIMENSION 'R' (IN).............(R)...            50.000
VARIABLE MOTOR SPEED FLAG......(MVAR)...              0  CONSTANT SPD
COUNTER-WEIGHT (LB)............(CBW)...      12000.000
C-WT PHASE ANGLE (+=CCW DEG)...(BETA)...           .000
UNBALANCE (+=HORSEHEAD HEAVY)..(UNBAL)...          .000
MOTOR SYNCHRONOUS SPEED (RPM)..(SYNSP)...      1200.000
FLUID VISCOSITY (CP)...........(MU)...           10.000
```

Figure C.1-Input Data - Case 1-1

```
                    ************************
                    * SUMMARY OF RESULTS *
                    ************************

MAXIMUM ROD STRESSES (PSI)
**************************

ELEMENT #  1:  24189.
ELEMENT #  2:  20262.
ELEMENT #  3:  16361.
ELEMENT #  4:  17883.
ELEMENT #  5:  13388.


POLISHED ROD LOADS (LB)
***********************
MAXIMUM PRL= 15629.
MINIMUM PRL=  6136.


GEARBOX/MOTOR TORQUES (IN-LB)
*****************************
MAXIMUM GEARBOX TORQUE=  333950.
MINIMUM GEARBOX TORQUE= -285133.
MAXIMUN MOTOR TORQUE=      2783.
MINIMUM MOTOR TORQUE      -2376.


PUMPING RATES (STROKES/MIN)
***************************
MAXIMUM= 10.00
MINIMUM= 10.00


MISCELLANEOUS
*************
SURFACE STROKE (IN)=                  87.40
PUMP STROKE (IN)=                     78.85
POLISHED ROD HORSEPOWER=               9.15
WEIGHT OF ROD IN AIR (LB)=          9126.87
WEIGHT OF ROD IN FLUID (LB)=        8078.73
MAX FLUID LD ON PLUNGER (LB)=       4221.27
```

Figure C.2-Output Data - Case 1-1

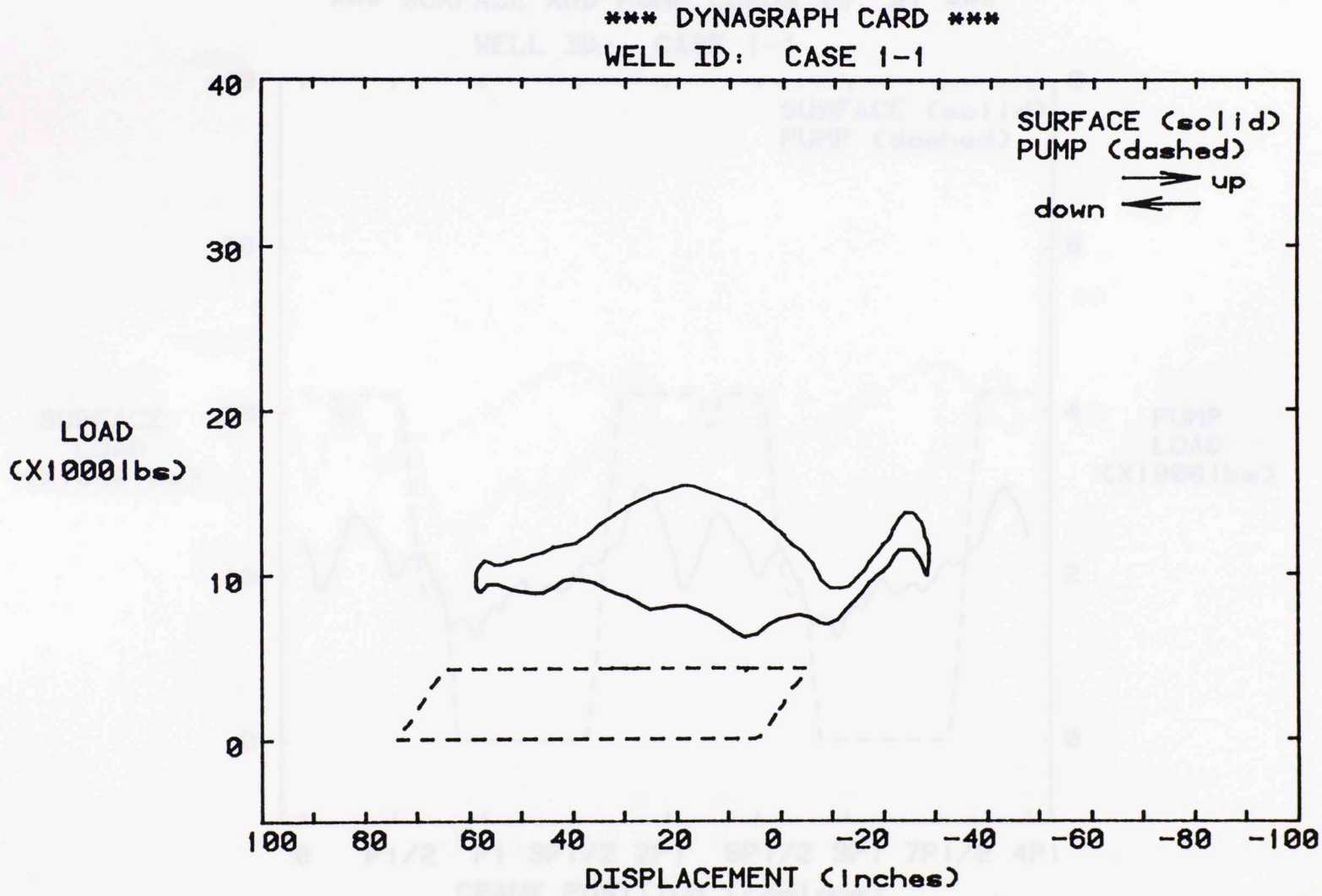

Figure C.3-Dynagraph - Case 1-1

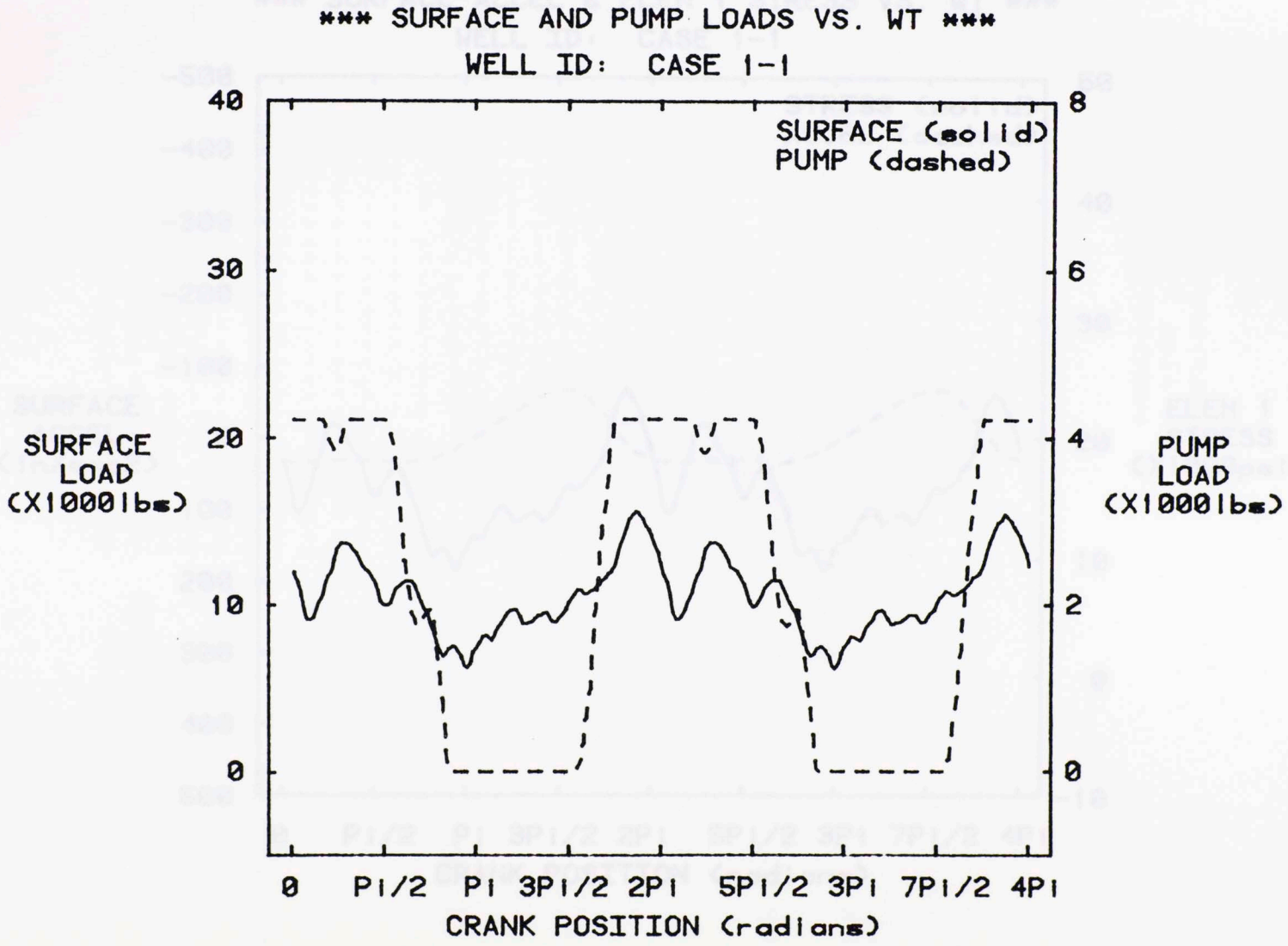

Figure C.4-Load Plot - Case 1-1

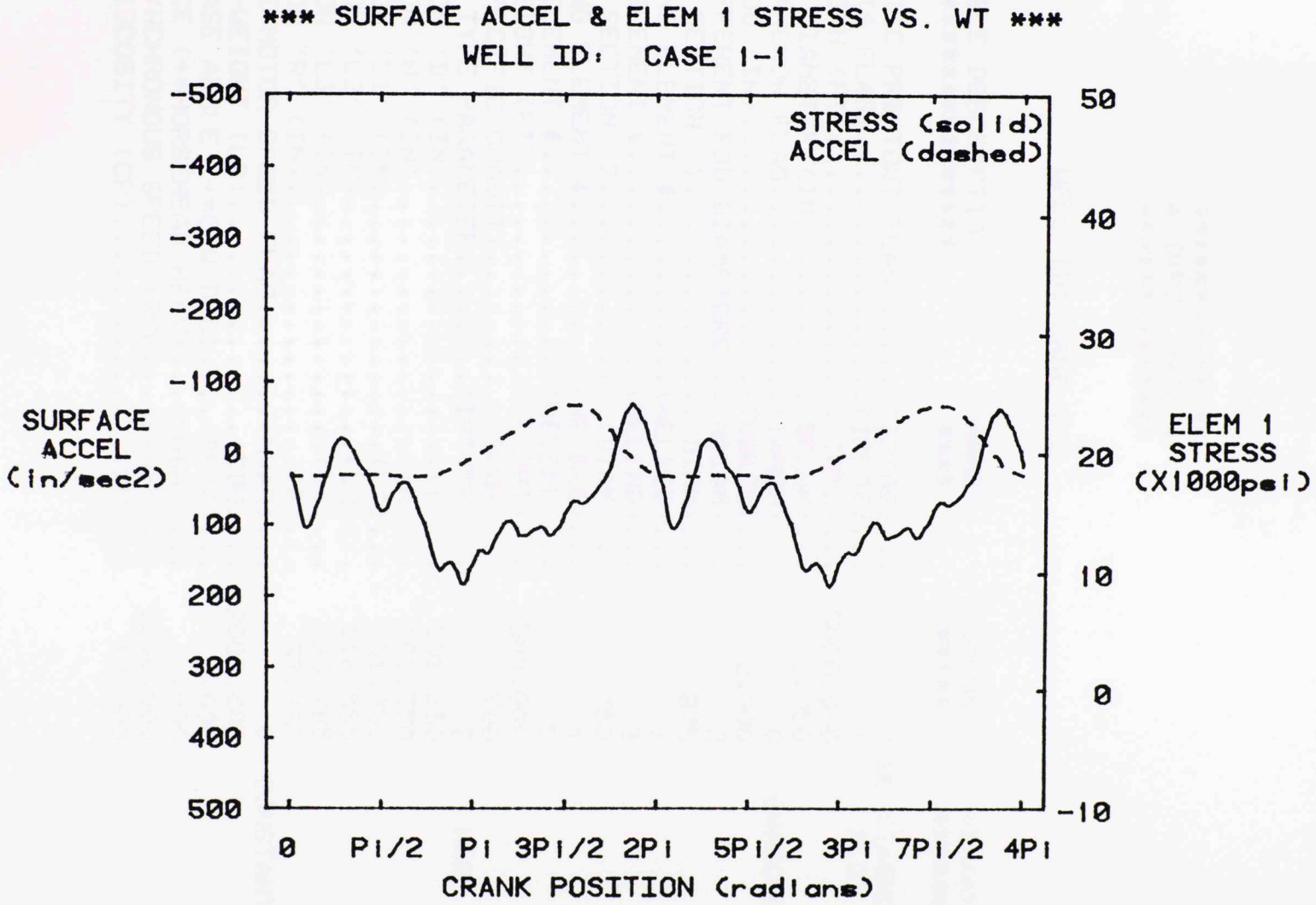

Figure C.5-Stress Plot - Case 1-1

****
* INPUT DATA *
****

WELL ID: CASE 1-2

VARIABLE DESCRIPTION	NAME	VALUE	REMARKS
DIAGNOSTIC PRINTOUT FLAG	(IDIAG)	0	NO DIAGNOSTICS
PLOT DATA FLAG	(IPLOT)	1	PLOT DATA
ROD LENGTH (FT)	(TOTL)	5000.000	
PLUNGER DIAMETER (IN)	(DPLUN)	1.750	
TUBING ANCHOR FLAG	(IANCH)	0	UNANCHORED
TUBING OD (IN)	(TUBEOD)	2.000	
# OF DIFFERENT ROD DIAMETERS	(NDIAM)	2	
DIAM OF SECTION 1	(DIAM)	.875	
BEGINNING ELEMENT #	(NELBEG)	1	
ENDING ELEMENT #	(NELEND)	3	
DIAM OF SECTION 2	(DIAM)	.750	
BEGINNING ELEMENT #	(NELBEG)	4	
ENDING ELEMENT #	(NELEND)	5	
FLUID HEIGHT (FT)	(FLDHT)	500.000	
FLUID SPECIFIC GRAVITY	(SPGR)	.900	
LINKAGE TYPE PARAMETER	(IPTYPE)	2	MARK II
DIMENSION 'D' (IN)	(D)	101.350	
DIMENSION 'H' (IN)	(H)	101.350	
DIMENSION 'L1' (IN)	(L1)	101.350	
DIMENSION 'L2' (IN)	(L2)	116.555	
DIMENSION 'L3' (IN)	(L3)	33.785	
DIMENSION 'R' (IN)	(R)	33.785	
VARIABLE MOTOR SPEED FLAG	(MVAR)	0	CONSTANT SPD
COUNTER-WEIGHT (LB)	(CBW)	12000.000	
C-WT PHASE ANGLE (+=CCW DEG)	(BETA)	.000	
UNBALANCE (+=HORSEHEAD HEAVY)	(UNBAL)	.000	
MOTOR SYNCHRONOUS SPEED (RPM)	(SYNSP)	1200.000	
FLUID VISCOSITY (CP)	(MU)	10.000	

Figure C.6-Input Data - Case 1-2

```
**********************
* SUMMARY OF RESULTS *
**********************

MAXIMUM ROD STRESSES (PSI)
**************************

ELEMENT #  1:  23046.
ELEMENT #  2:  19118.
ELEMENT #  3:  15211.
ELEMENT #  4:  16622.
ELEMENT #  5:  12435.


POLISHED ROD LOADS (LB)
***********************
MAXIMUM PRL= 14985.
MINIMUM PRL=  4759.


GEARBOX/MOTOR TORQUES (IN-LB)
*****************************
MAXIMUM GEARBOX TORQUE=  239019.
MINIMUM GEARBOX TORQUE= -154696.
MAXIMUN MOTOR TORQUE=      1992.
MINIMUM MOTOR TORQUE      -1289.


PUMPING RATES (STROKES/MIN)
***************************
MAXIMUM= 10.00
MINIMUM= 10.00


MISCELLANEOUS
*************
SURFACE STROKE (IN)=                  87.60
PUMP STROKE (IN)=                     81.49
POLISHED ROD HORSEPOWER=               8.85
WEIGHT OF ROD IN AIR (LB)=          9126.87
WEIGHT OF ROD IN FLUID (LB)=        8078.73
MAX FLUID LD ON PLUNGER (LB)=       4221.27
```

Figure C.7-Output Data - Case 1-2

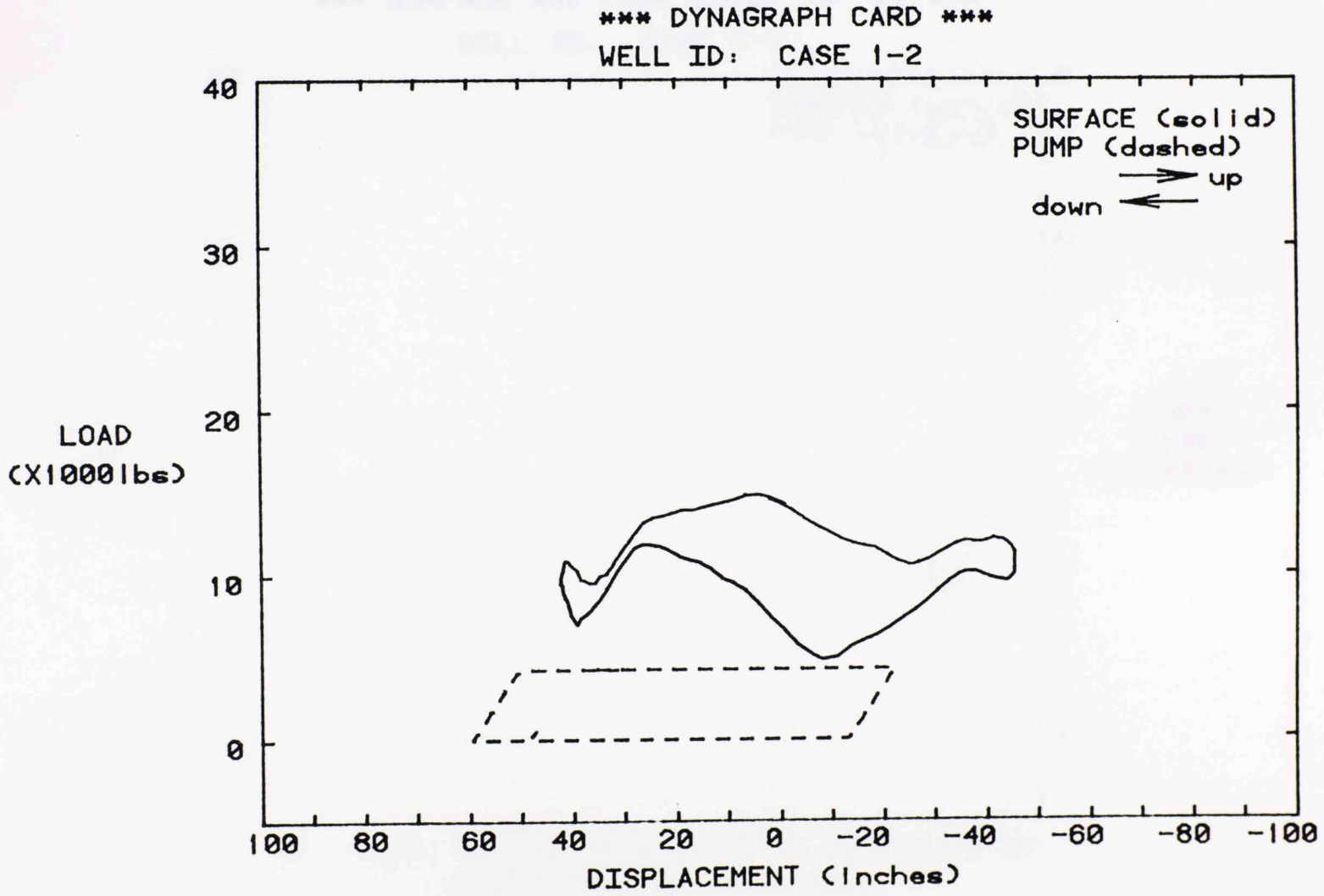

Figure C.8-Dynagraph - Case 1-2

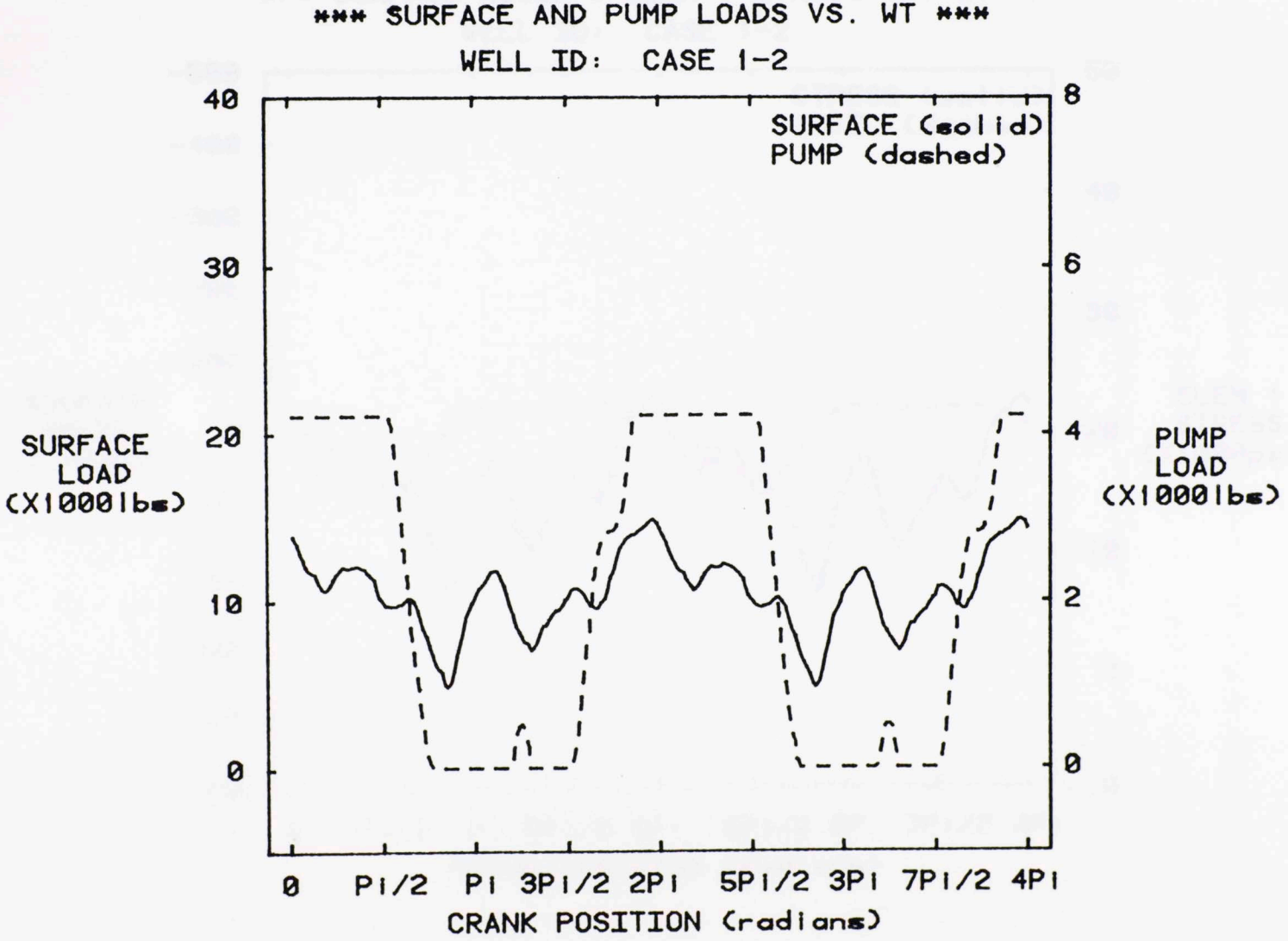

Figure C.9-Load Plot - Case 1-2

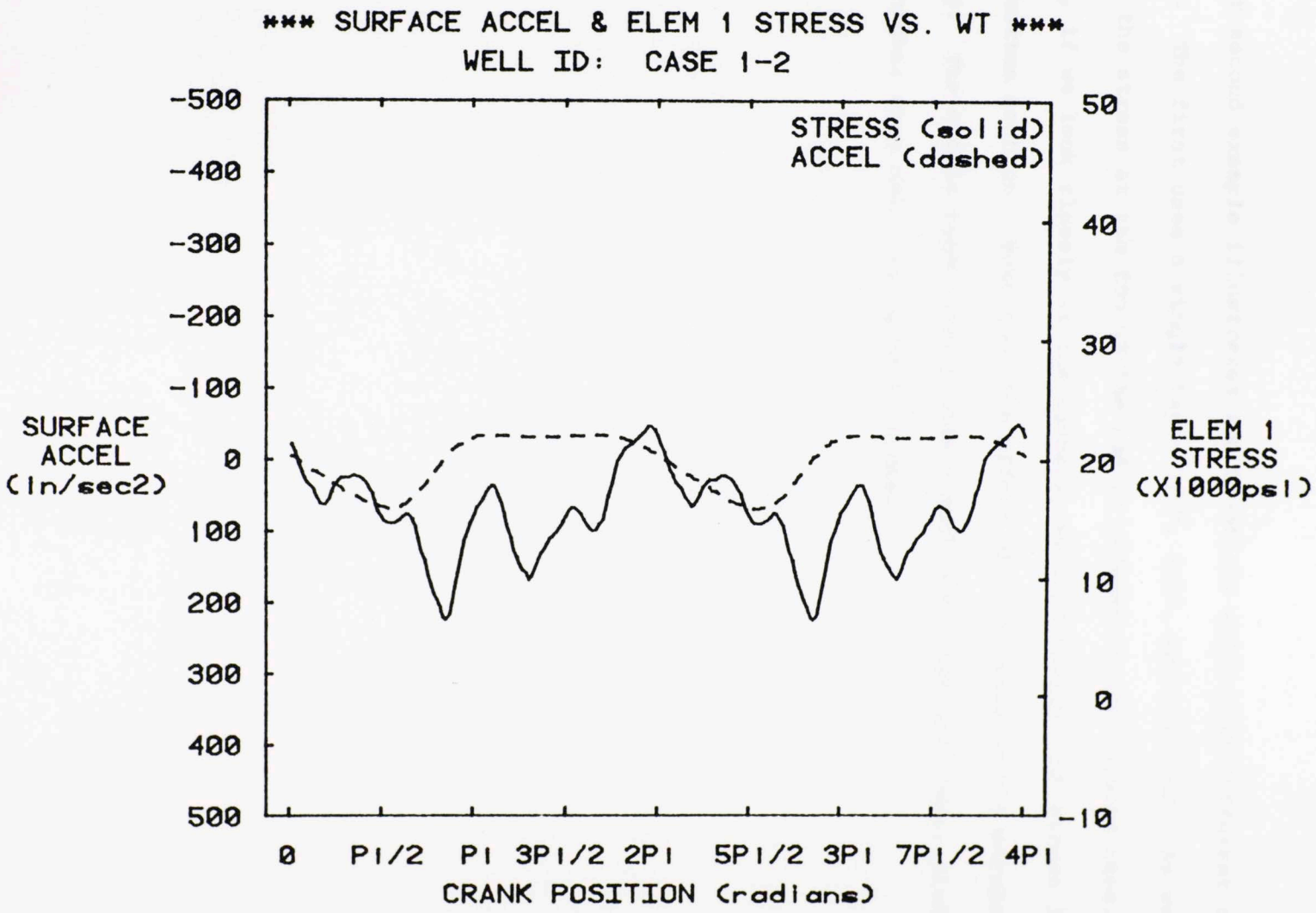

Figure C.10-Stress Plot - Case 1-2

Case 2

Our second example illustrates two identical wells with different rod strings. The first uses a single taper 7/8", 3/4", and 1/2" rod. As we might expect, the stress at the top of the rod is reduced in the tapered case. However, if we look closely at the summary, we find fairly high stress levels at the bottom section. Note too, the effect of both cases on the stroke at the pump. The single taper case yields a much more "springy" case, yielding a stroke higher even than the surface stroke.

```
               **************
               * INPUT DATA *
               **************

                WELL ID: CASE 2-1

  VARIABLE DESCRIPTION              NAME          VALUE        REMARKS
  ********************              ****          *****        *******

DIAGNOSTIC PRINTOUT FLAG.......(IDIAG)...            0 NO DIAGNOSTICS
PLOT DATA FLAG.................(IPLOT)...            1      PLOT DATA
ROD LENGTH (FT)................(TOTL)...     5000.000
PLUNGER DIAMETER (IN)..........(DPLUN)...        1.500
TUBING ANCHOR FLAG.............(IANCH)...            0    UNANCHORED
TUBING OD (IN).................(TUBEOD)...        2.000
# OF DIFFERENT ROD DIAMETERS...(NDIAM)...            1
DIAM OF SECTION  1.............(DIAM)...         .875
BEGINNING ELEMENT #............(NELBEG)...            1
ENDING ELEMENT #...............(NELEND)...            5
FLUID HEIGHT (FT)..............(FLDHT)...     500.000
FLUID SPECIFIC GRAVITY.........(SPGR)...         .900
LINKAGE TYPE PARAMETER.........(IPTYPE)...            1   CONVENTIONAL
DIMENSION 'D' (IN).............(D)...       150.000
DIMENSION 'H' (IN).............(H)...       150.000
DIMENSION 'L1' (IN)............(L1)...       150.000
DIMENSION 'L2' (IN)............(L2)...       172.500
DIMENSION 'L3' (IN)............(L3)...       150.000
DIMENSION 'R' (IN).............(R)...        50.000
VARIABLE MOTOR SPEED FLAG......(MVAR)...            0   CONSTANT SPD
COUNTER-WEIGHT (LB)............(CBW)...    12000.000
C-WT PHASE ANGLE (+=CCW DEG)...(BETA)...         .000
UNBALANCE (+=HORSEHEAD HEAVY)..(UNBAL)...        .000
MOTOR SYNCHRONOUS SPEED (RPM)..(SYNSP)...    1200.000
FLUID VISCOSITY (CP)...........(MU)...         10.000
```

Figure C.11-Input Data - Case 2-1

```
                    **********************
                    * SUMMARY OF RESULTS *
                    **********************

MAXIMUM ROD STRESSES (PSI)
**************************

ELEMENT #  1:  24419.
ELEMENT #  2:  20733.
ELEMENT #  3:  16867.
ELEMENT #  4:  12599.
ELEMENT #  5:   8081.


POLISHED ROD LOADS (LB)
***********************
MAXIMUM PRL= 15762.
MINIMUM PRL=  6395.


GEARBOX/MOTOR TORQUES (IN-LB)
*****************************
MAXIMUM GEARBOX TORQUE=  290105.
MINIMUM GEARBOX TORQUE= -276205.
MAXIMUN MOTOR TORQUE=      2418.
MINIMUM MOTOR TORQUE      -2302.


PUMPING RATES (STROKES/MIN)
***************************
MAXIMUM= 10.00
MINIMUM= 10.00


MISCELLANEOUS
*************
SURFACE STROKE (IN)=                  87.40
PUMP STROKE (IN)=                     89.58
POLISHED ROD HORSEPOWER=               8.47
WEIGHT OF ROD IN AIR (LB)=         10210.42
WEIGHT OF ROD IN FLUID (LB)=        9037.85
MAX FLUID LD ON PLUNGER (LB)=       3101.34
```

Figure C.12-Output Data - Case 2-1

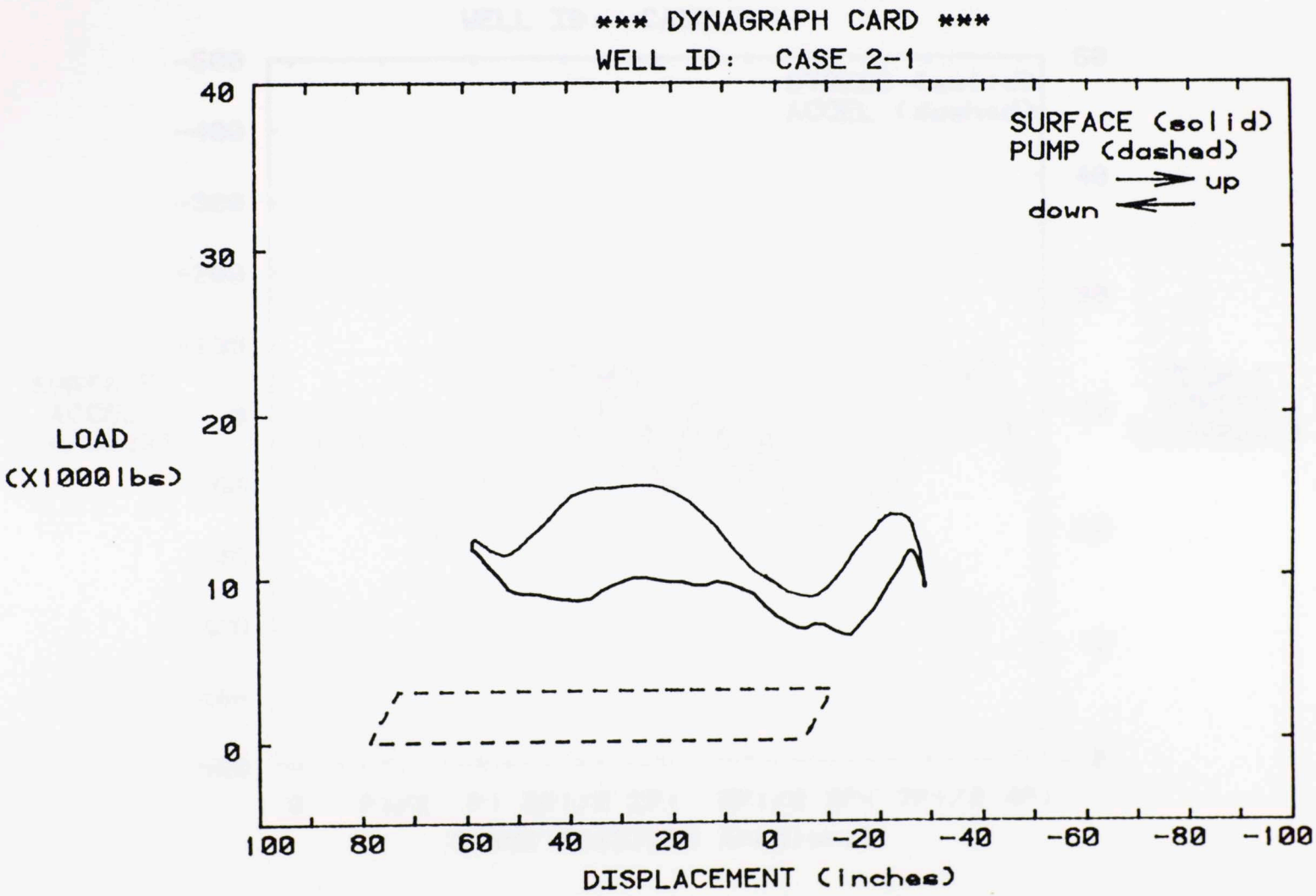

Figure C.13-Dynagraph - Case 2-1

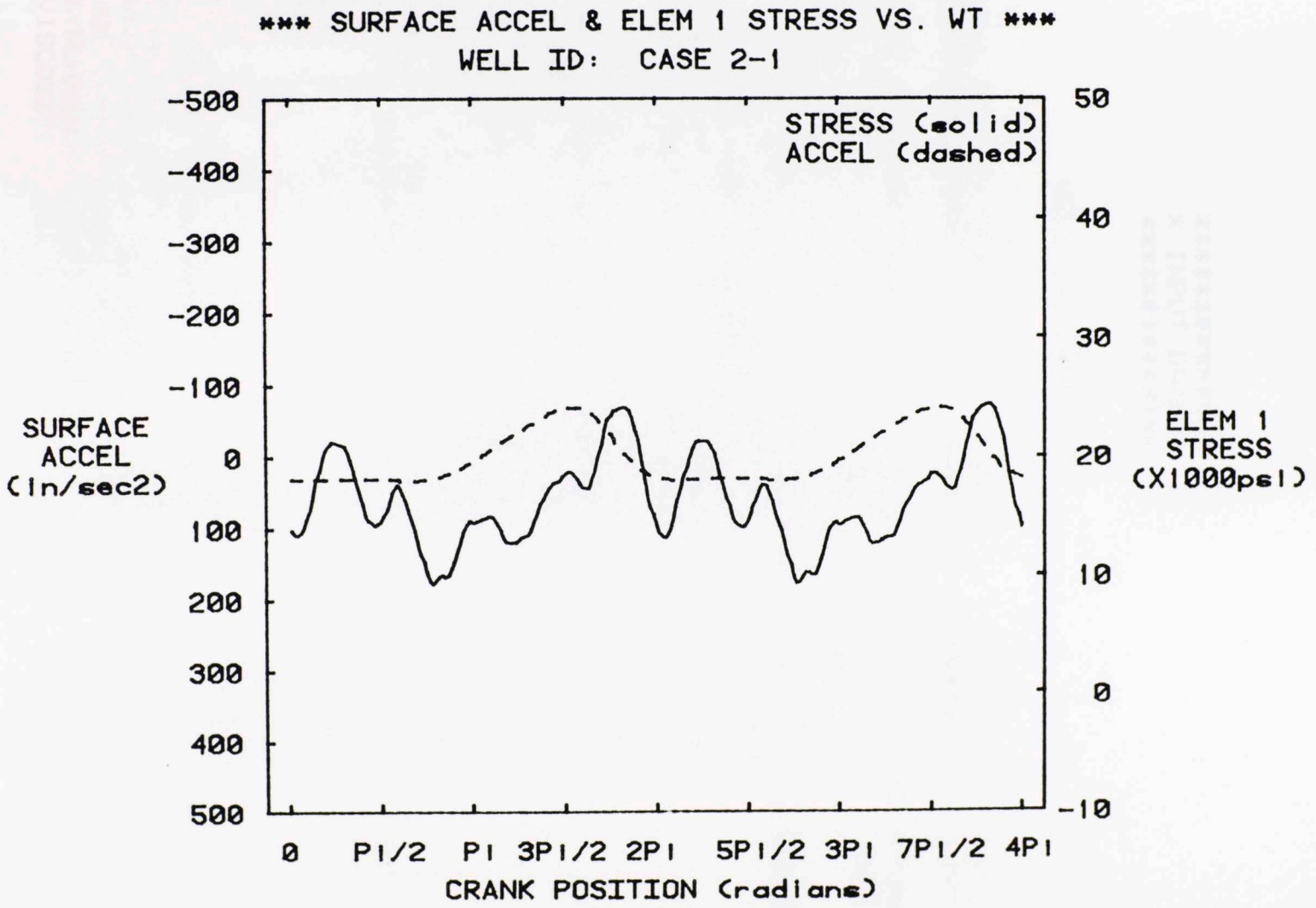

Figure C.14-Stress Plot - Case 2-1

****
* INPUT DATA *
****

WELL ID: CASE 2-2

VARIABLE DESCRIPTION	NAME	VALUE	REMARKS
DIAGNOSTIC PRINTOUT FLAG	(IDIAG)	0	NO DIAGNOSTICS
PLOT DATA FLAG	(IPLOT)	1	PLOT DATA
ROD LENGTH (FT)	(TOTL)	5000.000	
PLUNGER DIAMETER (IN)	(DPLUN)	1.500	
TUBING ANCHOR FLAG	(IANCH)	0	UNANCHORED
TUBING OD (IN)	(TUBEOD)	2.000	
# OF DIFFERENT ROD DIAMETERS	(NDIAM)	3	
DIAM OF SECTION 1	(DIAM)	.875	
BEGINNING ELEMENT #	(NELBEG)	1	
ENDING ELEMENT #	(NELEND)	2	
DIAM OF SECTION 2	(DIAM)	.750	
BEGINNING ELEMENT #	(NELBEG)	3	
ENDING ELEMENT #	(NELEND)	4	
DIAM OF SECTION 3	(DIAM)	.500	
BEGINNING ELEMENT #	(NELBEG)	5	
ENDING ELEMENT #	(NELEND)	5	
FLUID HEIGHT (FT)	(FLDHT)	500.000	
FLUID SPECIFIC GRAVITY	(SPGR)	.900	
LINKAGE TYPE PARAMETER	(IPTYPE)	1	CONVENTIONAL
DIMENSION 'D' (IN)	(D)	150.000	
DIMENSION 'H' (IN)	(H)	150.000	
DIMENSION 'L1' (IN)	(L1)	150.000	
DIMENSION 'L2' (IN)	(L2)	172.500	
DIMENSION 'L3' (IN)	(L3)	150.000	
DIMENSION 'R' (IN)	(R)	50.000	
VARIABLE MOTOR SPEED FLAG	(MVAR)	0	CONSTANT SPD
COUNTER-WEIGHT (LB)	(CBW)	12000.000	
C-WT PHASE ANGLE (+=CCW DEG)	(BETA)	.000	
UNBALANCE (+=HORSEHEAD HEAVY)	(UNBAL)	.000	
MOTOR SYNCHRONOUS SPEED (RPM)	(SYNSP)	1200.000	
FLUID VISCOSITY (CP)	(MU)	10.000	

Figure C.15-Input Data - Case 2-2

```
                    ************************
                    * SUMMARY OF RESULTS *
                    ************************

MAXIMUM ROD STRESSES (PSI)
**************************

ELEMENT #  1:  19360.
ELEMENT #  2:  15382.
ELEMENT #  3:  16608.
ELEMENT #  4:  12610.
ELEMENT #  5:  23014.


POLISHED ROD LOADS (LB)
***********************
MAXIMUM PRL= 12769.
MINIMUM PRL=  4792.


GEARBOX/MOTOR TORQUES (IN-LB)
*****************************
MAXIMUM GEARBOX TORQUE=  385130.
MINIMUM GEARBOX TORQUE= -321271.
MAXIMUN MOTOR TORQUE=      3209.
MINIMUM MOTOR TORQUE      -2677.


PUMPING RATES (STROKES/MIN)
***************************
MAXIMUM= 10.00
MINIMUM= 10.00


MISCELLANEOUS
*************
SURFACE STROKE (IN)=                  87.40
PUMP STROKE (IN)=                     79.77
POLISHED ROD HORSEPOWER=               7.34
WEIGHT OF ROD IN AIR (LB)=          7751.59
WEIGHT OF ROD IN FLUID (LB)=        6861.39
MAX FLUID LD ON PLUNGER (LB)=       3101.34
```

Figure C.16-Output Data - Case 2-2

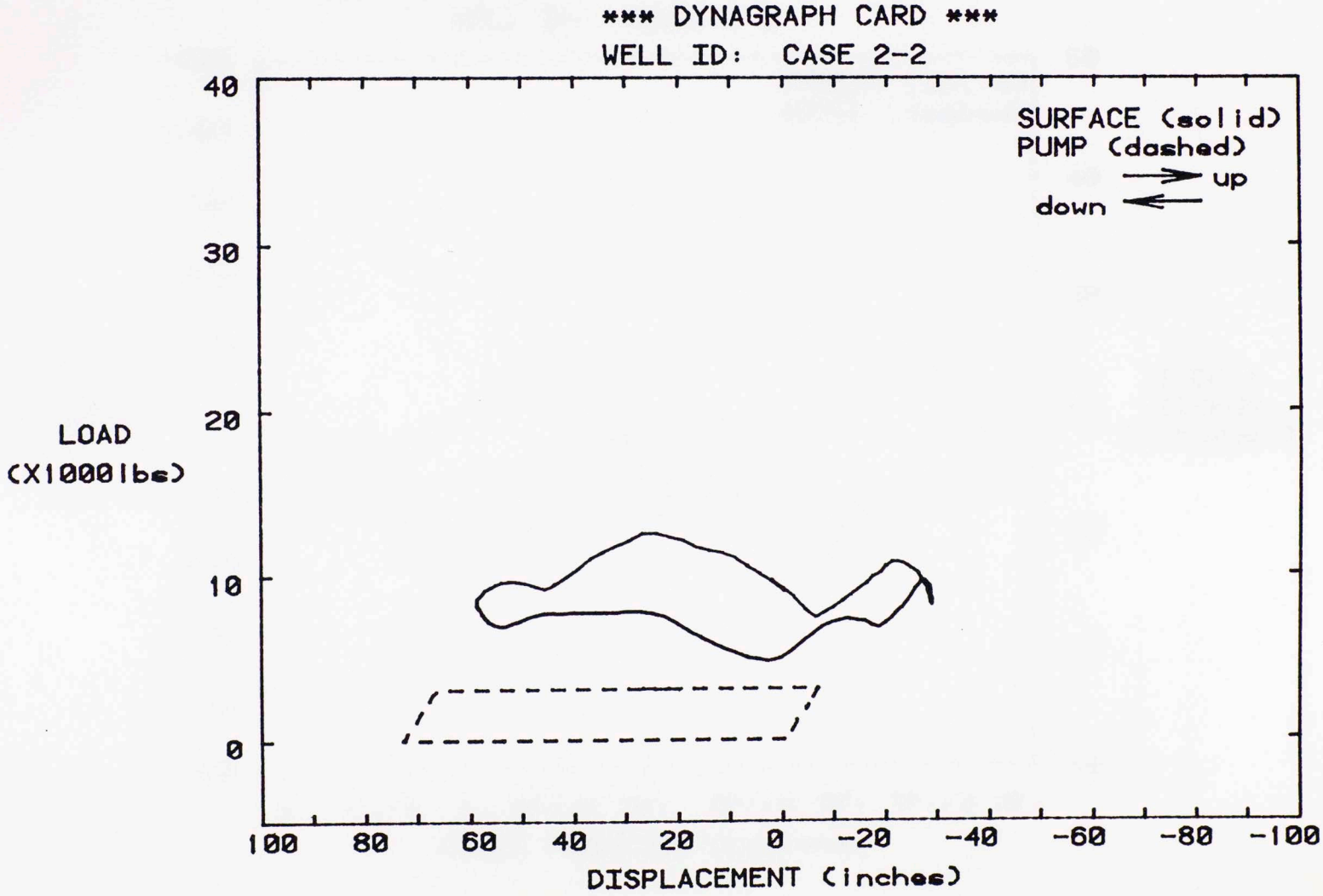

Figure C.17-Dynagraph - Case 2-2

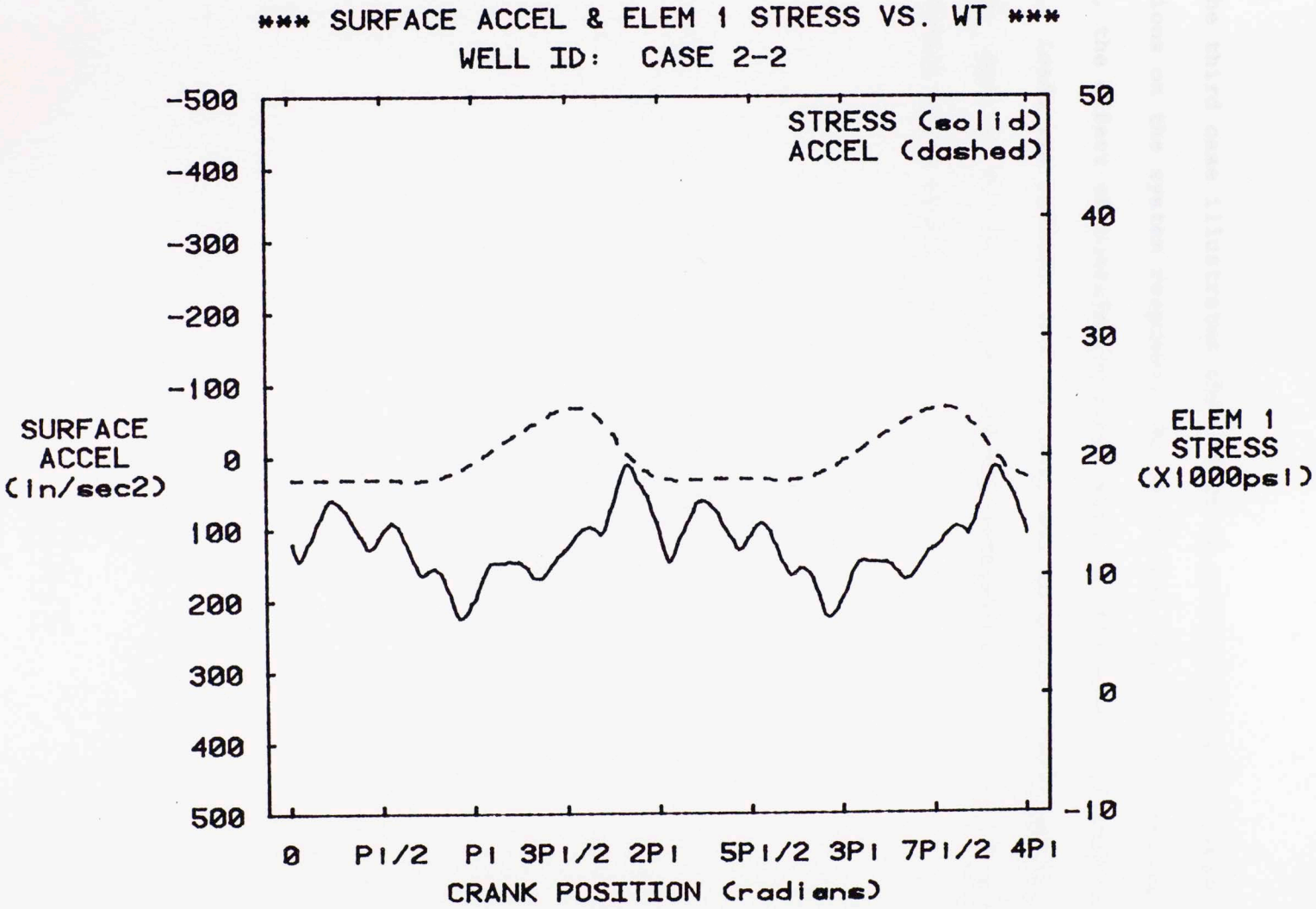

Figure C.18-Stress Plot - Case 2-2

Case 3

The third case illustrates the effect of considering motor speed variations on the system response. As we can see from the figures which follow, the effect of considering motor slip is effectively to "soften" the system. Loads are reduced, rod stresses, and horsepower requirements are reduced. But, so too is the pump stroke, indicating that a high slip motor would likely yield reduced production.

```
***************
* INPUT DATA *
***************

WELL ID: CASE 3-1

  VARIABLE DESCRIPTION                NAME          VALUE       REMARKS
  ********************                ****          *****       *******

DIAGNOSTIC PRINTOUT FLAG.......(IDIAG)...              0  NO DIAGNOSTICS
PLOT DATA FLAG.................(IPLOT)...              1       PLOT DATA
ROD LENGTH (FT)................(TOTL)...       6000.000
PLUNGER DIAMETER (IN)..........(DPLUN)...          1.750
TUBING ANCHOR FLAG.............(IANCH)...              0     UNANCHORED
TUBING OD (IN).................(TUBEOD)...         2.250
# OF DIFFERENT ROD DIAMETERS...(NDIAM)...              2
DIAM OF SECTION  1.............(DIAM)...           .875
BEGINNING ELEMENT #............(NELBEG)...              1
ENDING ELEMENT #...............(NELEND)...              3
DIAM OF SECTION  2.............(DIAM)...           .750
BEGINNING ELEMENT #............(NELBEG)...              4
ENDING ELEMENT #...............(NELEND)...              5
FLUID HEIGHT (FT)..............(FLDHT)...        750.000
FLUID SPECIFIC GRAVITY.........(SPGR)...           .900
LINKAGE TYPE PARAMETER.........(IPTYPE)...              1  CONVENTIONAL
DIMENSION 'D' (IN).............(D)...           150.000
DIMENSION 'H' (IN).............(H)...           150.000
DIMENSION 'L1' (IN)............(L1)...          150.000
DIMENSION 'L2' (IN)............(L2)...          175.000
DIMENSION 'L3' (IN)............(L3)...          150.000
DIMENSION 'R' (IN).............(R)...           50.000
VARIABLE MOTOR SPEED FLAG......(MVAR)...              0  CONSTANT SPD
COUNTER-WEIGHT (LB)............(CBW)...      15000.000
C-WT PHASE ANGLE (+=CCW DEG)...(BETA)...           .000
UNBALANCE (+=HORSEHEAD HEAVY)..(UNBAL)...       250.000
MOTOR SYNCHRONOUS SPEED (RPM)..(SYNSP)...      1200.000
FLUID VISCOSITY (CP)...........(MU)...           15.000
```

Figure C.19-Input Data - Case 3-1

```
                    **********************
                    * SUMMARY OF RESULTS *
                    **********************

MAXIMUM ROD STRESSES (PSI)
**************************

ELEMENT #  1:  26560.
ELEMENT #  2:  22026.
ELEMENT #  3:  17464.
ELEMENT #  4:  18811.
ELEMENT #  5:  14073.


POLISHED ROD LOADS (LB)
***********************
MAXIMUM PRL= 17226.
MINIMUM PRL=  7879.


GEARBOX/MOTOR TORQUES (IN-LB)
*****************************
MAXIMUM GEARBOX TORQUE=  396970.
MINIMUM GEARBOX TORQUE= -352724.
MAXIMUN MOTOR TORQUE=      3143.
MINIMUM MOTOR TORQUE      -2792.


PUMPING RATES (STROKES/MIN)
***************************
MAXIMUM=  9.50
MINIMUM=  9.50


MISCELLANEOUS
*************
SURFACE STROKE (IN)=                  86.31
PUMP STROKE (IN)=                     72.49
POLISHED ROD HORSEPOWER=               8.61
WEIGHT OF ROD IN AIR (LB)=         10952.24
WEIGHT OF ROD IN FLUID (LB)=        9694.47
MAX FLUID LD ON PLUNGER (LB)=       4924.81
```

Figure C.20-Output Data - Case 3-1

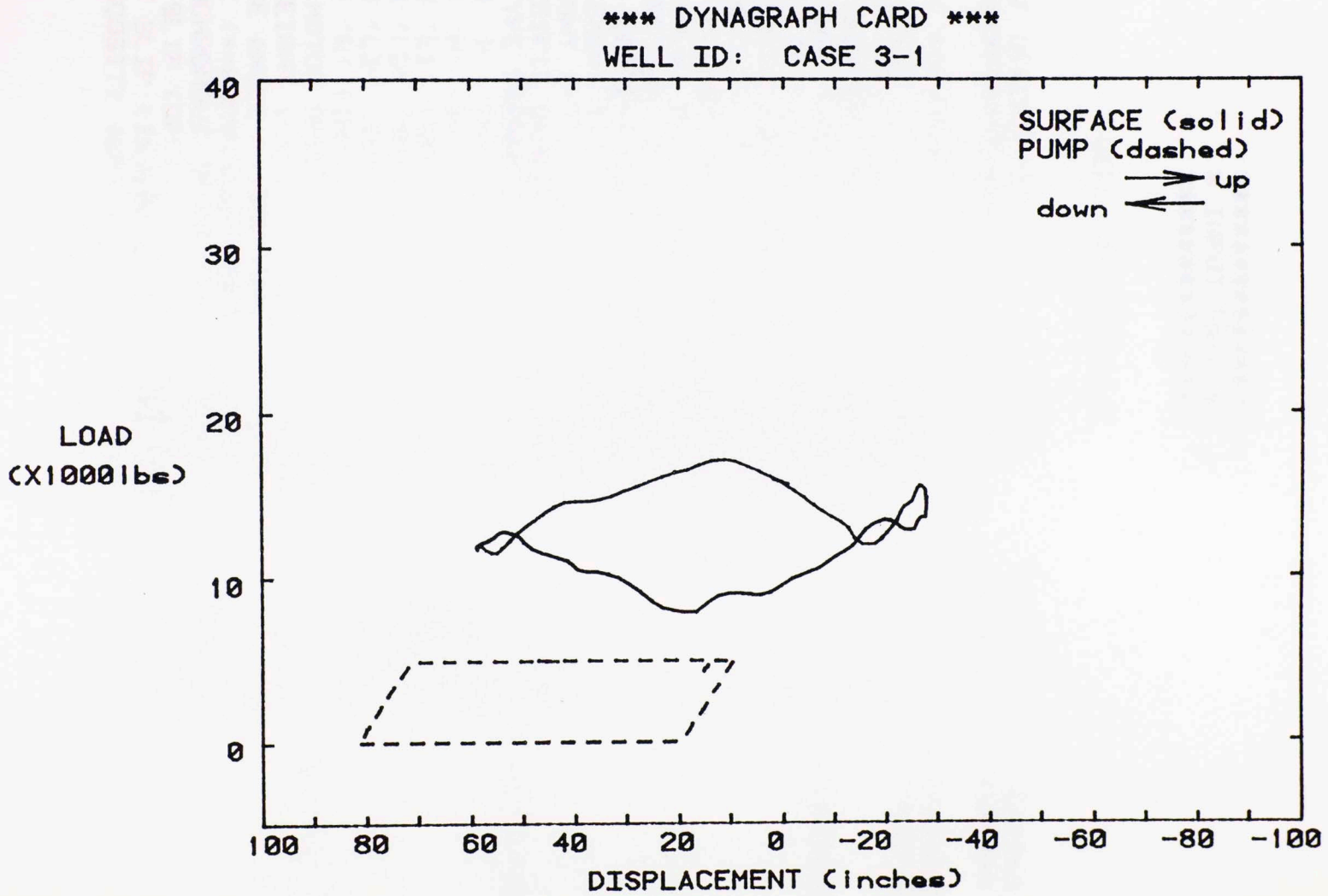

Figure C.21-Dynagraph - Case 3-1

```
***************
* INPUT DATA *
***************

WELL ID: CASE 3-2

  VARIABLE DESCRIPTION                NAME          VALUE       REMARKS
  ********************                ****          *****       *******

DIAGNOSTIC PRINTOUT FLAG.......(IDIAG)...              0 NO DIAGNOSTICS
PLOT DATA FLAG.................(IPLOT)...              1      PLOT DATA
ROD LENGTH (FT)................(TOTL)...      6000.000
PLUNGER DIAMETER (IN)..........(DPLUN)...         1.750
TUBING ANCHOR FLAG.............(IANCH)...              0    UNANCHORED
TUBING OD (IN).................(TUBEOD)...         2.250
# OF DIFFERENT ROD DIAMETERS...(NDIAM)...             2
DIAM OF SECTION  1.............(DIAM)...          .875
BEGINNING ELEMENT #............(NELBEG)...             1
ENDING ELEMENT #...............(NELEND)...             3
DIAM OF SECTION  2.............(DIAM)...          .750
BEGINNING ELEMENT #............(NELBEG)...             4
ENDING ELEMENT #...............(NELEND)...             5
FLUID HEIGHT (FT)..............(FLDHT)...       750.000
FLUID SPECIFIC GRAVITY.........(SPGR)...          .900
LINKAGE TYPE PARAMETER.........(IPTYPE)...             1  CONVENTIONAL
DIMENSION 'D' (IN).............(D)...          150.000
DIMENSION 'H' (IN).............(H)...          150.000
DIMENSION 'L1' (IN)............(L1)...          150.000
DIMENSION 'L2' (IN)............(L2)...          175.000
DIMENSION 'L3' (IN)............(L3)...          150.000
DIMENSION 'R' (IN).............(R)...           50.000
VARIABLE MOTOR SPEED FLAG......(MVAR)...              1  VARIABLE SPD
COUNTER-WEIGHT (LB)............(CBW)...      15000.000
C-WT PHASE ANGLE (+=CCW DEG)...(BETA)...           .000
UNBALANCE (+=HORSEHEAD HEAVY)..(UNBAL)...       250.000
MOTOR SYNCHRONOUS SPEED (RPM)..(SYNSP)...      1200.000
SPEED AT SLIP (RPM)............(SLPSP)...      1000.000
TORQUE AT SLIP (IN-LB).........(SLPTQ)...     12000.000
FLUID VISCOSITY (CP)...........(MU)...           15.000
```

Figure C.22-Input Data - Case 3-2

```
                    **********************
                    * SUMMARY OF RESULTS *
                    **********************

MAXIMUM ROD STRESSES (PSI)
**************************

ELEMENT #  1:  26409.
ELEMENT #  2:  22129.
ELEMENT #  3:  17558.
ELEMENT #  4:  18878.
ELEMENT #  5:  14020.


POLISHED ROD LOADS (LB)
***********************
MAXIMUM PRL= 17096.
MINIMUM PRL=  7952.


GEARBOX/MOTOR TORQUES (IN-LB)
*****************************
MAXIMUM GEARBOX TORQUE=  393437.
MINIMUM GEARBOX TORQUE= -357754.
MAXIMUN MOTOR TORQUE=      3115.
MINIMUM MOTOR TORQUE      -2832.


PUMPING RATES (STROKES/MIN)
***************************
MAXIMUM=  9.87
MINIMUM=  9.09


MISCELLANEOUS
*************
SURFACE STROKE (IN)=                 86.31
PUMP STROKE (IN)=                    71.38
POLISHED ROD HORSEPOWER=              8.43
WEIGHT OF ROD IN AIR (LB)=        10952.24
WEIGHT OF ROD IN FLUID (LB)=       9694.47
MAX FLUID LD ON PLUNGER (LB)=      4924.81
```

Figure C.23-Output Data - Case 3-2

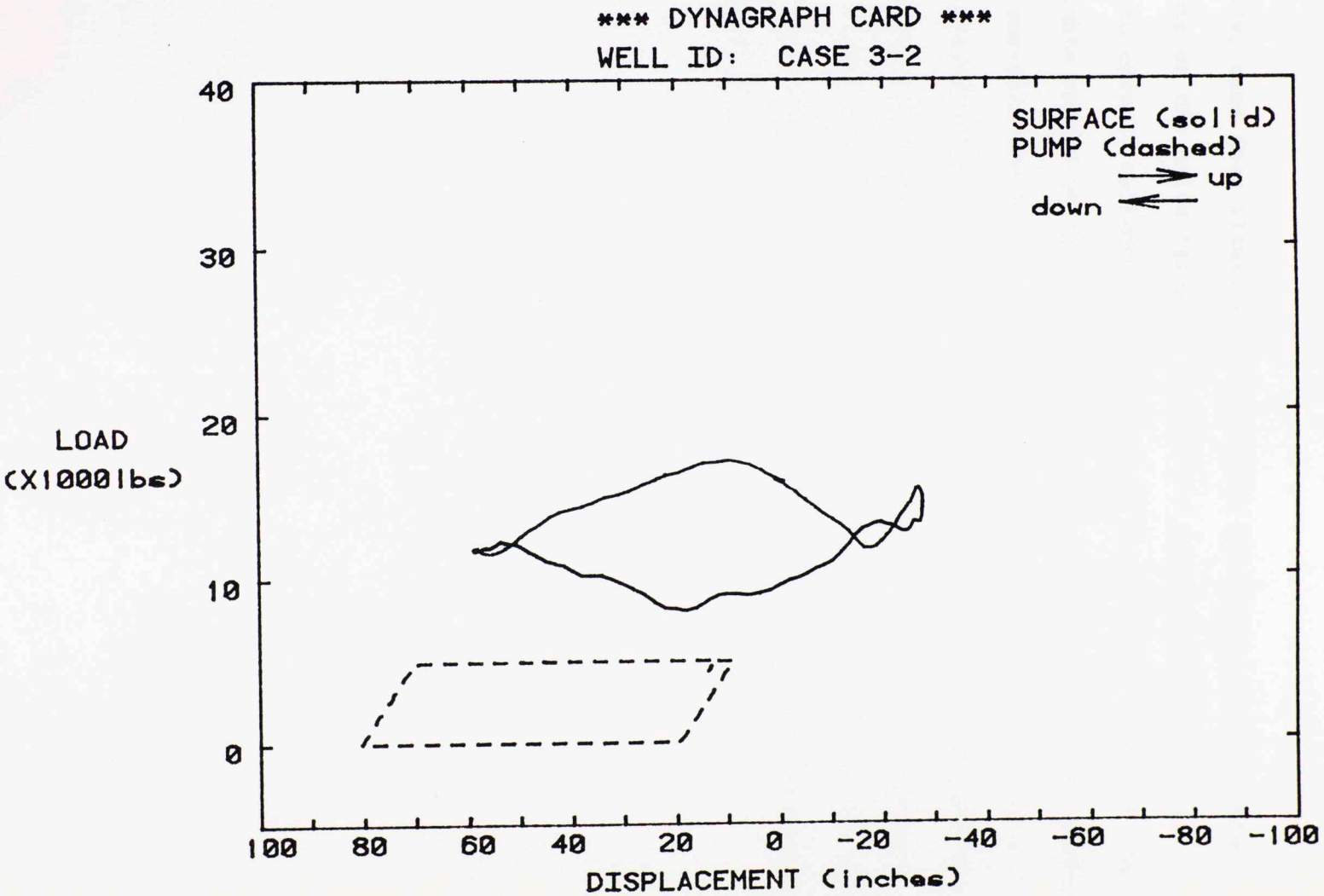

Figure C.24-Dynagraph - Case 3-2

Case 4

Finally, case four illustrates the effect of balance on the torque requirements of the drive train. In case 4-1, we see a unit in close proximity to correct balance. A rule of thumb is that the weight of the counterweights should be approximately equal to the sum of the rod weight in fluid and one-half the fluid load on the plunger. In this case, for 4-1, the resulting counterbalance weight is 11,150 lb.. For case 4-2, we take the same system but overcounterbalance by 20%. As can be seen in the following summaries, the resulting increase in gearbox torque is 34%. Were the system sized for the former case, the life of the gearbox in the overcounterbalanced state would clearly be significantly reduced.

```
***************
* INPUT DATA *
***************

WELL ID: CASE 4-1

  VARIABLE DESCRIPTION              NAME          VALUE        REMARKS
  ********************              ****          *****        *******

DIAGNOSTIC PRINTOUT FLAG.......(IDIAG)...           0 NO DIAGNOSTICS
PLOT DATA FLAG.................(IPLOT)...           1     PLOT DATA
ROD LENGTH (FT).................(TOTL)...   5000.000
PLUNGER DIAMETER (IN)..........(DPLUN)...      2.000
TUBING ANCHOR FLAG.............(IANCH)...           0   UNANCHORED
TUBING OD (IN).................(TUBEOD)...      2.500
# OF DIFFERENT ROD DIAMETERS...(NDIAM)...          2
DIAM OF SECTION  1.............(DIAM)...       .875
BEGINNING ELEMENT #............(NELBEG)...          1
ENDING ELEMENT #...............(NELEND)...          3
DIAM OF SECTION  2.............(DIAM)...       .750
BEGINNING ELEMENT #............(NELBEG)...          4
ENDING ELEMENT #...............(NELEND)...          5
FLUID HEIGHT (FT)..............(FLDHT)...       .000
FLUID SPECIFIC GRAVITY.........(SPGR)...       .900
LINKAGE TYPE PARAMETER.........(IPTYPE)...          1  CONVENTIONAL
DIMENSION 'D' (IN).................(D)...   150.000
DIMENSION 'H' (IN).................(H)...   150.000
DIMENSION 'L1' (IN)...............(L1)...   150.000
DIMENSION 'L2' (IN)...............(L2)...   172.500
DIMENSION 'L3' (IN)...............(L3)...   150.000
DIMENSION 'R' (IN).................(R)...    50.000
VARIABLE MOTOR SPEED FLAG.......(MVAR)...           0  CONSTANT SPD
COUNTER-WEIGHT (LB).............(CBW)... 11150.000
C-WT PHASE ANGLE (+=CCW DEG)....(BETA)...       .000
UNBALANCE (+=HORSEHEAD HEAVY)..(UNBAL)...       .000
MOTOR SYNCHRONOUS SPEED (RPM)..(SYNSP)...  1200.000
FLUID VISCOSITY (CP)............(MU)...    10.000
```

Figure C.25-Input Data - Case 4-1

```
                    **********************
                    * SUMMARY OF RESULTS *
                    **********************

MAXIMUM ROD STRESSES (PSI)
**************************

ELEMENT #  1:  28290.
ELEMENT #  2:  24437.
ELEMENT #  3:  20438.
ELEMENT #  4:  23505.
ELEMENT #  5:  19300.


POLISHED ROD LOADS (LB)
***********************
MAXIMUM PRL= 18053.
MINIMUM PRL=  5343.


GEARBOX/MOTOR TORQUES (IN-LB)
*****************************
MAXIMUM GEARBOX TORQUE=  325561.
MINIMUM GEARBOX TORQUE= -213461.
MAXIMUN MOTOR TORQUE=      2713.
MINIMUM MOTOR TORQUE      -1779.


PUMPING RATES (STROKES/MIN)
***************************
MAXIMUM= 10.00
MINIMUM= 10.00


MISCELLANEOUS
*************
SURFACE STROKE (IN)=                87.40
PUMP STROKE (IN)=                   70.17
POLISHED ROD HORSEPOWER=            11.03
WEIGHT OF ROD IN AIR (LB)=        9126.87
WEIGHT OF ROD IN FLUID (LB)=      8078.73
MAX FLUID LD ON PLUNGER (LB)=     6126.11
```

Figure C.26-Output Data - Case 4-1

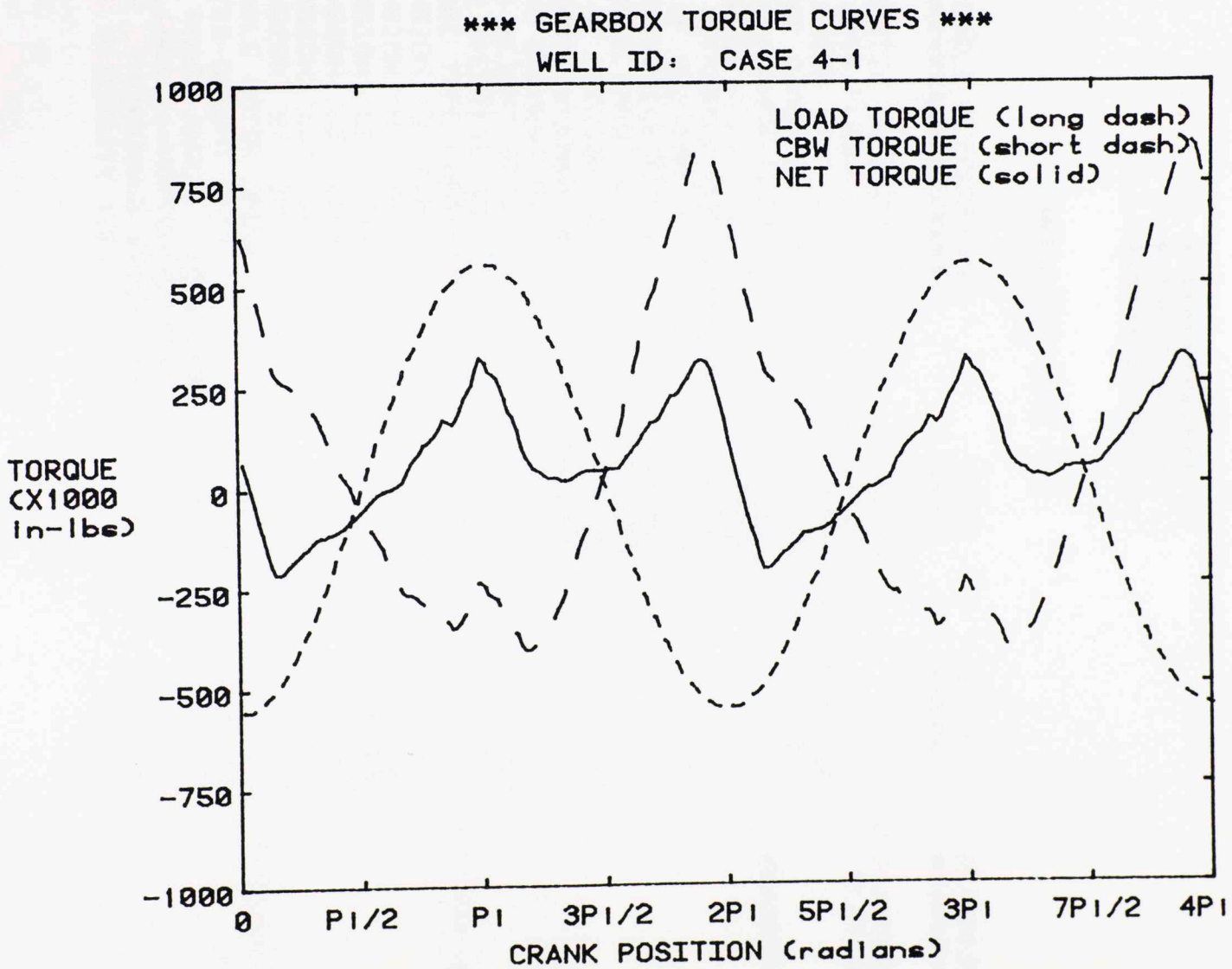

Figure C.27-Torque Plot - Case 4-1

```
               ***************
               * INPUT DATA *
               ***************

                    WELL ID: CASE 4-2

  VARIABLE DESCRIPTION                NAME          VALUE        REMARKS
  ********************                ****          *****        *******

DIAGNOSTIC PRINTOUT FLAG.......(IDIAG)...            0 NO DIAGNOSTICS
PLOT DATA FLAG.................(IPLOT)...            1    PLOT DATA
ROD LENGTH (FT).................(TOTL)...  5000.000
PLUNGER DIAMETER (IN)..........(DPLUN)...     2.000
TUBING ANCHOR FLAG.............(IANCH)...            0   UNANCHORED
TUBING OD (IN).................(TUBEOD)...     2.500
# OF DIFFERENT ROD DIAMETERS...(NDIAM)...         2
DIAM OF SECTION  1.............(DIAM)...      .875
BEGINNING ELEMENT #............(NELBEG)...         1
ENDING ELEMENT #...............(NELEND)...         3
DIAM OF SECTION  2.............(DIAM)...      .750
BEGINNING ELEMENT #............(NELBEG)...         4
ENDING ELEMENT #...............(NELEND)...         5
FLUID HEIGHT (FT)..............(FLDHT)...      .000
FLUID SPECIFIC GRAVITY.........(SPGR)...      .900
LINKAGE TYPE PARAMETER.........(IPTYPE)...         1  CONVENTIONAL
DIMENSION 'D' (IN).................(D)...   150.000
DIMENSION 'H' (IN).................(H)...   150.000
DIMENSION 'L1' (IN)................(L1)...   150.000
DIMENSION 'L2' (IN)................(L2)...   172.500
DIMENSION 'L3' (IN)................(L3)...   150.000
DIMENSION 'R' (IN).................(R)...    50.000
VARIABLE MOTOR SPEED FLAG.......(MVAR)...            0  CONSTANT SPD
COUNTER-WEIGHT (LB)............(CBW)... 13380.000
C-WT PHASE ANGLE (+=CCW DEG)....(BETA)...      .000
UNBALANCE (+=HORSEHEAD HEAVY)..(UNBAL)...      .000
MOTOR SYNCHRONOUS SPEED (RPM)..(SYNSP)...  1200.000
FLUID VISCOSITY (CP)...........(MU)...      10.000
```

Figure C.28-Input Data - Case 4-2

```
          **********************
          * SUMMARY OF RESULTS *
          **********************

MAXIMUM ROD STRESSES (PSI)
**************************

ELEMENT #  1:  28290.
ELEMENT #  2:  24437.
ELEMENT #  3:  20438.
ELEMENT #  4:  23505.
ELEMENT #  5:  19300.


POLISHED ROD LOADS (LB)
***********************
MAXIMUM PRL= 18053.
MINIMUM PRL=  5343.


GEARBOX/MOTOR TORQUES (IN-LB)
*****************************
MAXIMUM GEARBOX TORQUE=  436964.
MINIMUM GEARBOX TORQUE= -311720.
MAXIMUN MOTOR TORQUE=      3641.
MINIMUM MOTOR TORQUE      -2598.


PUMPING RATES (STROKES/MIN)
***************************
MAXIMUM= 10.00
MINIMUM= 10.00


MISCELLANEOUS
*************
SURFACE STROKE (IN)=                  87.40
PUMP STROKE (IN)=                     70.17
POLISHED ROD HORSEPOWER=              11.03
WEIGHT OF ROD IN AIR (LB)=          9126.87
WEIGHT OF ROD IN FLUID (LB)=        8078.73
MAX FLUID LD ON PLUNGER (LB)=       6126.11
```

Figure C.29-Output Data - Case 4-2

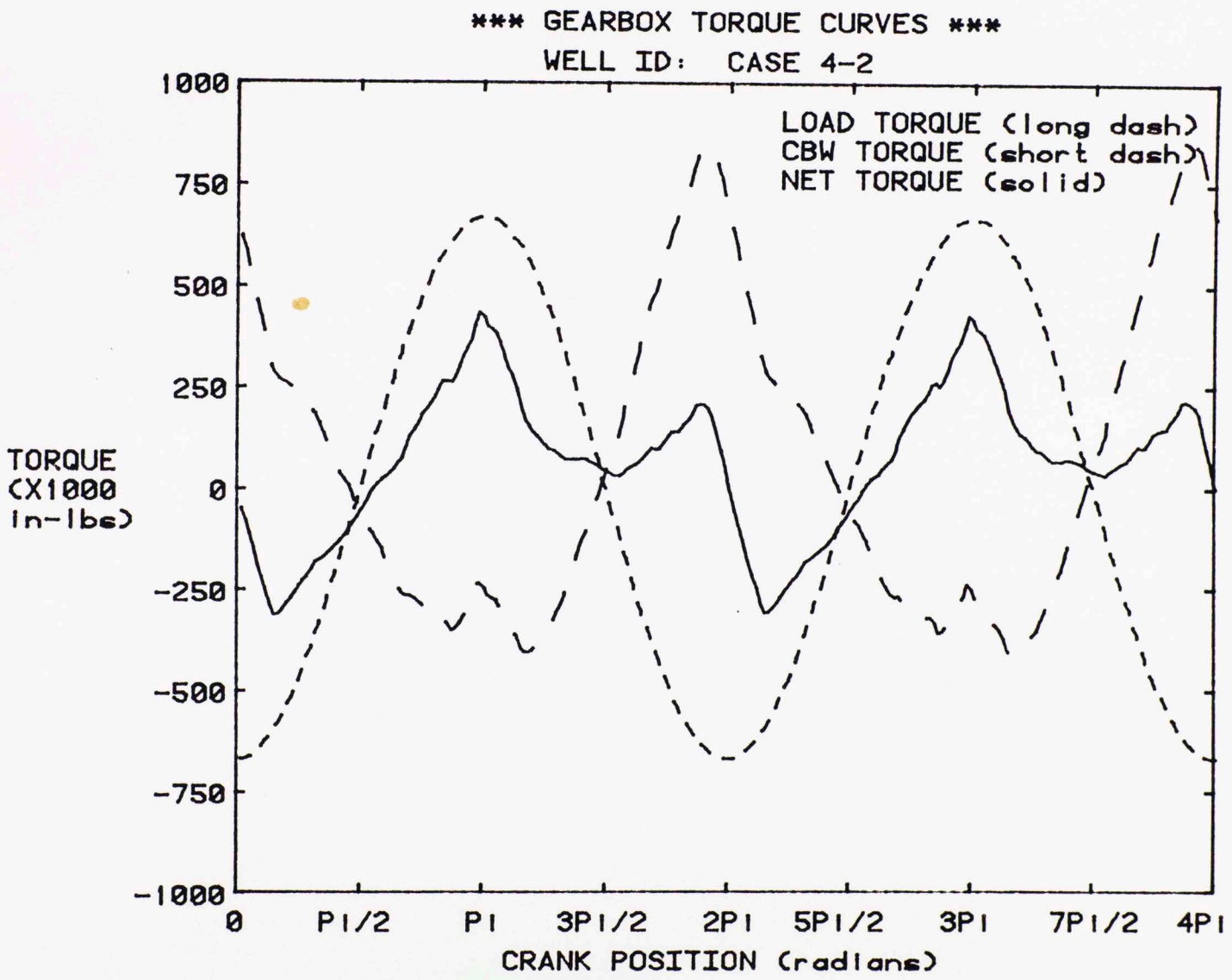

Figure C.30-Torque Plot - Case 4-2